QUEENSLAND WATER MODELLING NETWORK

Water planning, integration and management

MEDLI science review: Modelling of water and solute transport in MEDLI

Final report

Report prepared by

Prof Freeman J Cook

for the Queensland Water Modelling Network

Queensland Government

The Queensland Water Modelling Network (QWMN) is an initiative of the Queensland Government that aims to improve the state's capacity to model its surface water and groundwater resources and their quality. The QWMN is led by the Department of Environment and Science with key links across industry, research and government.

Prepared by: Prof Freeman J Cook, Freeman Cook & Associates

Citation

Cook FJ (2021). MEDLI science review: Modelling of Water and Solute Transport in MEDLI. Report to the Queensland Water Modelling Network, Department of Environment and Science by Freeman Cook & Associates.

Acknowledgements

QWMN commissioned a review of MEDLI (Model for Effluent Disposal using Land Irrigation) to assess the science underpinning its Hydrology, Nutrient & Pond Chemistry modules, to identify gaps, and suggest possible improvements. This report is one of five reports written for the MEDLI Science Review by a team led by Prof Ted Gardner. Other reports from the MEDLI Science Review are "Hydrology – Model and process" by Dr Tony Ladson, "Methodologies used by biophysical models for simulating soil nutrient pools and processes in pasture systems - Carbon, nitrogen and phosphorus" by Dr Phil Moody, "MEDLI Science Review: Pond chemistry module" by Dr Mike Johns and Dr Bronwen Butler, and "MEDLI Science Review: Synthesis" by Prof Ted Gardner. The author would like to thank Prof Ted Gardner (Victoria University), Alison Vieritz and other members of the Department of Environment and Science review team that made numerous editorial suggestions and technical questions of clarification that substantially improved the readability of this review. The author also thanks the reviewers of this document including Dr Melanie Roberts, Prof Calvin Rose and Dr Afshin Ghahramani.

Table of Contents

Table of Figures

Table of Tables

Executive Summary

Water and solute transport are the pivotal processes in the MEDLI model. A recent review of MEDLI suggested that the modelling of these processes needed to be examined given advances in soil physics since MEDLI was developed. This report presents a review and recommendations for how water and solute transport could be revised in MEDLI.

The water transport is broken down into infiltration, drainage, and evapotranspiration. The Green and Ampt (GA), linear soil and Philip two-term infiltration models are considered for infiltration. The GA model has received considerable development recently and this was considered to be the best model if the present Curve Number (CN) infiltration model was to be replaced. This model assumes that water is ponded on the soil surface during infiltration but can be adapted using the time-to-ponding concept to include mixed (flux controlled, and concentration controlled) surface boundary conditions. In addition, it can be adapted for non-uniform initial conditions and layered soils. The equations for all of these adaptions are presented in this report (Appendix 1). The time step in MEDLI of 1 day will have to be reduced when infiltration is occurring to use the GA model. Methods are available for disaggregation of daily rainfall into duration and intensity. There is a need for further investigation comparing the GA and CN models before the infiltration model in MEDLI is changed.

The drainage method used in the present MEDLI and cascading box models is shown to be dependent on the time step of the model. Two alternative drainage models, one, the Sisson et al. (1980) model, based on gravitational drainage and the Youngs (1960) model based on a shallow water table are presented and reviewed. Sites where shallow water tables are present are unlikely to be considered for wastewater irrigation and hence modelled in MEDLI. Thus, the Sisson model has been suggested as a drainage model that could be adopted in MEDLI. Developments of this model for non-uniform initial conditions and layered soils are presented in Appendix 3. The evapotranspiration and drainage are convolved, so the order that the processes are calculated will have an effect mainly on drainage.

Root water uptake was considered with transpiration and is based on a recent review. The Feddes model for determining the actual transpiration compared with the potential transpiration is considered. This is a bent stick model and has two zones where the actual transpiration will differ from potential, one near saturation where aeration limits transpiration and one when the soil is drier than a predetermined value and transpiration is again limited. A weighting function for water extraction from depth is developed from published information. A simple method similar to that presently in MEDLI but using a weighting function is also presented. This latter method could be easily incorporated into MEDLI and may be a first step in any modifications of the transpiration function. Soil evaporation is reviewed, and the method presented for stage potential evaporation is similar to that already used in MEDLI. However, the plant cover function of Sutanto et al. (2012) presented here would give a lower potential evaporation rate than the model used in MEDLI; further investigation using data is suggested. A crop residual cover function is also presented, and this could and probably should be included in MEDLI.

Solute transport is reviewed with both convective dispersion equation (CDE) and transfer function (TF) models discussed. The simple piston flow model, which is what is presently used in MEDLI, is introduced and an adaption using a velocity distribution and streamtubes is used to show how this could be used to develop a model that gives more realistic solute distributions. The CDE model is too complicated and computationally intensive for MEDLI, but the introduction of the mobile/immobile concept is the connection between this and the TF models. The simple method suggested by Scotter and Ross (1994) to determine the mobile pore space region when used with piston flow model would result in the Corwin et al. (1991) bypass model and this could be easily used to provide more realistic solute transport in the MEDLI model without extensive modification.

The Burns equation is another simple model that could be adapted to MEDLI by treating each wastewater irrigation as a separate event and using the super positioning principle to combine these together. The problem with this method is it does not allow for plant uptake and gains and losses of solutes from mineralisation/immobilisation. However, it may be possible to do this with a time-based function, but this would have to be investigated further. The Burns equation would be a particularly

effective way of determining the potential leaching of solute out of the soil to deep drainage even if this was an overestimate due to plant uptake and other gains and losses not being accounted for.

This report and the accompanying spreadsheet provide options for the further development of MEDLI. The report also indicates where further investigation is required before any modifications to MEDLI.

Implications of the issues identified in this report are summarised and provided in Table 1.

Table 1. Strategic overview of the issues and implications raised by this review. (From p.66)

Model Process	Issue(s) identified	Current handling	Proposed alternative(s)	Implications	Degree of difficulty	Importance	Recommendation
Infiltration/ Runoff quantity	Curve number (CN) – Dryland only, not tested under irrigation. Datasets underlying model testing limited to heavy textured soils.	CN used as a pragmatic solution in most daily time-step hydrological models	Green & Ampt (G&A) improved with better approach to calculating time to ponding, be considered to replace CN.	Can't be adopted immediately into MEDLI. Need to compare the improved GA model with the CN model before the infiltration model in MEDLI is changed. Proposed G&A model will require the rainfall input to be at a time step of less than 1 day. and also requires additional parameters for each soil horizon: • Sub-daily rainfall data • Lambda – defines relationship between water content and matric potential. • Sorptivity – a measure of the how rapidly a dry soil is wetted due to capillarity only. • Air-entry matric potential	Currently high, as limited resources to adapt the model; Limited availability of datasets (with the exception of sub-daily rainfall for many areas), Limited in-house soil physics expertise	Infiltration is a key factor in determining deep drainage and solute transport and if incorrectly handled, will have significant implications reef models.	Investigate need and develop a detailed case for dedicated resource(s) to: Adapt G&A model to non-uniform soils and to develop datasets for new parameters using pedo-transfer functions (PTFs) where possible which will need to involve both field studies and "mining" of the soil physics literature.

Model Process	Issue(s) identified	Current handling	Proposed alternative(s)	Implications	Degree of difficulty	Importance	Recommendation
Deep drainage	The prediction of drainage in the soil by MEDLI and other cascading box models is dependent on the thickness of the soil layers chosen and time step used in the model. The draining profile shape is also unrealistic. Hence, daily cascading box models poorly represent actual drainage. Also, the order of calculation of the drainage and evaporation process can affect the drainage if they are implemented sequentially Datasets underlying model testing limited to heavy textured soils – possibly under rain-fed conditions.	Cascading bucket using daily time-step where the drainage factor (proportion of drainable water draining) is calculated using an exponential function based on the saturated hydraulic conductivity and drainable porosity of the soil layer. As such, the drainage factor has no real physical meaning.	Consider using the Sisson model, based on gravitational drainage (must have no shallow water tables). NOTE: *shallow water tables are unlikely to be modelled by MEDLI.* Refer Appendix 3	Sisson model requires additional parameters as it is based on the K-**θ** function, but these may be able to be estimated from known parameters. Sisson method assumes that at the soil surface, the water content reduces to a specified value (less than DUL) as drainage proceeds. A value of 0.83 x DUL may be suitable, but this will need to be checked by comparison with numerical models such as HYDRUS1D.	Currently high, proposed Sisson model not currently built or tested. Limited resources to adapt the MEDLI model Limited availability of datasets (with the exception of sub-daily rainfall for many areas) Limited in-house soil physics expertise	High	Investigate need and develop a detailed case for dedicated resource(s) to: • Adapt Sisson model to non-uniform soils • Develop datasets for new parameters using pedo-transfer functions (PTFs) - methods to predict the hydraulic properties of soils from simpler soil measurements - where possible which will need to involve field studies.
Root water uptake	MEDLI transpiration algorithm does progressively reduce root water uptake as plant available soil water approaches zero.	Partitioning of potential transpiration favours wetter layers and excludes layers with no plant available water. The upper two soil layers are also weighted more heavily as these layers will contain more roots. The actual transpiration from each layer is then limited to the amount of plant available water stored in that layer.	Feddes model uses a *bent stick* approach with two zones– • for near saturation/ aeration limitation. • for when soil dried below a specified limit.	Relatively easy to adopt into MEDLI. Will need extra parameter for the soil lower water content threshold. Note: Transpiration and soil evaporation will affect drainage predictions. Order of calculations important	Low.	Improves transpiration modelling in schemes where irrigation is well below irrigation demand.	Include in current planning for model development with current resources

Model Process	Issue(s) identified	Current handling	Proposed alternative(s)	Implications	Degree of difficulty	Importance	Recommendation
Soil evaporation for soils with dead cover (crop residues)	MEDLI poorly models the impact of crop residual cover on soil evaporation.	The fraction of soil surface with any cover (transpiring or non-transpiring) is deemed to show zero soil evaporation.	The residual cover function from HOWLEAKY? should be considered/adopted to account for the mass of residual dead plant material reducing soil evaporation.	Relatively easy to adopt into MEDLI. No new parameters would be required. A "Desorptivity" parameter is equivalent to "CONA" used in MEDLI. Improved soil evaporation modelling in schemes where residual cover occurs following crop removal or as plant canopy regrows following harvest.	Moderate as some further investigation into the HOWLEAKY residual cover function is required. However, adoption into the MEDLI model appears straight forward	Moderate to high Transpiration and soil evaporation will affect irrigation demand and drainage predictions. Order of calculations important	Consider including in current planning for model development subject to availability of resources
Soil evaporation from bare soil	MEDLI does not model re-wetting of soil surface towards the second soil moisture content in the absence of rain or evaporation, potentially underestimating soil evaporation from bare soils.	Ritchie (1972) evaporation algorithms are used to estimate soil evaporation which is then subtracted from the water content of the top two soil layers. Upward flux is ignored.	Force-restore method proposed by Cook et al. (2008).	As bare soil scenario would be rarely modelled within MEDLI, the extra complication may be unwarranted.	Moderate – need for investigation	Low	Consider including in current planning for model development subject to availability of resources
Plant cover factor	Sutanto et al. 2012 calculates a plant cover factor from LAI uses Beers law with an extinction coefficient of -0.463 while MEDLI uses and extinction coefficient of -0.65.	In the pasture model, MEDLI uses a sine curve function of plant transpiring cover over thermal time. The transpiring cover, expressed as the proportion of soil area is then used to calculate potential transpiration. The crop module taken from EPIC uses LAI which is converted to transpiring cover using Beers law with an extinction coefficient of -0.65.	Plant cover function of Sutanto et al. (2012) (used in HYDRUS1D)	This would apply to the crop module.	Moderate as some further investigation into the Sutanto model is required. Adoption into the MEDLI model appears straight forward. Need further investigation of LAI on evaporation with measured data.	Transpiration and soil evaporation will affect irrigation demand and drainage predictions. Order of calculations important	Consider including in current planning for model development subject to availability of resources

Model Process	Issue(s) identified	Current handling	Proposed alternative(s)	Implications	Degree of difficulty	Importance	Recommendation
Solute Transport	Simple piston-flow model assumes all the existing soil water with its dissolved solutes is displaced by the infiltrating solution, hence overestimating leaching. For a model such as MEDLI, the development of the actual shape of the solute distribution may not be as important as calculating where the solute front is.	Simple piston-flow model	Adopt Corwin et al. bypass model (uses mobile/ immobile concept) + Scotter & Ross (1994) to determine mobile/immobile regions for a more realistic solute transport model. The solute would be transported in the mobile pore space during drainage. Adopt the split suggested by Corwin et al. (1991) and have only 50% of the solute mass in a box available for transport. And/or The Burns equation could be incorporated into MEDLI using the leaching fraction algorithms to give the fraction of solute mass leaching out of the bottom boundary of the soil model domain to deep drainage. .	This would require only a minimal recoding of the MEDLI model and the computational methodology is well set out by Corwin et al. (1991). Extra parameters include a fixed bypass flow coefficient for the soil. The Burns equation works on cumulative drainage and either a uniform profile or pulse input. Unlike the Corwin et al. model, It would be more difficult to incorporate into MEDLI's bucket model approach. The Burns equation also assumes that the solute is conserved within the soil (does not allow for plant uptake and gains and losses of solutes from mineralisation/ immobilisation). However, it may be possible to do this with a time-based function, but this would have to be investigated further	Moderate as the Corwin model is well described and the Burns equation is also easily implemented. Equations need explanation for implementation. The Burns equation approach only requires knowledge of one soil factor (the water content of the mobile region).	High	Investigate need and develop a detailed case for dedicated resource(s) to: Develop solute transport model and to develop datasets for new parameters using PTFs where possible which will need to involve field studies.

Model Process	Issue(s) identified	Current handling	Proposed alternative(s)	Implications	Degree of difficulty	Importance	Recommendation
Runoff Quality*	Need to estimate dissolved P concentration and hence P loss in runoff from effluent irrigation areas.	No attempt to model quality of runoff water. MEDLI will indicate any effluent-sourced P lost in runoff if the runoff is likely to contain effluent.	A relationship between soil solution P and soil Colwell-P and Phosphorus buffer index could be used to estimate runoff P concentration	Cannot be adopted immediately into MEDLI. This will need further development and testing against field data	Currently high, due to requirement of investigations and due to limited resources.	High. P loss in runoff is of greater concern than P leaching losses in most soils (with the exception of sandy soils)	Investigate need and develop a detailed case for dedicated resource(s) to: Field trials/data needed; Soil Chemist input needed
Denitrification*	No denitrification model has been validated against datasets. Models assume a potential denitrification rate for the soil (depends on soil pH etc) which can then be scaled back within the model according to soil water content (> DUL) and temperature and soil carbon. This potential value needs validation.	A first order kinetic equation between nitrate-N and denitrification per mass soil per day is assumed which is suitable for high strength effluents. The potential denitrification rate is defined by the user for the soil but uses 10%/day as default. This is scaled back according to soil water content (> DUL) and temperature and presence of labile soil carbon.	Approaches used in APSIM and DairyMod and others need to be reviewed in the light of data.	Cannot be adopted immediately into MEDLI.	Limited availability of datasets. Uncertainty of predictions from such an approach could be high (e.g., see Cook et al 2019; Wallach et al 1990).	High Denitrification is a poorly estimated in the nitrogen mass balance. It represents a possible legitimate sink for nitrogen during effluent irrigation.	Investigate need and develop a detailed case for dedicated resource(s) to: Field trials/data needed (see Beggs et al. 2011 for a good review and method); Soil Chemist input needed
Soil organic carbon specification	The current MEDLI suite of lab analysis only offers to measure OC in topsoil layer.		The need to specify the full thickness of organic carbon layer in the soil rather than just use the default value could be made more explicit?				

* From QWMN MEDLI Science Review Report by Phil Moody.

1. Background

MEDLI is a software tool that is used to design the application of wastewater by irrigation onto land for treatment by soil and plant processes. A recent review of the MEDLI model (Gardner, 2021) suggested that soil hydrology aspects of this model should be reviewed with regard to the underlying physics of water and solute transport. In particular, processes that should be looked at are the infiltration, redistribution and deep drainage of water and solutes in the soil profile.

2. Water transport

Water movement in soil at the pore scale is governed by the Navier-Stokes equation (Narsilio et al. 2009) but trying to use this in any practical application is difficult as we cannot measure all the properties and parameters required in any practical applications. This means that we have to use approximate macroscopic models. At the next scale up, we find that Darcy's law can describe the flow of water from centimetres to tens of metres. This "phenomenological law" was discovered by Darcy when considering water flow through sand filters. He found that the flow rate through the sand filter was proportional to the difference in hydraulic head. The proportionality constant is now called the saturated hydraulic conductivity (K_s (m s^{-1})) and the law has the form (for vertical flow):

$$J_w = K_s \frac{dh}{dz} \tag{1}$$

where

J_w is the rate of water flow (m s^{-1})

h is the hydraulic head (m)

z is the depth of the media (m).

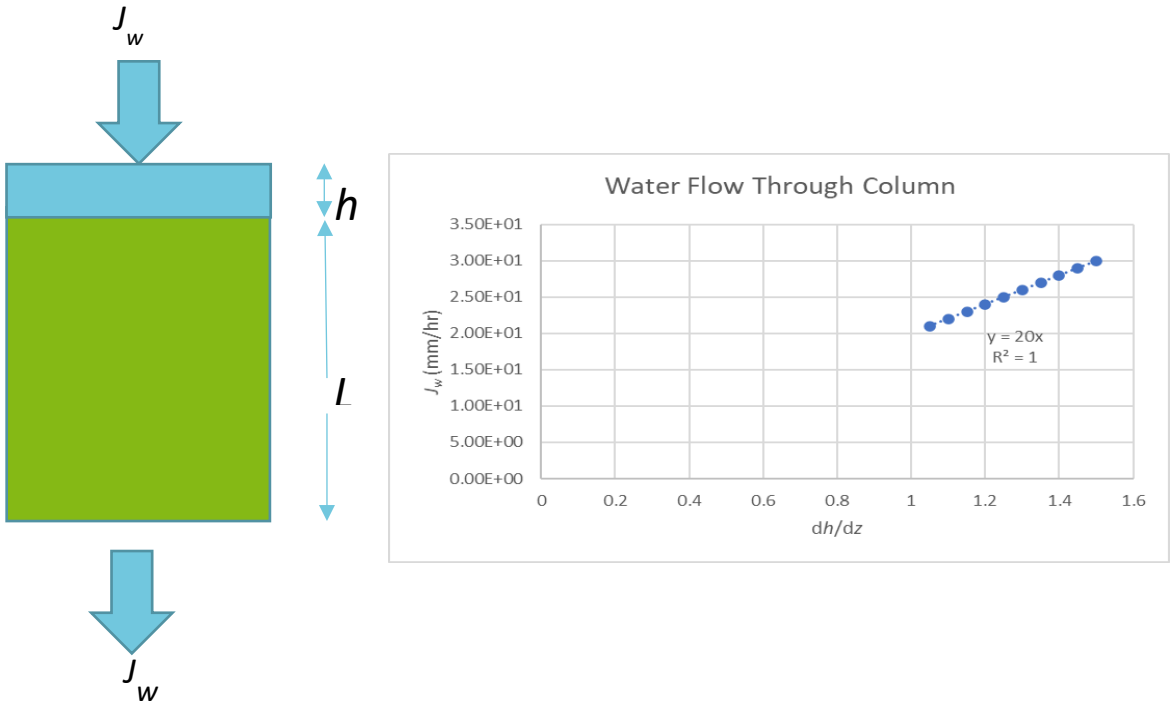

Figure 1. Simple diagram of a column of soil with a head of water on the surface and steady water flow J_w through it. If h is varied and J_w is plotted versus dh/dz = (h+L)/L, the slope of the resulting straight line gives the value of K_s, which in this case is 20 mm/h.

A schematic of steady state water flow through a column of soil is shown in Figure 1. This is similar to Darcy's sand beds.

When water flow through a media is not steady, we need to consider the law of conservation of mass. In Figure 2 a steady horizontal flux density, J_{in} (m s^{-1}), occurs into a small volume of soil of length Δx (m) and initially at a water content of θ at time t, and steady flux density out, J_{out}, over a small increment of time Δt (s). This will result in a change of water content in the volume of soil to $\theta+\Delta\theta$ at the end of Δt. By considering conservation of mass, the flow difference ($J_{in} - J_{out}$) $\Delta t = \Delta\theta\Delta x$. As the space and time steps are made smaller and smaller, we get the conservation equation:

$$\frac{dJ}{dx} = \frac{d\theta}{dt} \tag{2}$$

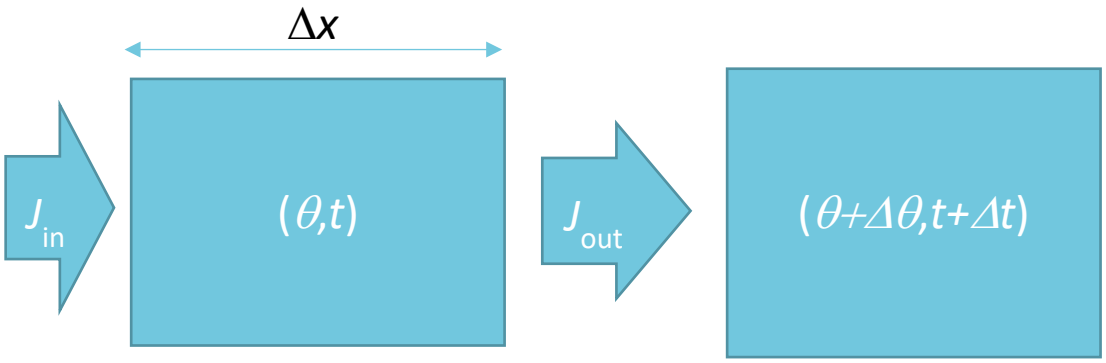

Figure 2. Schematic of horizontal water flow through an element of soil to describe the mass conservation concept.

Combining equations (1) and (2) results in an equation for water transport through soil which was first devised by Richardson (Richardson, 1922) and independently rediscovered by Richards (Richards, 1931). This can be written for horizontal flow as (Warrick, 2003):

$$\frac{\partial\theta}{\partial t} = \frac{\partial}{\partial x}\left(k(\theta)\frac{\partial\psi}{\partial x}\right) = \frac{\partial}{\partial x}\left(D(\theta)\frac{\partial\theta}{\partial x}\right) \tag{3}$$

where

θ is the volumetric water content (m^3 m^{-3})

t is time (s)

x is the horizontal distance (m)

ψ is the matric potential (potential energy per unit weight of water) (m)

k is the hydraulic conductivity (which is a strong function of θ) (m s^{-1})

D is the soil water diffusivity given by $D(\theta) = k(\theta)\frac{d\psi}{d\theta}$ (m^2 s^{-1})

Equation (3) describes the change in water content with time at any distance, x, due to the flux of water caused by the matric potential gradient ($\partial\psi / \partial x$) mediated by the hydraulic conductivity or water content gradient mediated by the diffusivity. The use of diffusivity in Eqn (3) results in an equation equivalent to Fick's Law, which states that the rate of transfer of water content in the direction x per unit time is due to the water content gradient ($\partial\theta / \partial x$), and a proportional parameter, the diffusivity. This makes Eqn (3) into a form that is equivalent to heat flow in solids. This allows the

many mathematical solutions that have been developed for heat flow to be adapted to describe water flow in soil.

To make Eqn (3) useful in a practical sense we need to provide initial and boundary conditions, so that this can be integrated to give the water content, θ, distributed in space (x) and time (t). It can also be solved numerically using models such as HYDRUS (Simunek, 2008) and SWIM (Verburg et al., 1996) but these require considerable amounts of soil hydraulic information, are time consuming, and require considerable computing power. Physicists have been exploring analytical solutions over 4 to 5 decades (Philip, Parlange, Gardner, Youngs, White, Knight, Raats, Clothier etc.) because the equation is analogous to heat transport in solids for which there are textbooks with analytical solutions (Carslaw and Jaeger, 1959).

When vertical flow is considered, a further term to account for the flow due to the unit gravitational potential unit gradient ($\partial k(\theta) / \partial z$) (s^{-1}) must be added to the right-hand side of Eqn (3) and the spatial coordinate changed from x to z (i.e. depth (m)). The vertical flow equation with a sink term (S_p) added for root water uptake by plants, is given below in Eqn (4).

Infiltration of water into soil was one of the first processes modelled, using the model of Green and Ampt (1911). This was developed before the discovery of Eqn (3). Since that time there have been major advances in modelling of infiltration, initially in the 1950s by Philip (summarised in Philip (1969)) and numerous other authors, and then a further advance in the 1970s by Parlange (1971) and Philip and Knight (1974). These models and the approaches taken will be discussed below and evaluated as to how MEDLI might be modified to incorporate some of the physical understanding gained from these studies.

Drainage is the other aspect of the water transport that will be considered in this report. This process commences following the infiltration of water into a soil profile and redistributes the water within the soil. Of particular interest to the MEDLI users is the water that passes beyond a *certain depth* and is then “lost” eventually to the groundwater. This *certain depth* is usually the depth below which soil water cannot be extracted by plant roots.

This extraction of water by plant roots is not considered in Eqn (3) and requires a sink term (S_p (s^{-1})) to be added to Eqn (3) and the spatial coordinate changed to vertical giving:

$$\frac{\partial \theta}{\partial t} = \frac{\partial}{\partial z}\left(k(\theta)\frac{\partial \psi}{\partial z} \right) + \frac{\partial k(\theta)}{\partial z} + S_p(t,z) \qquad (4)$$

This sink varies both in time, due the potential evapotranspiration (PET) and depth via a combination of soil matric potential and root length density. Thus, when we come to consider the drainage, we also need to consider how the sink term will affect this, as water uptake and redistribution can be simultaneous processes. Models for root water uptake at all scales have been reviewed by Feddes and Raats (2004).

In this report, we will divide the models on water transport into the following processes: infiltration, drainage, evaporation and transpiration. Most of these solutions have been developed for discrete events i.e., infiltration into soils with uniform properties with depth and uniform initial water content with depth, or drainage from an initially saturated soil profile. These have been very useful in advancing understanding of the driving forces and development of sound theory upon which to base predictions of soil water transport processes. But for more practical field situations where both the flow conditions and soil properties vary in space and time, numerical models have been developed that can cope with these variable boundary conditions. Such models use very fine space and time steps such that they closely approximate Eqn (4). Models such as SWIM (Verburg et al. 1996) and HYDRUS (Simunek et al. 2008) use this approach.

There are also models that use much simpler approximations of the space and time scales, often with fixed time steps of one day. These models usually have simplifications, such as that water only moves

downward in the soil and only when the soil is wetter than a certain value (field capacity or drained upper limit). Numerous examples of these water balance models such as SoilWat (Probert et al., 1988), Perfect (Littleboy et al., 1989), and EPIC (Steiner et al., 1987) exist. MEDLI is a model that is also based on this simplified approach.

These work by dividing the time and space into small increments and move the water in the space by transferring water according to rules based on Eqn (4), but often with considerable simplifications with fixed time steps.

In this report we will consider how understanding about water transport could be used to enhance some of the approximations used in MEDLI. These will need to be adapted so that they can be used in an approximate framework like MEDLI. They will also need to be well tested before inclusion in MEDLI, but this is beyond the scope of this report.

2.1. Infiltration

Infiltration is an important process as it determines how water from the atmosphere enters the terrestrial ecosystem to provide water for plant growth, runoff, and drainage to groundwater, which is a source of water for freshwater bodies such as rivers and lakes. It is a process of fundamental importance and has been researched in depth over the years.

Infiltration has a long history in soil physics with the earliest model being that of Green and Ampt (GA) (1911). This model has had a resurgence of interest following a publication by Mein and Larson (1973) who applied it to rainfall conditions rather than just surface ponded conditions. The fundamental features of the GA model are: the soil is divided into two sections by a sharp wetting front, which is defined by a fixed matric potential; above this wetting front the soil is saturated and below the wetting front the soil is at the initial water content (Figure 3). As originally written, the equation results in an implicit equation (see Eqn (7) below), which can only be solved using iterative methods such as Newton-Raphson (Ralston, 1965). However, this can be time consuming, so various authors have developed explicit equations that use different functions to overcome the implicit nature of the original equation. This is explained in more detail below in Section 2.1.3.

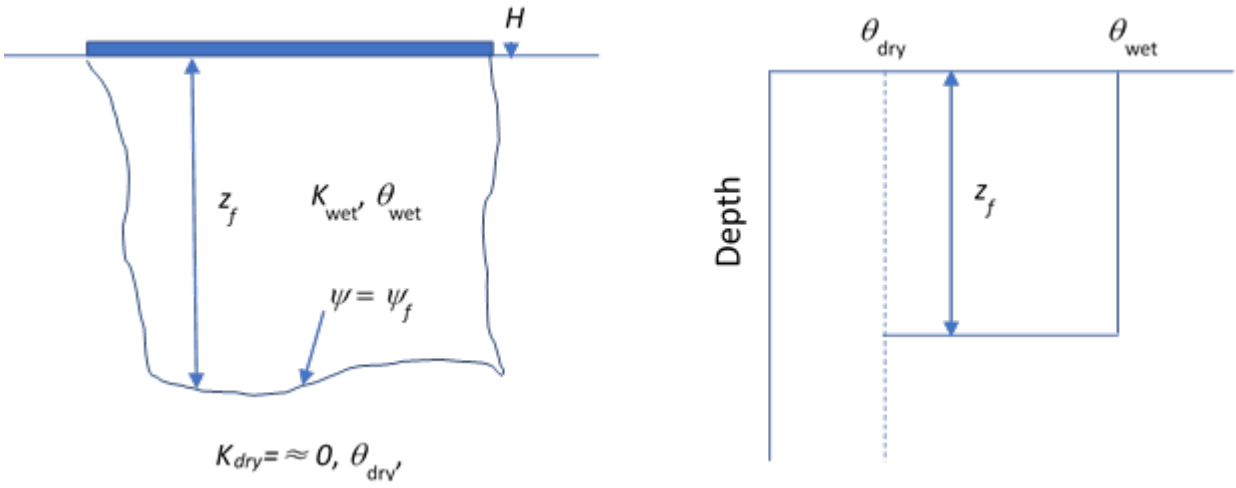

Figure 3.Schematic of Green and Ampt infiltration behaviour under ponded surface conditions with a head of water of H. The left-hand panel indicates infiltration into a dry soil with a water content of θ_{dry} and hydraulic conductivity ($K_{dry} \approx 0$). The wetting front is represented by the line has reached a depth of z_f and the wetting front potential is ψ_f. Behind the wetting from the water content is θ_{dwet} and hydraulic conductivity (K_{wet}) In the right-hand panel this is idealised as a square wave (or delta function) as is assumed in the Green and Ampt model.

Subsequently, Philip published extensively on the topic in the 1950s and 60s and summarised his understanding of infiltration in his landmark publication (Philip, 1969). The 1950s work resulted in the two-term algebraic infiltration equation (Philip, 1957), which is now commonly referred to as the Philip equation. This work also introduced the concept of sorptivity. A definition of sorptivity based on Philips' work is given by Minasny and Cook (2011). Sorptivity is what drives the infiltration of water into dry soil due to the capillarity. For horizontal infiltration, the cumulative infiltration, when plotted

against the square root of time, gives a straight line with the slope being the sorptivity value. This scaling with the square root of time occurs because as the wetting proceeds, the wetting front gets further and further away from the intake surface, and so the matric potential gradient at the intake surface gets less and less, such that the driving force diminishes, and the infiltration rate inexorably decreases. Typical infiltration curves with only sorptivity acting are shown in Figure 4.

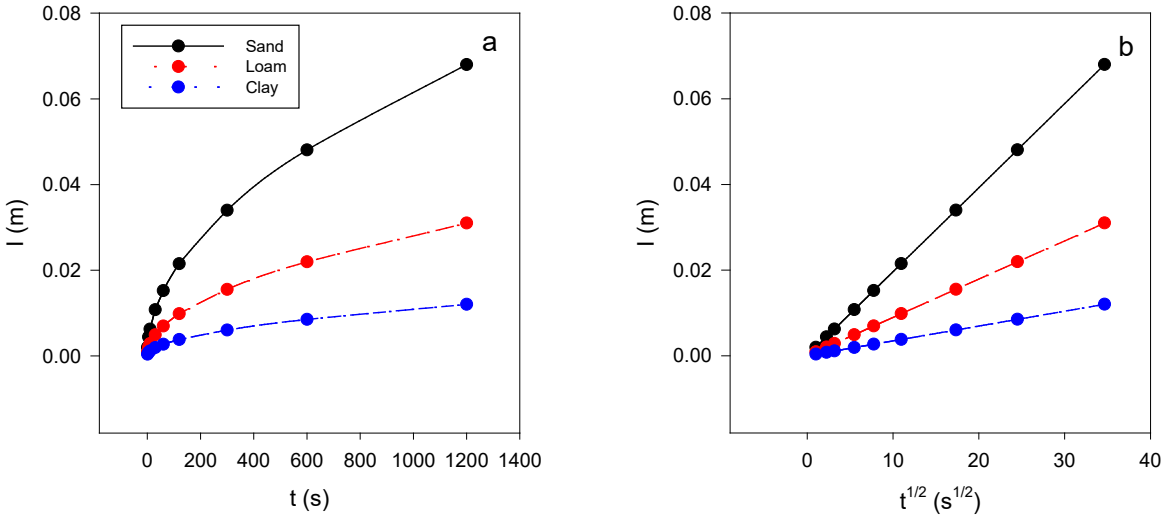

Figure 4. Calculated infiltration (I) into horizontal columns of sand, loam and clay with a) time (t) and b) the square root of time ($t^{1/2}$). The slope of the $t^{1/2}$ graphs is the Sorptivity value of the soil. Note that S also varies with antecedent soil moisture content.

When vertical infiltration occurs, the sorptivity dominates the initial rate of water intake into the soil, but as the wetting front moves deeper into the soil, the unit gravitational potential gradient becomes more dominant, and this results in a deviation from the square root of time behaviour towards a constant value of slope with time. At large times, the infiltration rate is equal to the saturated hydraulic conductivity. This is shown for a sand in Figure 5 where the infiltration rate (d*I*/d*t*) tends towards a straight line as elapsed time increases. The same data plotted against the square root of time shows an upward curvature. The insert in Figure 5b shows a straight line with the square root of time at small, elapsed times when sorptivity still dominates the flow process.

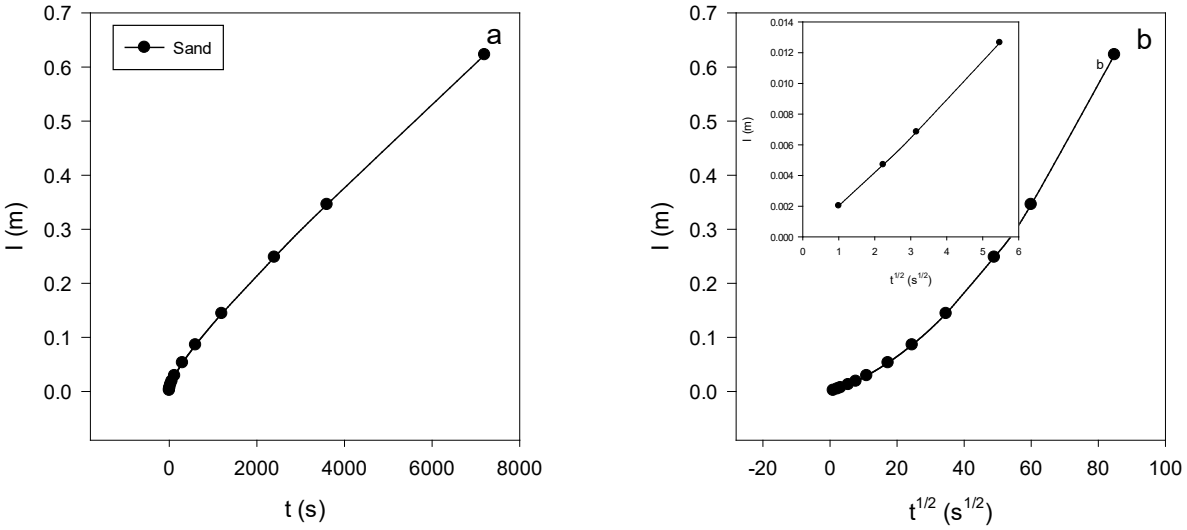

Figure 5. Cumulative infiltration (I) into a sand a) with time (t), and b) with square root of time ($t^{1/2}$). The insert is for time less than 36 s.

This led to the Philip two-term infiltration equation (Philip, 1957) but this was only suitable for ponded infiltration, and then only for early to moderate elapsed infiltration times. Philip (1987) published an

extension to this model that allowed it to be applied to longer times by joining a long-time steady-state flow model to it. This will be described in more detail below in Section 2.1.3.3.

Philip (1969) showed that the Green and Ampt model is a delta function solution. This means that at a specified water content value (in this case the saturated water content) the value of the diffusivity shows very small values with all water content except at saturation, where it shows a very large value. This behaviour can be described by a Dirac delta function. The integral of the diffusivity with water content for a delta function is 1. For the Green and Ampt model, the sharp wetting front is an example of delta function behaviour. Philip (1969) also presented solutions for a linearised diffusivity where its value is constant over the water content range of interest. These two types of solutions provide bounds to the likely soil water infiltration behaviour. However, the linearized solution is poor at estimating the water content distribution due to the assumption of constant diffusivity.

A summary of solutions up to 1969 is given in Philip (1969). In the 1970s, the *flux concentration* idea was introduced by Parlange (1971) and improved by Philip and Knight (Knight and Philip, 1973; Philip and Knight, 1974). White and co-workers (White and Sully 1987; Broadbridge et al. 1988; Broadbridge and White 1987; Broadbridge and White 1988; White and Broadbridge 1988) then used these methods to reduce the number of parameters down to one factor they called *C*, which ranges from 1 for Green and Ampt soils, to ∞ for soils based on Burger's equation (Raats, 2001). These solutions have been used to develop numerical models that solve Eqn (4) (Dawes and Short, 1993; Short et al. 1995). The time to ponding concept developed from these methods is particularly useful and will be introduced in Section 2.1.4 below.

During infiltration, runoff can occur due to one of two possible limits being reached. The first of these limits is the *infiltration rate limit*. During infiltration, the potential infiltration rate (i (m s^{-1})) decreases with time towards the saturated hydraulic conductivity of the soil. If the surface flux density (R (m s^{-1})) (either rainfall rate or irrigation rate) is greater than the potential infiltration rate then water will accumulate on the soil surface after some time, t_p (the time to ponding), and the excess water will runoff. This process is illustrated in Figure 6a.

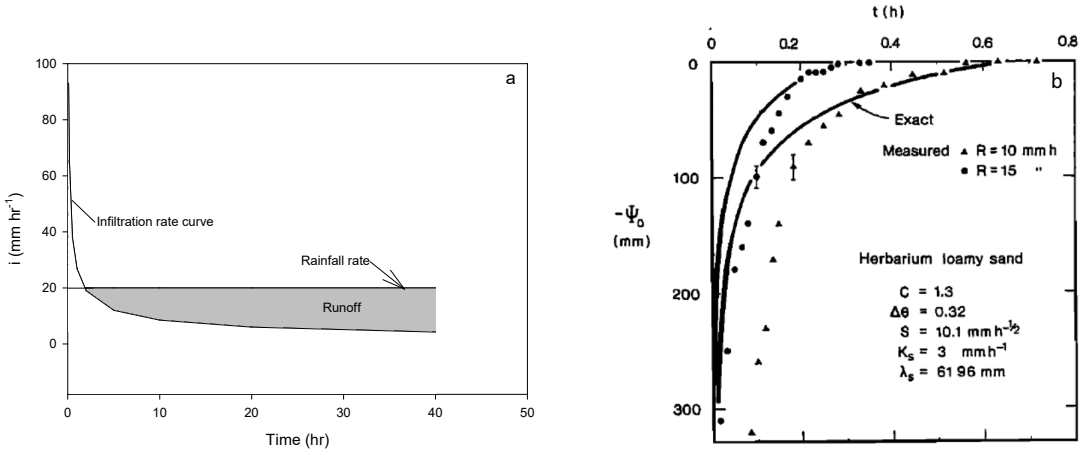

Figure 6. Illustration of a) potential infiltration and rainfall rate showing when ponding would occur and runoff rate (grey area) and b) example from White and Broadbridge (1988) of the surface matric potential during infiltration at two different rainfall rates.

An example from White and Broadbridge (1988) of the change in surface matric potential with time during constant rainfall shows that the time at which ponding occurs increases from about 0.3 hr to 0.7 hr as the rainfall rate decreased from 15 to 10 mm hr^{-1} (Figure 6b).

The second way runoff can be generated is due to the *storage limit* of the soil being exceeded. This can occur if there is a shallow water table or a shallow layer that impedes the water flow through the soil. At the start of infiltration for such a soil, the amount of storage capacity (I_c (m)) is the difference between initial water content of the soil and the saturated water content summed over the depth of soil to the water table or the impeding layer. If the cumulative infiltration at some time ($I(t^*)$ (m)) equals I_c then no further infiltration into the soil can occur, and all further application of water to the soil surface will result in this water becoming runoff. This is often termed saturation overland flow in

hydrology. The example in Figure 7 (from Salvucci and Entekhabi 1995) is for ponded infiltration but shows how the soil water storage is filled up as the wetting front advances into the soil until all the storage has been filled.

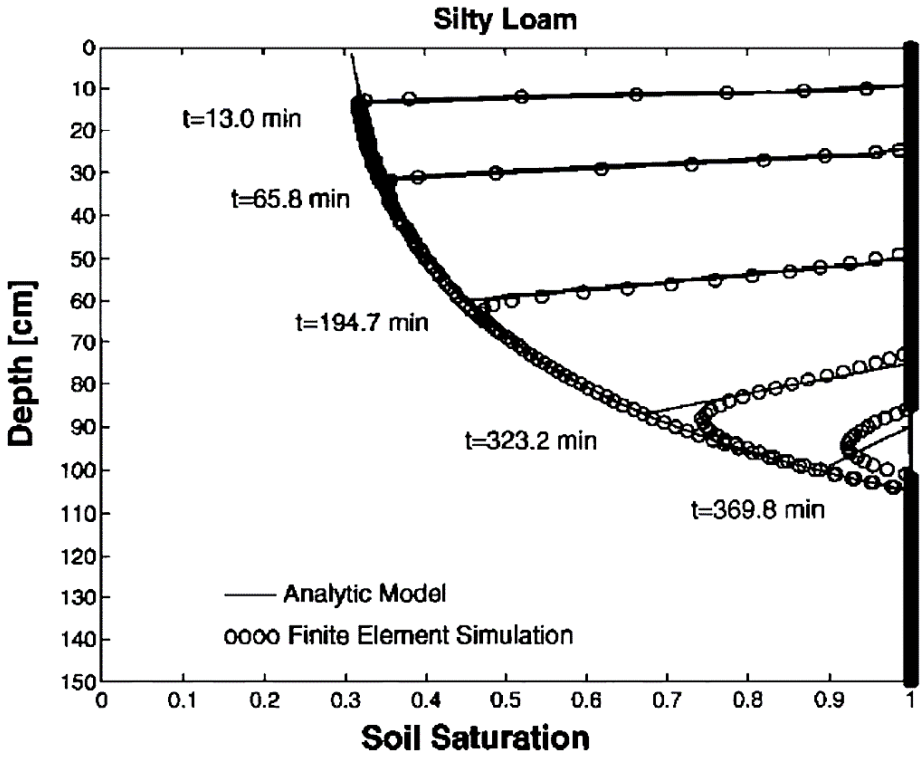

Figure 7. An example taken from Salvucci and Entekhabi (1995, Figure 3) of infiltration into a silty loam soil with a water table at a depth of 150 cm. There is saturated soil to approximately 100 cm depth due to capillary rise from the water table. This shows the soil progressively wetting to saturation (soil saturation = 1) and no further infiltration can occur sometime after 369.8 minutes, when the wetting front joins up with the saturated soil.

In both these cases, the flow regime into the soil will change from being flux controlled - the rate of infiltration is controlled by the flux to the soil surface, to being concentration controlled as the surface water content reaches saturation. Analytical solutions have been developed for flux-controlled flow regimes (absorption solutions) and for concentration-controlled flow regimes (ponded solutions). However, solutions for a mixed boundary condition where the surface boundary condition changes from flux to concentration controlled are problematic, and as will be discussed below, the *time-compression-analysis* is one way to allow concentration-controlled solutions to be used for mixed boundary conditions.

2.1.1. Macro-pores, Layering and Uneven Wetting

Analytical models for infiltration assume that water flows evenly through the soil, has a well-defined wetting front, and the surface boundary is uniform (i.e., does not vary with space). When flux is occurring, and the surface soil is unsaturated, these assumptions are generally true (Clothier and Heiler 1983). However, when the soil surface undergoes ponding, water can enter macropores (such as cracks and wormholes) and the distribution can vary with a proportion of the water moving to greater depth than the infiltration model(s) would otherwise predict (Germann and Beven 1985; Germann and Beven 1986). These macropores do not have an effect on the distribution of water in the soil when the soil surface is less than saturation (Clothier and Heiler 1983). However, when water ponds on the surface, this “free” water (potential greater than zero) can enter the macropores and flow down them as well as laterally into the soil (Figure 8). This results in an uneven wetting front and can result in water and solutes being transferred beyond the rooting depth of plants. This “bypass flow” is undesirable as it can result in greater nutrient losses from the root zone to the groundwater (Prendergast, 1995).

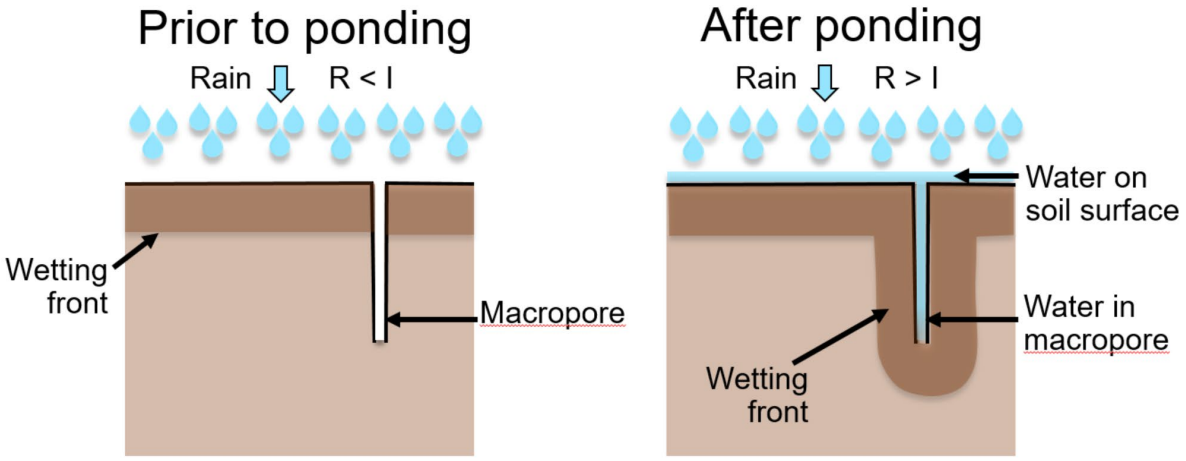

Figure 8. Schematic of effect of macropores of water flow in soil during infiltration. The left-hand panel shows infiltration with the rainfall rate, R, less than the potential infiltration rate, I, and no flow through the macropore. The right-hand panel shows infiltration with R > I and water ponded on the soil surface and entering the macropore which results in an uneven wetting front.

When ponding occurs on the surface, the distribution in ponded depth due to surface micro-topography can also result in very uneven water distribution in the soil (Cook 1983). These effects can occur when applying wastewater with sprinkler irrigation, and hence surface ponding should be avoided if possible (Cook 1988).

Layering in the soil can also result in uneven wetting. When water moving through a coarse textured soil layer meets the boundary of a deeper soil layer of finer texture with a saturated hydraulic conductivity lower than the flux occurring in the coarse textured soil, then ponding can occur at the boundary. This can result in water flow into macro-pores and uneven distribution. The opposite can also occur when flow through finer textured soil overlays a coarser textured layer and wetting front instabilities can occur, which leads to fingering, which is flow occurring down wet fingers separated by dry soil (Du et al. 2001; Yao and Hendrickx 2001; Parlange and Hill, 1976). Fine texture over coarse texture also results in a transient perched water table that can result in a higher plant available water content in the finer soil (Clothier et al., 1977), a technique used in the design of golf greens.

While these issues need to be considered when planning a wastewater irrigation system, they are of second-order importance especially if the irrigation system is designed to avoid ponding. The issues of variation in the flow due to larger pores and the distribution of pores will be discussed in more detail when considering solute transport in Section 3.

2.1.2. Scale and Uncertainty

The issue of scale is of practical concern as soil physics theory and measurement have been based at volume scales of cm^3 to m^3 (Raats, 2001). This limitation is partially due to instrumentation that only measures a limited volume of soil in the range of cm^3. This is still the case today except for the recent development of the cosmic neutron probe (Franz et al. 2012; 2013), which measures water content over approximately a 40 ha area to a depth that varies with water content.

For practical purposes we still use and assume that the Richards equation can be applied at scales of greater than tens of m^3 although Addiscot (1995) argued that Darcy's Law was only applicable up to soil areas of about 10 m^2. However, the Richards equation has really transformed into a transfer-function model, as the hydraulic conductivity and the water potential gradient will be an ensemble of the point scale values.[1]

[1] The ensemble value is the average value we get when we calculate flow at the point scale using many (usually thousands) of different values of the soil properties. To do this, usually Markov chain

This means that when using point scale models (discussed below), the use of a single valued average implies that 50% of the area is likely to have physical parameter values greater than, and 50% less than the flux, and hence water content distribution. This then raises the question: is this good enough for predictive purposes and what probability should be considered appropriate?

When using point scale models for wastewater, we contend their acceptability depends on the environmental hazard created by substances in the wastewater. For relatively benign substances, the mean probability of runoff and drainage may be acceptable. But for hazardous wastes, a much lower probability should be considered.

2.1.3. Specific Infiltration Models

2.1.3.1 Green and Ampt

The Green and Ampt infiltration as originally derived for ponded conditions is given by

(Bouwer, 1978):

$$i(t) = K_s\left[1 + \frac{H + \psi_f}{z_f(t)}\right] \tag{5}$$

where

$i(t)$ is the infiltration rate (volume per unit area) at time t (m s^{-1})

K_s is the saturated hydraulic conductivity (m s^{-1})

H is the ponded head of water on the soil surface (m)

ψ_f is the wetting front matric water potential (m)

z_f is the wetting front depth at time t (m)

These concepts were shown schematically in Figure 3.

The z_f can be replaced in Eqn (5) by the ratio of the cumulative infiltration $I(t)$ (m) and the change in water content $\Delta\theta = \theta_{wet} - \theta_{dry}$ to give:

$$i(t) = K_s\left[1 + \frac{\Delta\theta\left(H + \psi_f\right)}{I(t)}\right] \tag{6}$$

For constant H, $i(t) = dI(t)/dt$ which leads to the well know **implicit** equation:

$$I(t) = K_s t + \Delta\theta\left(H + \psi_f\right)\ln\left[1 + \frac{I(t)}{\Delta\theta(H + \psi_f)}\right] \tag{7}$$

The reason this is called an implicit equation is that $I(t)$ appears in both sides of the equation (7), so a simple algebraic solution is not possible and can only be solved using iterative methods. Mein and Larson (1973) showed that Eqn (7) could be used to describe infiltration under rainfall by calculating

---

Monte Carlo (MCME) methods are used (Beven and Freer, 2001), which are computationally intensive and time consuming.

the elapsed time when ponding occurred on the soil surface. The infiltration of water into a soil where ponding occurs during infiltration is shown in Figure 9.

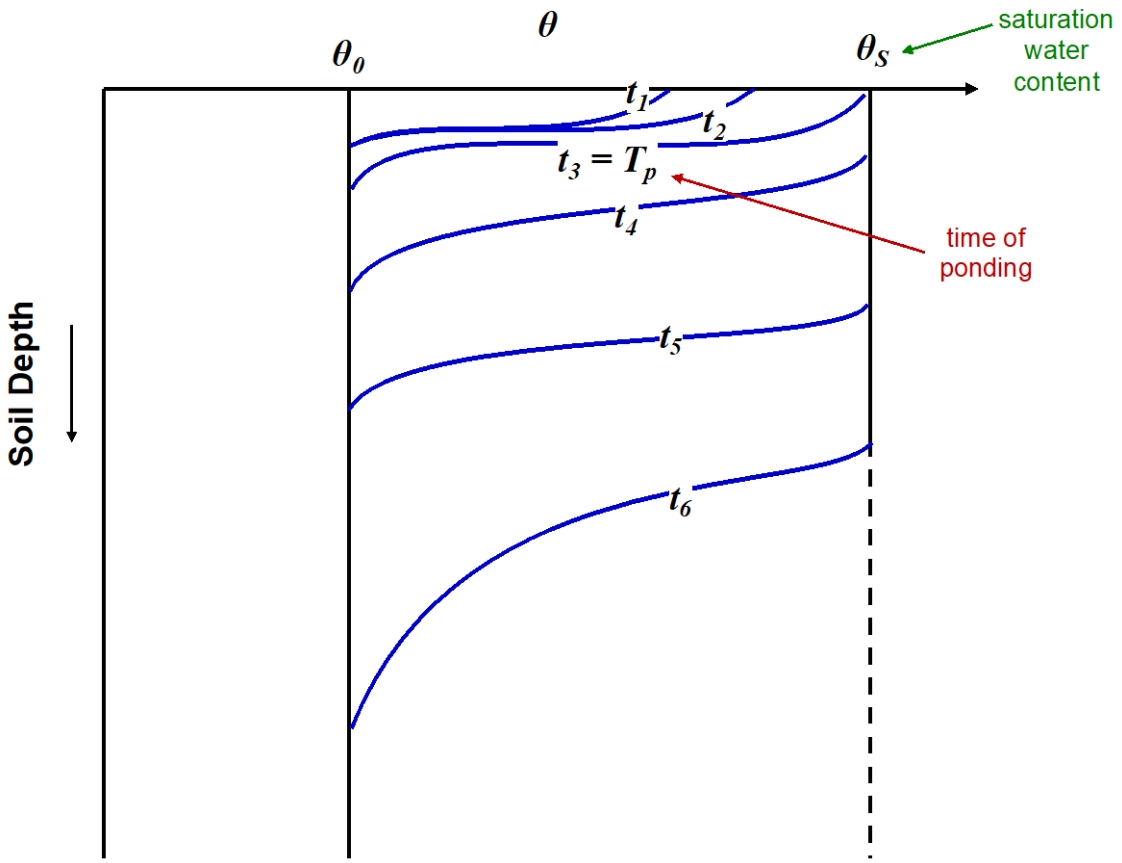

Figure 9. Schematic diagram of water content (θ) increasing with depth as wetting occurs during rainfall. In this figure the rainfall rate is such that at time t_3 the water content at the soil surface reaches the saturation. This is the time to ponding (T_p). After ponding the water content at the surface remains at saturation as the wetting front moves down into the soil with saturated soil occurring behind the wetting front.

Prior to the ponding, the infiltration rate equals the rainfall rate, and after ponding, infiltration is described by Eqn (7). Mein and Larson's seminal publication has led to an increased interest in the Green-Ampt (GA) approach for modelling infiltration in hydrology models.

This has resulted in various authors developing **explicit** methods that approximate Eqn (7) and transform Eqn (7) into an algebraic equation that is amenable to solution. Ali et al. (2016) evaluated these methods and found that the explicit solution proposed by Barry et al. (1995, 2005) was the solution that was the most accurate comparison with Eqn (7) and is given by:

$$I(t) = \frac{S^2}{2K_s}\left\{-1-\left[\frac{t^* + \ln\left(1+t^*+A\right)}{\left(1+t^*+A\right)^{-1}-1}\right]\right\},$$

$$A = \frac{6\sqrt{2t^*}}{6+\sqrt{2t^*}}, \quad (8)$$

$$t^* = \frac{2K_s^2 t}{S^2}$$

where

t^* is dimensionless time

A is a dimensionless time parameter

S is the sorptivity (m $s^{-1/2}$) and for a GA (delta function) soil is given by (Parlange 1975, Neuman, 1976):

$$S^2 = 2\Delta\theta K_s\left(H+\psi_f\right) \quad (9)$$

The value of the wetting front potential can be obtained from the Brooks and Corey (1964; 1966) moisture retention parameters, as described by Gowdish and Munoz-Carpena, (2009):

$$\psi_f = \psi_b \frac{2+3\lambda}{1+3\lambda} \quad (10)$$

where

ψ_b is the air entry water potential (m)

λ is the pore size distribution parameter.

The value of ψ_f for most soils falls in the range of -0.10 to -0.5 m. The relationship between water content and matric potential (termed the moisture characteristic) is illustrated in Figure 10, where ψ_b is the soil suction (*aka* matric potential) when a saturated soil will first start to drain as air enters the soil, and λ is the slope of the linear $\log(\theta)$ and $\log(\psi)$ relationship. This relationship is known as the Brooks and Corey model and is described in its simplest form as:

$$\psi(\theta) = \psi_b\left(\frac{\theta}{\theta_s}\right)^{-\lambda} \quad (11)$$

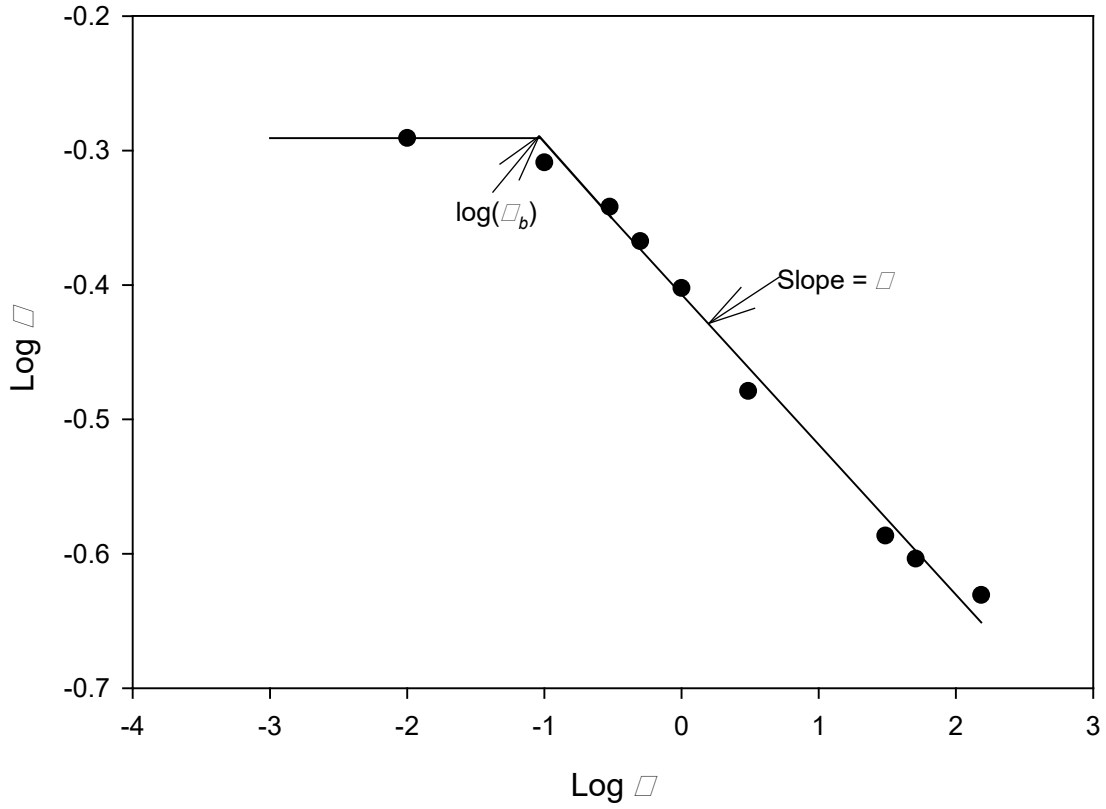

Figure 10. The soil moisture characteristic of a sandy soil where the log volumetric moisture content (θ) is plotted against the matric potential (units of m) using a log scale. The soil suction when the saturated soil first starts to drain (the air entry potential or bubbling pressure) and the slope of line define Ψ_b and λ respectively of the Brooks & Corey equation.

The infiltration rate is determined using $I(t)$ from Eqn (8) and substituting Eqn (9) into Eqn (6) to give (Ali et al., 2016):

$$i(t) = K_s\left[1+\frac{S^2}{2K_s^2 I(t)}\right] \tag{12}$$

The depth of the wetting front is then easily calculated as $z_f(t) = \frac{I(t)}{\Delta\theta}$.

The GA equations discussed above are for soils uniform in both the water content difference profile ($\Delta\theta$) with depth, and the constant soil hydraulic conductivity with depth. Bouwer (1969) developed methods to alleviate these restrictions on the use of the GA method. To use his method, it is easier to use the explicit solution (Eqn (7)), and a description of the Bouwer (1969) methodology and a solution method for a box model[2] like MEDLI is given in Appendix 1.

[2] A box model is where the spatial domain is split into boxes of discrete lengths and the flow between these boxes for a given time step is described by simplified approximations of the actual flows. The difference between water flow into the box and out of the box in the time step allow the change in the water content to be calculated. This then gives the new value of the state variable (i.e. water content) at the end of the time step.

2.1.3.2 Linear Soil

For describing heat conduction in solids, the diffusivity is usually constant, or approximately constant, with temperature. Philip (1966, 1969) used this assumption to develop the linear soil solution for infiltration.

A linear soil is assumed to have a constant diffusivity ($D_* = \pi S^2 / \left(4\Delta\theta^2\right)$) and a constant slope of the K - θ characteristic $\kappa = dK(\theta)/d\theta = (K_{wet} - K_{dry})/\Delta\theta$ for the range of $\Delta\theta$. This approximation can be used as the conductivity (K) is a function of the water content with a positive slope and $d\psi / d\theta$ is a function with a negative slope (see Figure 10).

The cumulative infiltration for ponded conditions is then given by (Philip, 1969):

$$I(t) = \frac{\pi S^2}{2\Delta K}\left\{\sqrt{\frac{T}{\pi}}.\exp(-T) + \frac{1}{2}\operatorname{erf}\left(\sqrt{T}\right) - T.\operatorname{erfc}\left(\sqrt{T}\right)\right\}$$
$$T = \frac{\kappa^2 t}{4D_*} = \frac{(\Delta K)^2 t}{\pi S^2} \qquad (13)$$

where

$$\Delta K = (K_{wet} - K_{dry})/\Delta\theta$$

erf(x) is the error function

erfc(x) = 1 – erf(x) is the complimentary error function

The water content profile can be obtained using (Philip, 1969):

$$\theta(z,t) = \theta_{dry} + \frac{\Delta\theta}{2}\left\{\operatorname{erfc}\left[\frac{z-\kappa t}{2\sqrt{D_* t}}\right] + \exp\left(\frac{\kappa z}{D_*}\right)\operatorname{erfc}\left[\frac{z+\kappa t}{2\sqrt{D_* t}}\right]\right\} \qquad (14)$$

A comparison of water content profiles at three selected times for the GA and linear soil infiltration models are shown in Figure 11. This clearly shows the enhanced dispersion of the water content profile predicted for the linear soil. However, neither the GA nor the linear infiltration equations give the true water content profiles (z,t), which will lay somewhere between these two extremes.

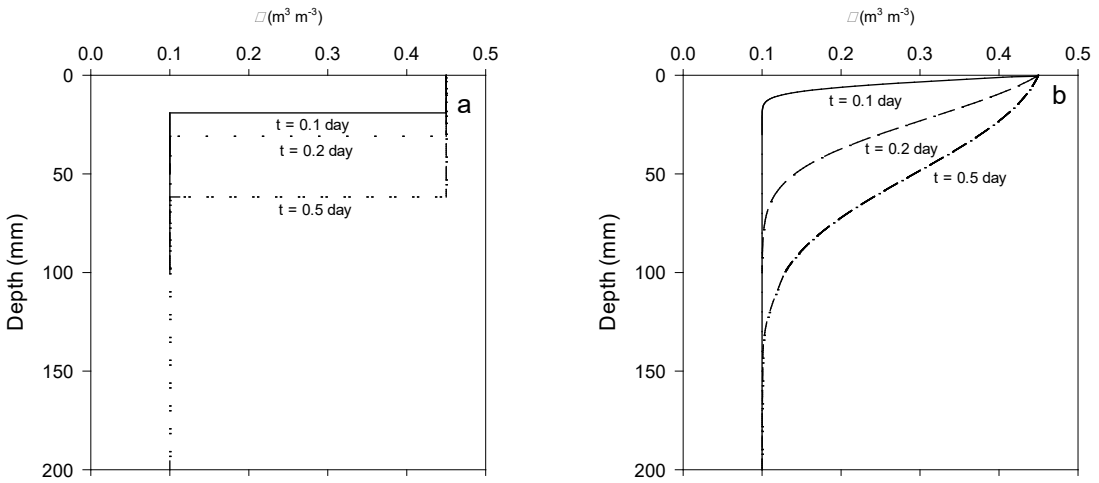

Figure 11. Comparison of water content with depth for ponded infiltration into a clay soil using: a) Green and Ampt model, Eqn (8) and b) linear model based on Philips equation, Eqn (14) (soil hydraulic properties were taken from Salvucci and Entekhabi (1994) and given in Table A1.

2.1.3.3 Philip two-term infiltration model

The Philip two-term algebraic infiltration model (Philip, 1957) is only applicable during the early to medium time period of infiltration. This was overcome by coupling a long-time solution infiltration equation to the two-term equation (Philip, 1987). This results in a ponded infiltration model that can be used for the whole time period, and is given by Cook et al. (2008):

$$
\begin{aligned}
I(t) &= St^{1/2} + 0.36K_s t, \quad 0 < t \le t_g \\
I(t) &= St_g^{1/2} + K_s\left[t - t_g\left(1 - 0.36\right)\right], \qquad t > t_g \\
t_g &= \left(\frac{S}{(1-0.36)K_s}\right)^2
\end{aligned}
\tag{15}
$$

The value t_g, the gravity time, is the time at which gravity becomes the dominant force driving the infiltration of the water into the soil.

The constant 0.36 in Eqn (15) is for a soil with Burger's equation properties, which is close to the properties exhibited by real soils. More information on Burger's equation is given in Knight (1973).

This equation does not provide a solution for the water content profile, but a square wave solution similar to that of the GA model, which would fit well with the box model spatial discretisation as used in the MEDLI model, can be calculated.

Eqn (15) describes ponded infiltration, and hence is only applicable **after** ponding occurs for rainfall infiltration. The time compression analysis given below can be used with Eqn (15) to adjust the time at which infiltration calculated with Eqn (15) occurs. The method used for nonuniform initial water content profiles and non-uniform soil properties given in Appendix 1 are also applicable to Eqn (15).

However, the Green and Ampt soil is more amenable to being included in the MEDLI model and has been shown widely to give good estimates of the infiltration of water into soil. Thus, I suggest that the Green and Ampt model be adopted for use in MEDLI. The GA model as given in Section 2.1.3.1 is for ponded infiltration into a soil with uniform initial water content and soil properties. Its adaption for rainfall rates where the initial infiltration will be flux controlled using the time-compression analysis is

given below in Section 2.1.4, and adaption for nonuniform initial water content and soil properties is given in Appendix 1.

2.1.4. Time to Ponding and Time Compression Analysis

During rainfall and sprinkler irrigation, the soil surface will remain unsaturated if the **average** rate of application, R (m s^{-1}), is less than the potential infiltration rate, i_{pot} (m s^{-1}). If $R > i_{pot}$ the soil surface will become saturated at some elapsed infiltration time t_p, which will depend on the ratio of R/K_s. White et al. (1989) showed the following equation was able to determine the **time to ponding** for exact solutions, as well as for experimental data:

$$\begin{aligned} \bar{R}_p t_p &= M\left[\frac{S^2(\theta_{dry})}{K_s}\right]\ln\left[\frac{R(t_p)}{R(t_p)-K_s}\right] = I_p(t_p) \\ t_p &= \frac{M}{\bar{R}_p}\left[\frac{S^2(\theta_{dry})}{K_s}\right]\ln\left[\frac{R(t_p)}{R(t_p)-K_s}\right] \end{aligned} \tag{16}$$

where

$\bar{R}_p = t_p^{-1}\int_0^{t_p} R(t)dt$ is the **average** water application = surface flux (m s^{-1}) up to the time of ponding

$R(t)$ is the variable water application rate (=surface flux) with time (m s^{-1})

M is a soil specific property, which White and Broadbridge (1988) suggested range from 0.5 to 0.66

$S(\theta_{dry})$ is the sorptivity of the dry soil (m s$^{-1/2}$)

t_p (s) is the time of surface ponding

$R(t_p)$ is the surface flux into the soil at t_p (m s^{-1})

I_p is the cumulative infiltration up to t_p (m)

White and Broadbridge (1988) suggested that a value of M = 0.55 was consistent with measurements and this has been widely adopted in solutions of water flow including measurements using disc permeameters (Cook and Broeren, 1994).

For a Green and Ampt soil, Broadbridge and White (1987) showed that t_p in Eqn (16) can be simplified to the Mein and Larson (1973) version of the Green and Ampt equation:

$$t_p = S^2/\left[2R(R-K_s)\right] \tag{17}$$

for constant surface flux R. However, Broadbridge and White (1987) found this considerably overestimated t_p when R and hence i_{pot} approached K_s. An example is given in Figure 12 for a soil with clay soil properties (Table A1 in Appendix 2) and shows the comparison of t_p calculated with Eqns (16) and (17). This shows that as R approaches K_s the value of t_p from Eqn (17) becomes large and diverges markedly from that calculated with Eqn (16) with M = 0.55. This was noted in Broadbridge and White (1987) who advised that the Green-Ampt solution substantially overestimates t_p as R/Ks approaches 1.

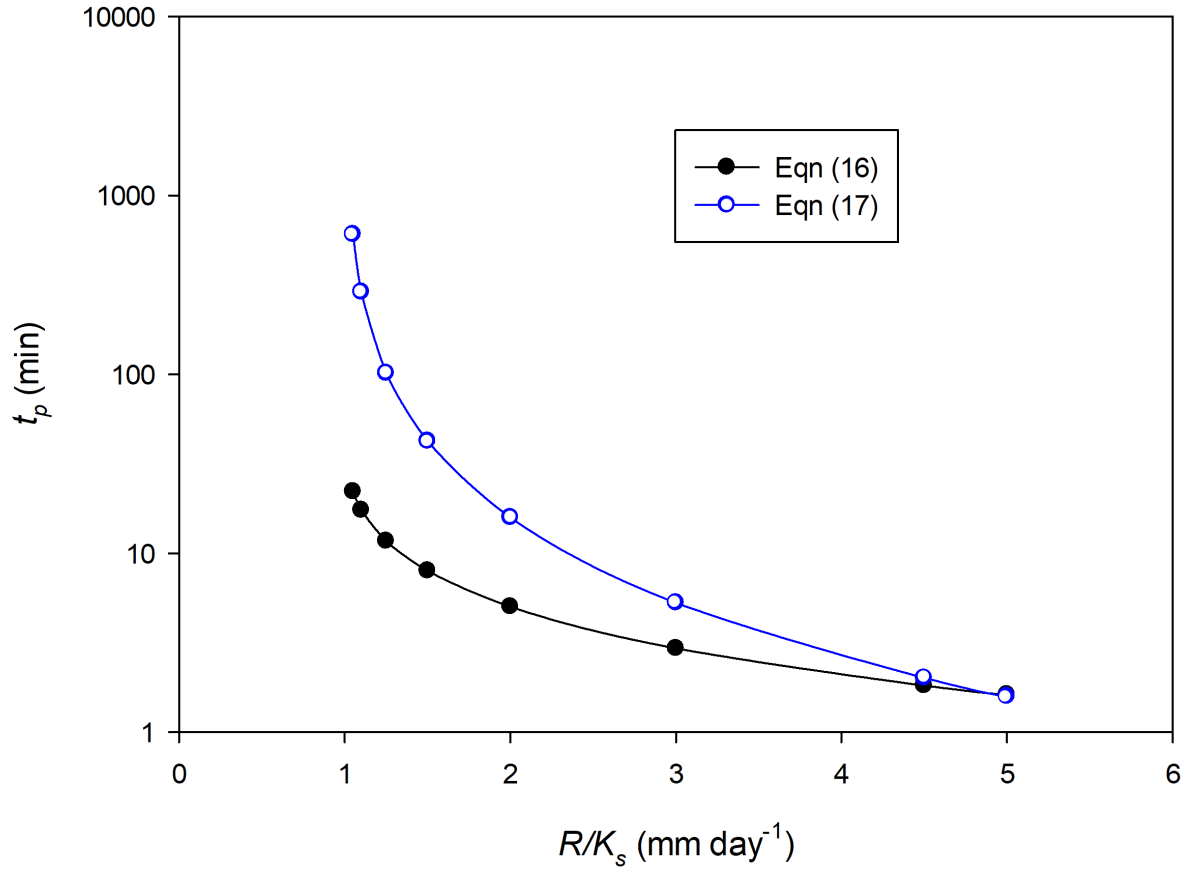

Figure 12. Comparison of time to ponding for various infiltration solutions (Eqns 16 and 17) for a sandy loam soil (Table A1). t_p is plotted on a log scale due to the large range in values at low R.

Accepting that Eqn (16) gives the more realistic value of t_p allows the use of the time-compression analysis (TCA) of Salvucci and Entekhabi (1994) with a small variation for the cumulative infiltration, which is given below.

For the TCA analysis, the surface flux at t_p ($R(t_p)$) is matched to the infiltration rate from Eqn (12) to get the time parameter (t_c) (Figure 13). The value of t_c is the time at which the GA model gives an infiltration rate $i(t_c)$ equal to the surface flux ($R(t_p)$) at t_p. This can be achieved using recursive methods such as Newton-Raphson (Ralston, 1965). The cumulative infiltration $I(t_c)$ calculated with Eqn (8) will be equal to the actual cumulative infiltration Rt_p, so $t_p = I(t_c)/R$. The cumulative infiltration and infiltration rate can then be calculated with Eqns (8) and (12) respectively, but with an adjusted time (t') given by $t' = t - (t_p - t_c)$.

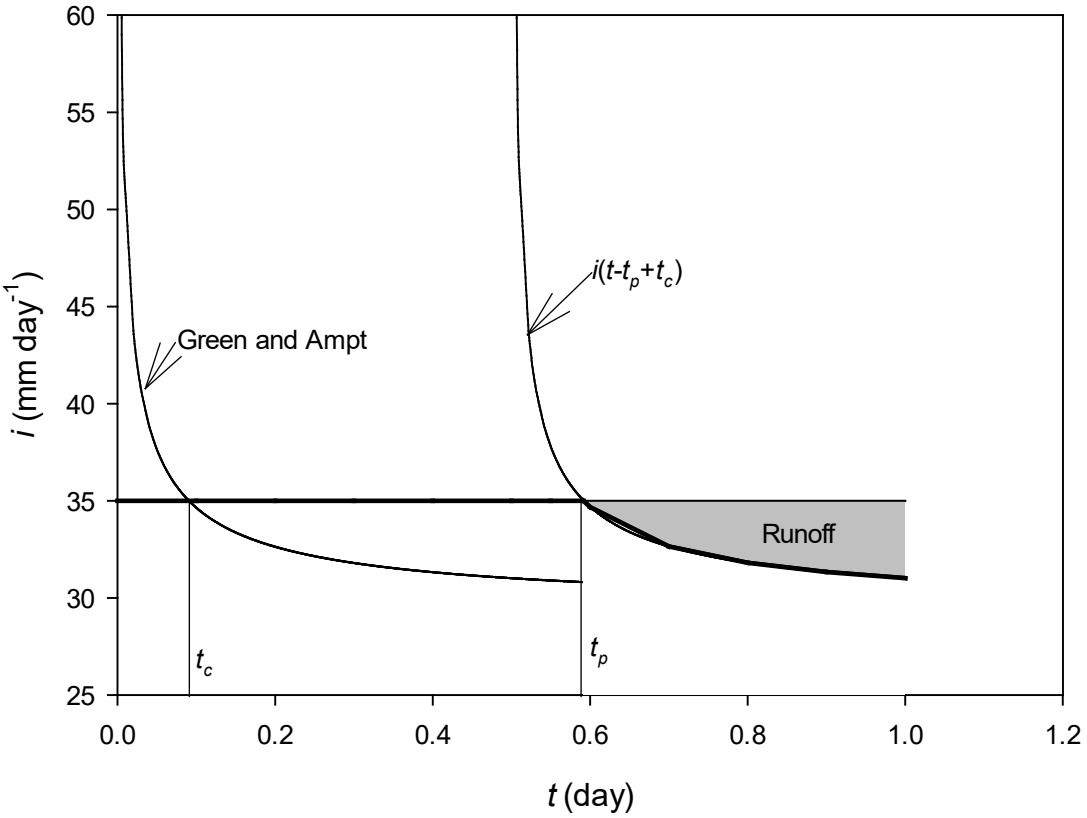

Figure 13. Illustration of the time compression analysis method (TCA) using the same data as in Figure 12 with a value of R = 35 mm day^{-1}. This shows that the matching of the fluxes (GA vs real world behaviour) occurred at t_c = 0.090 day. Solving Eqn (16) gives the value of t_p = 0.59 day. The heavy dark line shows the actual infiltration and the difference between the actual infiltration rate and the steady rainfall rate R is the runoff rate. The shaded area is the cumulative runoff.

We then shift the infiltration rate curve so that $i(t_c)$ from Eqn (12) now matches R at t_p by adjusting the time so that the infiltration rate is now given by:

$$\begin{aligned} i(t) &= R(t), && t \le t_p \\ i(t-(t_p-t_c)) &= K_s\left[1+\frac{S^2}{2K_s^2 I(t)}\right], && t > t_p \end{aligned} \tag{18}$$

The cumulative infiltration ($I(t)$) will be given by:

$$I(t) = \int_0^t R(t)\,dt, \qquad t < t_p$$

$$I(t_p) = \int_0^{t_p} R(t)\,dt = \bar{R}.t_p, \qquad t = t_p$$

$$I(t) = I_{GA}\left(t - (t_p - t_c)\right) = \frac{S^2}{2K_s}\left\{-1 - \left[\frac{t^* + \ln\left(1 + t^* + A\right)}{\left(1 + t^* + A\right)^{-1} - 1}\right]\right\}, \quad t > t_p \qquad (19)$$

$$t^* = \frac{2K_s^2\left(t - (t_p - t_c)\right)}{S^2}$$

$$A = \frac{6\sqrt{2t^*}}{6 + \sqrt{2t^*}}$$

where I_{GA} is the cumulative infiltration calculated with Eqn (8) (m).

The methods described here will require the rainfall input to be at a time step of less than 1 day.

An example of using the TCA analysis on a sandy loam soil (hydraulic properties are given in Table A1) is presented in Figure 14. This shows the change in the infiltration rate and the shifting of the curve so that the rate matches at t_p (Figure 14a) and the cumulative infiltration compared to the cumulative surface flux (Figure 14b). The difference between the cumulative surface flux (cumulative rainfall) and the cumulative infiltration is the runoff. By 20 minutes, the cumulative runoff has reached 10.6 mm (20.8 -10.2).

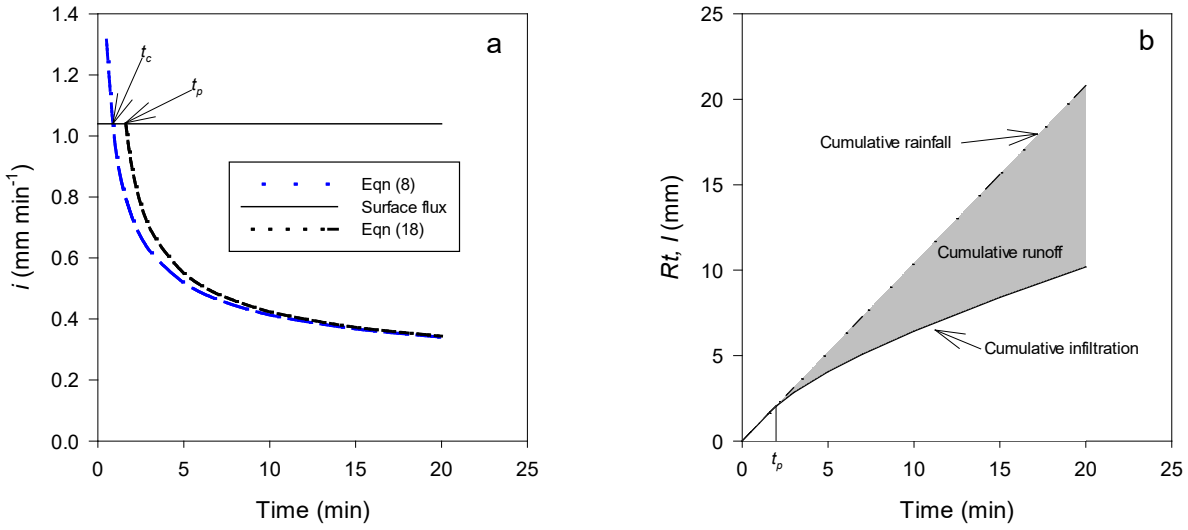

Figure 14. An illustration of the TCA analysis for a sandy loam soil with a surface rainfall flux of 5K_s: a) infiltration rate with elapsed time showing the time when the infiltration rate is the same as the surface flux and the shifting of Green and Ampt curve to match at t_p; b) cumulative rainfall (Rt) and cumulative infiltration calculated with TCA (I). The shaded area is cumulative runoff, which is simply Rt -I.

Using Eqn (16) as R approaches K_s, t_p can become less than t_c. This occurs as R approaches Ks but the correct value of t_c and t_p and I(t) will be calculated if Eqns (16) and (19) are used.

The analysis that has been done here has used a constant rate of surface flux, but as is implied in Eqn (16) a variable rate with time can be used when determining the value of t_p. Cook (1988) used the time to ponding approach in designing a lateral move irrigator.

2.1.5. Layered Soils

The GA model has been extended to layered soils by (Bouwer 1969) and this method has been adapted for the MEDLI model approach in Appendix 1.

2.1.6. Infiltration Model for MEDLI

The use of the GA model with the combination of the White et al. (1989) time to ponding, the TCA analysis and the nonuniform initial water content profile (see Appendix 1) and layered soils would provide a robust infiltration model for MEDLI. The mathematics to implement such a model are given in Appendix 1 along with the list of equations. Also, a spreadsheet with the above methods and those in Appendix 1 have been provided to assist with implementation.

To implement this will require the following soil physical properties for each soil horizon:

- Saturated water content (θs)
- Saturate hydraulic conductivity (Ks)
- The air entry potential (ψ_b)
- The pore size distribution parameter λ
- The soil separated into discrete boxes
- The thickness of each soil horizon.
- Measured Sorptivity or determined from Eqn (9).

In addition, the following data will be required:

- The rainfall rate (R) at time steps of less than 1 day. This could be obtained from the daily rainfall using a disaggregation model such as that of Connolly et al. (1998) or from rate duration curves (www.bom.gov.au/water/designRainfalls/revised-ifd/). At present this may be difficult to implement in MEDLI and further consideration of this aspect needs to be considered before the GA method is implemented in MEDLI. This is beyond the scope of this report.
- The initial soil water content profile

The rainfall rate may only be available from total rainfall depth and length of event. This data only allows the average rainfall intensity to be estimated, so will result in underestimation of runoff and overestimation of infiltration. One final point, if the wetting front depth, z_f, exceeds the depth of the modelled soil profile (z_{max}), then any infiltration once $z_f > z_{max}$ will become deep drainage.

2.2. Drainage

Sisson et al. (1980) and Raats (1983) provide solutions where the drainage flux and the water content at a specific depth and time can be described by the average water content above that depth at that time. Another useful solution that used the Green and Ampt approach for drainage was developed by Youngs (1960) and extended by Youngs and Aggelides (1976) to a situation where infiltration is still occurring at the soil surface but at a rate much less than the saturated hydraulic conductivity. Cook et al. (2008) used the linear soil concept to develop a drainage model. On further examination during this report, I now conclude that this approach may result in some anomalous behaviour, which is a feature of box models and described below in more detail, will not be pursued any further here. The approaches by Sisson et al. (1980) and Youngs (1960) are different in the way in which the profile will drain. With the Sisson approach, the soil drains with the water content profile moving from right to left in Figure (15a). This shows water decreasing at all depths with time. While for the Youngs approach, a square wave moves down the soil profile, with water content above the draining front draining to the drained upper limit water content and that below the draining front remaining at the initial water content (Figure 15b). This is similar to a cascading bucket model (e.g., MEDLI) but requires a high water table to become valid. This would not be a condition that would be suitable for wastewater irrigation.

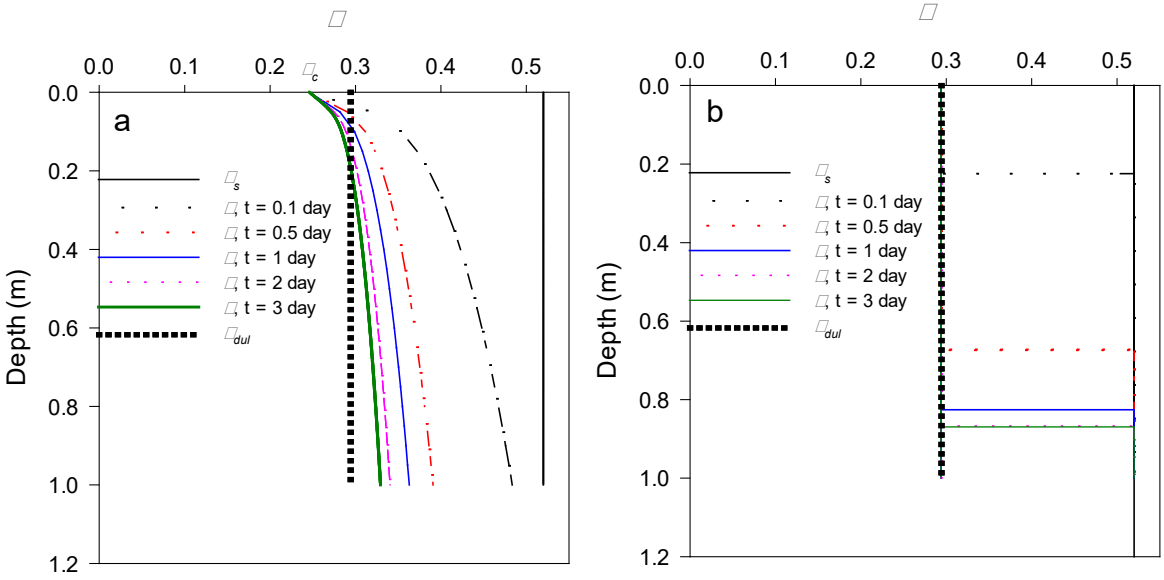

Figure 15. Drainage of water from a uniform soil profile with a) Sisson method (Eqn (20)) and b) Youngs method. The soil properties are taken from Sisson et al. (1980). For the Youngs method a water table at 2 m was assumed to exist. θ_{dul} is the water content at the drained upper limit.

Each of these methods has some merit as measurements have shown that the development of either of the soil water content profiles during drainage can occur, but more soils follow the Sisson type profiles. John Knight (pers. comm.) found that these different draining profiles are due to the bottom boundary condition in the models. He found that a model like the Sisson model applies if free drainage occurs at the bottom boundary, which means any water table is far enough below this lower boundary to have no influence on the drainage. The Youngs model is appropriate if a water table is close or is the bottom boundary which results in a restriction to the amount of drainage. Both solutions assume a thoroughly wetted initial soil profile. The Sisson method assumes that at the soil surface, the water content reduces to θ_c for $t > 0$. This can be seen in Figure 15a with all the curves converging on this point at $z = 0$. The value of θ_c is less than θ_{dul} otherwise the profile will only drain very slowly towards θ_{dul}. These methods do not account for evapotranspiration, which will also reduce the water content of the soil. Both methods can be adapted to nonuniform initial water contents and nonuniform soil properties.

For uniform soil profiles, the equations for the Sisson method are:

$$\theta(z,t') = \theta_c + (\theta_s - \theta_c)\left[\frac{z}{At'}\right]^{1/(m-1)} \quad ,0 < z < At'$$

$$\theta(z,t') = \theta_s \quad ,z \geq At' \qquad (20)$$

$$A = \frac{K_s m}{\theta_s - \theta_c}$$

where

$m = 2\lambda+3$ is the pore size distribution parameter for the Brooks and Corey hydraulic conductivity function. The value of λ can be found from the relationship between θ and ψ (see Fig. 10) or by pedo-transfer functions (Cook and Cresswell, 2007) or from tables such as those in Table A2 from Clapp and Hornberger (1978).

K_s = saturated hydraulic conductivity (m s^{-1})

z depth (m) at t' (s)

θ_c is the water content that the surface of the soil drains to

t' is the time since the start of the drainage event (s)

Youngs (1960) method relies on there being a water table at some known shallow depth. Where MEDLI is applied this is unlikely as such sites would not be suitable for wastewater irrigation. This method is unlikely to be as useful as Sisson's method, so is not developed further here.

Another way to use the Sisson et al. (1980) method can be developed from the fact that the flux can be given by:

$$j(z,t') = K_s \left(\frac{z}{At'} \right)^{m/(m-1)} \tag{21}$$

where

$j(z,t')$ is the flux rate at depth z at time t' (m s^{-1}).

Integration of Eqn (21) with time will give the total amount of water that has passed beyond z at time t'. This provides a perfect solution for calculating the drainage in a box model like MEDLI, as the values of z can be the depth of the bottom of the boxes (z_1, z_2 …z_n). The integral of Eqn (21) with time is:

$$\begin{aligned} J(z,t') &= \int_{t_0'}^{t'} K_s \left(\frac{z}{At'} \right)^{m/(m-1)} dt' = \frac{B(z)}{1-M} \left[\left(t_0' \right)^{1-M} - \left(t' \right)^{1-M} \right], \quad t' > t_0' \\ t_0' &= z / A \\ M &= m / \left(m-1 \right) \\ B(z) &= K_s \left(\frac{z}{A} \right)^{M} \end{aligned} \tag{22}$$

t' is the time since the start of the drainage event (s),

t_0' (s) is the time when the draining front reaches the depth z. Prior to t_0' the water content is maintained at a constant value of θ_s due to the drainage water from above z.

$J(z,t')$ is the cumulative drainage of water from the soil profile above a depth z at the time t'.

The water storage W (m) above z at time t' and water content $\theta(z,t')$ (m^3 m^{-3}) are calculated by:

$$\begin{aligned} W(z,t') &= W(z,t_0') - \left[J(z,t_0') - J(z,t') \right], && t' > t_0', 0 < z < At' \\ W(z,t_0') &= \theta_c z + \left(\frac{m}{m-1} \right) z \left(\theta_s - \theta_c \right) \left[\frac{z}{At'} \right]^{1/(m-1)} \\ \theta(z,t') &= W(z,t') / z, && 0 < z < At' \\ \theta &= \theta_s, && z \geq At' \end{aligned} \tag{23}$$

The valuable feature of Eqns (22) and (23) is that the flux ($j(z,t')$) as a function of depth and time is known, so this can be coupled with solute transport solutions. Also, it is relatively easy to calculate drainage for nonuniform soil water profiles and nonuniform soil properties. The values of $\theta(z,t')$ calculated with Eqns (22) and (23) are identical to $\theta(z,t')$ calculated with Eqn (20), as they should be. The adaption of Eqn (22) to nonuniform water contents at the start of drainage and the computational procedure is given in Appendix 3. For the clay loam soil with only wetting to 0.45 m, the profile drains quickly with the redistribution of water further down the soil profile. This should be checked out further before adoption in MEDLI.

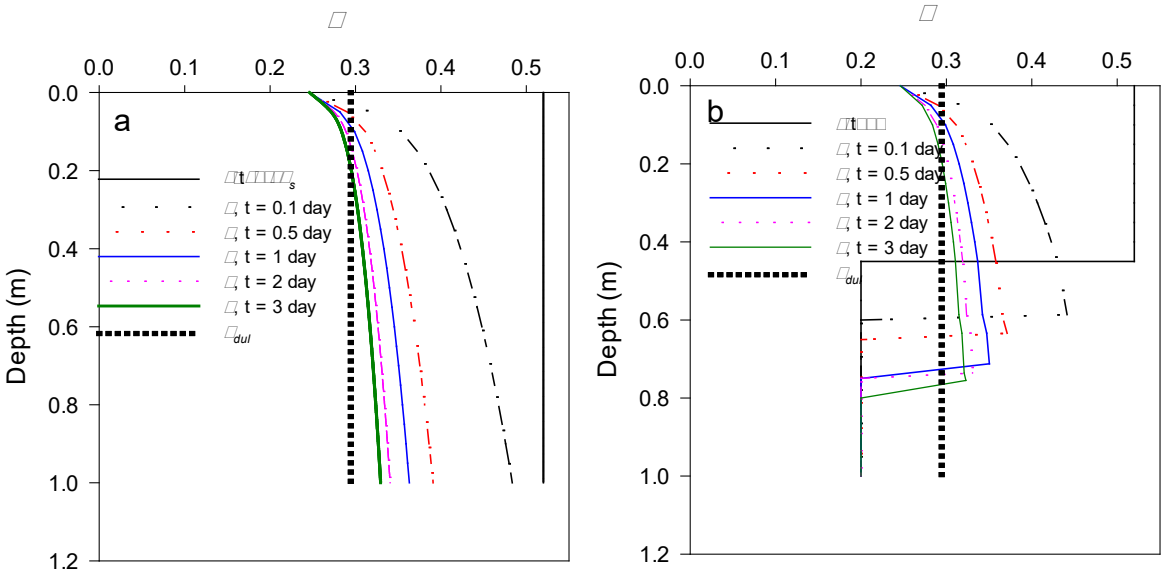

Figure 16. Drainage of water from: a) a uniform soil profile with: a) Sisson method (Eqn (20)); b) nonuniform profile using a method described in Appendix 3. The soil properties are taken from Sisson (1980).

The drainage method of Sisson et al. (1980) would appear to give more realistic results than that of Youngs (1960). The Sisson method requires the following soil properties: K_s, θ_s, m and θ_c. Of these, only θ_c is not readily available, but this could be estimated as a fraction of θ_{dul}. A value of $0.83\theta_{dul}$ was used in Figures 15 and 16 and this is a suitable value. For uniform soil profiles this seems to work well but will need to be checked by comparison with numerical models such as HYDRUS1D. Evapotranspiration is going to reduce the water content at each time step, so that if $\theta_c = \theta_{dul}$ was used this may lead to only a small difference in the drainage.

The present MEDLI model is based on the cascading bucket model from EPIC (Sharpley and Williams, 1990) and given by:

$$\begin{aligned} Dr_i &= U_i\left(Sw_i - fc_i\right) \\ U_i &= 1 - \exp(-1/TT_i) \\ TT_i &= \left(Sw_{\max} - fc_i\right)/K_{s_i} \end{aligned} \qquad (24)$$

where

Dr_i is the drainage rate from the ith layer (m) during the time step of the model

Sw_i is the soil water storage in the ith layer (m)

fc_i is the field capacity or drained upper limit storage of the ith layer (m)

U_i is the proportional drainage factor for the ith layer

TT_i is the travel time for the *i*th layer (s)

Sw_{max} is the maximum soil water storage in the *i*th layer (m)

K_{s_i} is the saturated hydraulic conductivity of the *i*th layer (m s^{-1})

All such cascading box drainage models with a fixed time step are fundamentally flawed. The reason is that in a uniform soil draining from saturation with layers of equal thickness in the first time step, only the first layer will drain - as the same volume of water coming from layer 1 will also be going out of layer 2 and so forth to the last layer, with the same volume then being lost to deep drainage. What this means is that the drainage of the soil is dependent on the thickness of the layers and the time step used in the model. This is shown in Figure 17 where the Sisson model is compared to the MEDLI for different layer thicknesses and time steps.

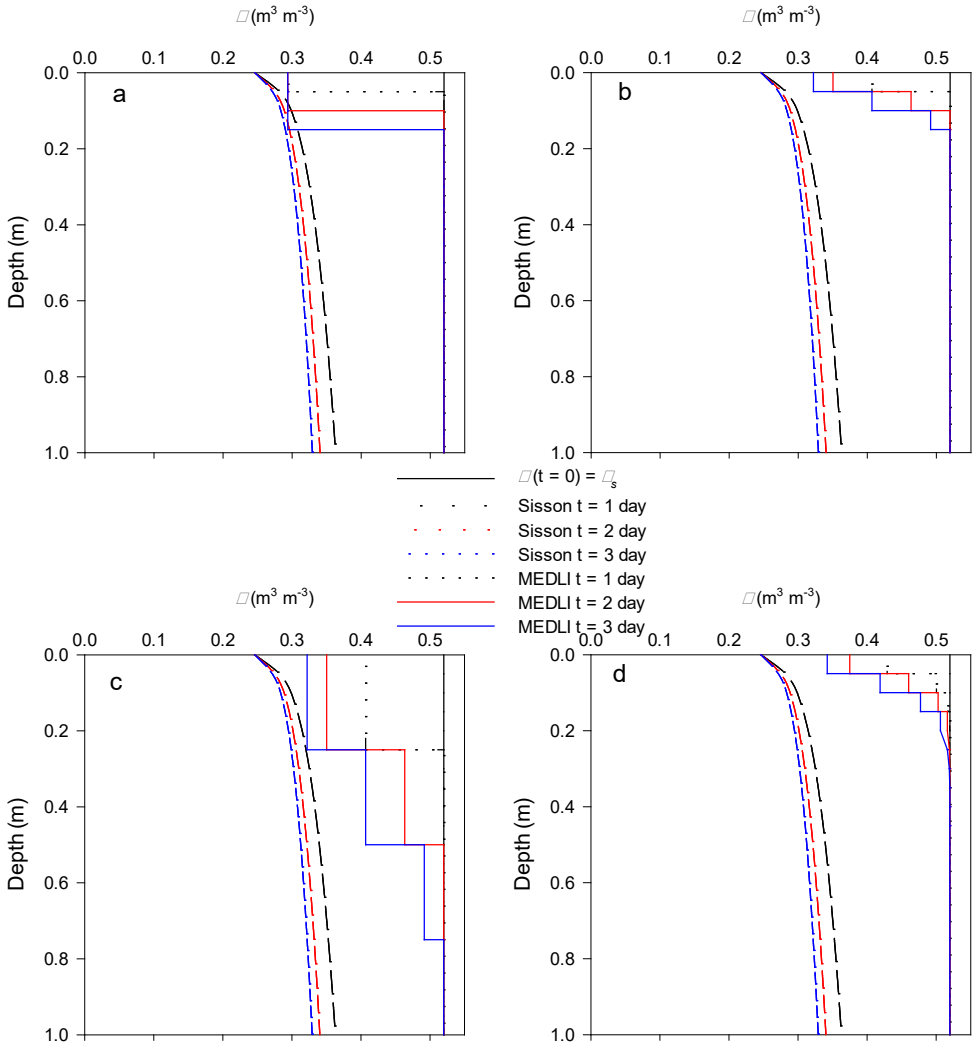

Figure 17. Comparison of the Sisson models and MEDLI drainage model with the soil properties from Sisson (1980): a) U_i = 1 for MEDLI model, space steps of 5 cm and time steps of 1 day, b) same as Figure 17a but with U_i = 0.5, c) U_i = 0.5 for MEDLI model, space steps of 25 cm and time steps of 1 day, d) U_i = 0.05 for MEDLI model, space steps of 5 cm and time steps of 0.1 day.

When the values of soil in Sisson et al. (1980) were used (Table A1) the value of TT_i was 0.0113 day and U_i was 1. With U_i = 1, spatial steps of 0.05 m and time steps of 1 day the drainage front would only reach a depth of 0.15 m as only 3 depth boxes will be drained (Figure 17a). Changing the value of U_i to 0.5 changes the shape of the drain front but not the depth (Figure 17b). Changing the spatial

steps to 0.25 m changes the depth of the drainage front dramatically (Figure 17c) while changing the time step does not dramatically change the drainage front. These results show that not only MEDLI, but any cascading box model is very dependent on the spatial step size. Cumulative drainage plots (Figure 18a) highlight these model differences. When the drainage time is extended to 10 days (Figure 18b), the number of timesteps (10) now exceeds the number of soil layers (4) being modelled for scenario shown in Figure 17c. After day 4, the quantity of draining water exiting the bottom of the soil profile at each timestep declines, as the accumulated deep drainage approaches total profile drainable water (Profile SWmax – Profile FC) at time = 0. The Sisson curve shown in Figure 18b supports field observations that downward drainage from saturated covered plots materially decreases (to say ≤1mm/day) after 2 to 3 days of drainage. However, the slower deep drainage rate predicted by the MEDLI algorithm would allow transpiration to use some of this water in the drainable store, which would lead to further underestimating deep drainage by the integrated MEDLI model.

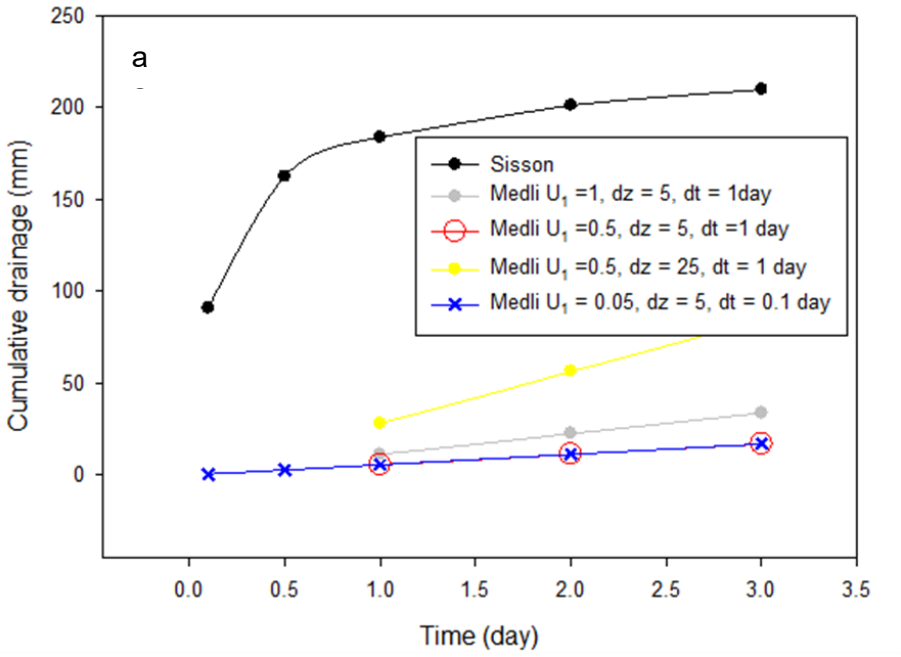

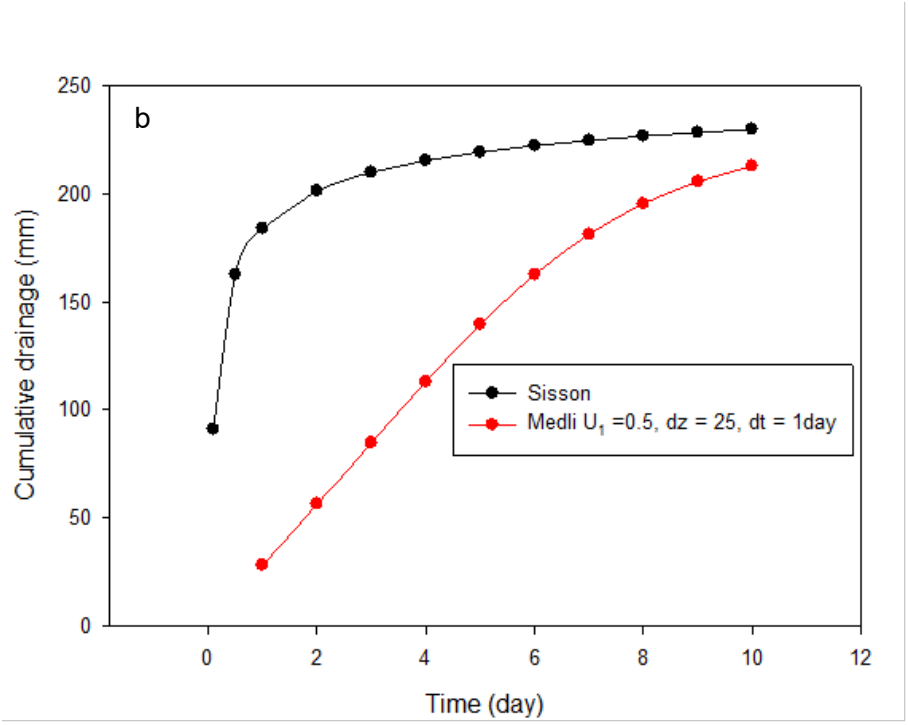

Figure 18. Comparison of the cumulative drainage shown by Sisson method and MEDLI for a) the four scenarios defined in Figure 17 and b) for the scenario defined in Figure 17c, extended to 10 days cumulative drainage time.

What this also means is that the deep drainage (*DD*) for a soil profile with only drainage loss starting at saturation is given by:

$$DD(t_d) = \sum_{i=1}^{n} Dr_i \qquad (25)$$

$$n = t_d / \Delta t$$

where

t_d is the time since the start of drainage (s)

Δt is the time step (s).

Soil data from Sisson et al. (1980) using a value of Δt = 1 day would result in a value of Δz = 15.5 m. This value of Δz is unrealistic but indicates that daily cascading box models will have problems representing actual drainage. Evapotranspiration will also extract water from the soil profile changing the shape of the water content profile and hence the drainage at the next time step. This means that the models used for drainage and evapotranspiration will be convolved and being able to determine each component from experimental data will be difficult. This also means that the order that processes are carried out in the water balance models will change the amounts of water determined as drainage and/or evapotranspiration. This means that the evapotranspiration models need to be considered as affecting the drainage process.

The problems shown here for the MEDLI model will also occur in all cascading box drainage models including WASOM1, which was developed by the author. For these cascading box drainage models the order of calculation of the drainage and evaporation process can affect the drainage if they are implemented sequentially. If evapotranspiration losses are calculated before drainage, then there will be less water for drainage, whereas if drainage is calculated first then transpiration can be affected if the water content of the box is greater than the aeration limit (see Section 2.3 below).

2.3. Root water uptake and transpiration

A comprehensive review of soil water plant root systems has been undertaken by Feddes and Raats (2004). The water uptake in a root zone is a combination of potential root sink term S_p (s^{-1}) and a dimensionless function (h_s) related to the availability of the water to the plant such that the actual sink term (S_u (s^{-1})) is given by (Feddes et al., 1978):

$$S_u(\psi) = h_s(\psi) S_p \tag{26}$$

The value of h_s is defined by the soil matric potential in Figure (19).

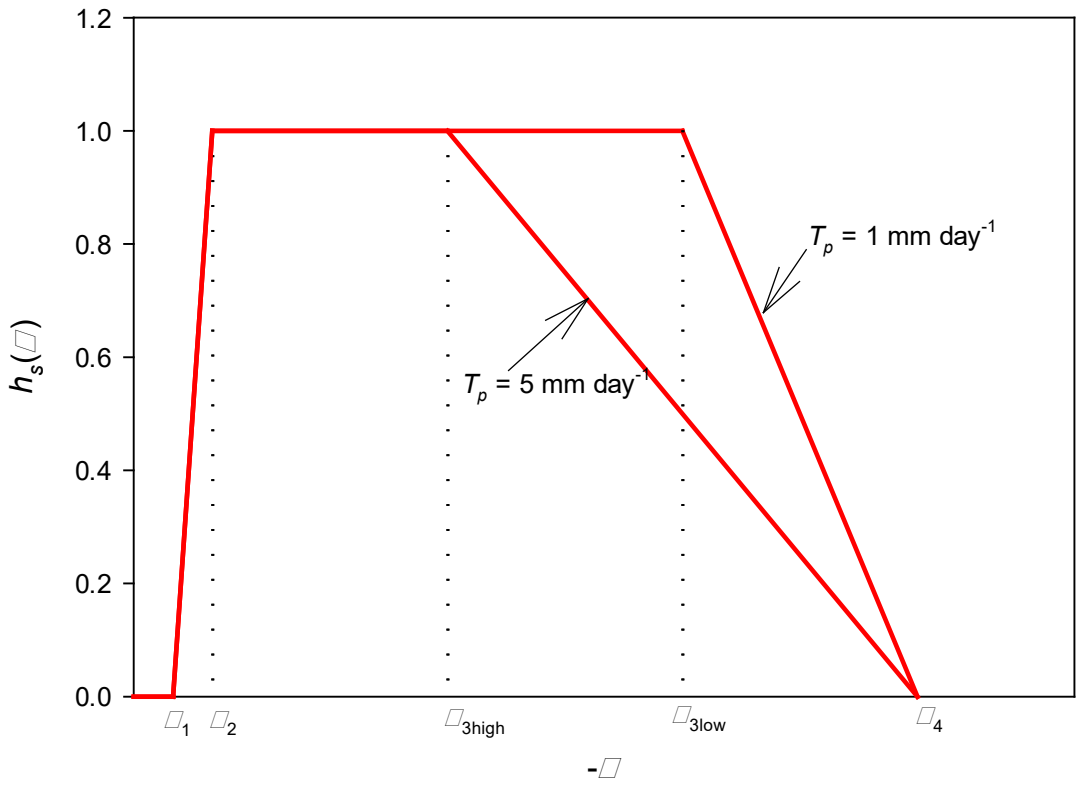

Figure 19. Schematic of h_s function with matric potential for the following turning points: $\psi > \psi_1$ zero uptake due to a lack of aeration; $\psi_1 \leq \psi > \psi_2$ the uptake increases up to a maximum at ψ_2; $\psi_2 \leq \psi > \psi_3$ the uptake is at a maximum; $\psi_3 \leq \psi > \psi_4$ the uptake decreases due to limited available water; $\psi < \psi_4$ zero uptake as at the lower limit of water extraction. This also shows that ψ_3 changes depending on the potential transpiration rate (T_p).

The matric potential points in Figure 19 can easily be converted to water contents if the moisture retention characteristic of the soil is known. The values of the potentials for various crops can be found in the literature and are also found in HYDRUS1D, which can be downloaded for free. The root distribution in the soil will also have an effect on where the water is taken from in the soil. In their original publication Feddes et al. (1978) considered the root uptake to be homogeneous throughout the root depth of the crop so that:

$$S_p(z) = \frac{T_p}{Z_r} \tag{27}$$

where

S_P is the potential root sink term (s^{-1})

T_P is the potential transpiration rate ($m\ s^{-1}$)

Z_r is the rooting depth of the crop (m)

This was modified by Prasad (1988) to have a linear decrease in uptake with depth. McAneney and Judd (1983) observed that the percentage uptake for pasture varied non-linearly with the proportion of the root depth (Figure 20).

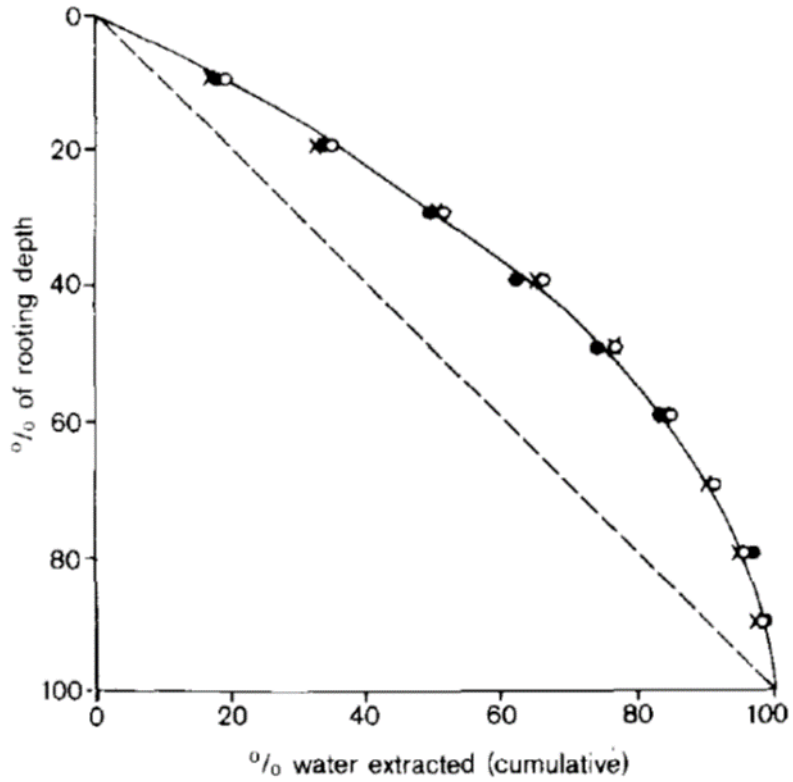

Figure 20. Normalised water extraction from McAneney and Judd (1983, Fig.4) and surface soil moisture measurements versus normalised rooting depth for the 198—1981 season. The dashed line is a 1:1 plot and demonstrates what would occur if each depth increment contributed equally to water extraction. The figure is taken from (McAneney and Judd (1983, Fig. 5).

The data of McAneney and Judd (1983) can be used to develop a weighting function ($f(z)$) with rooting depth that then modifies Eqn (27) to:

$$S_p(z) = T_p f(z), \qquad 0 \le z \le Z_r \tag{28}$$

where $f(z)$ is a weighting function (m^{-1}).

The function developed is shown in Figure 21.

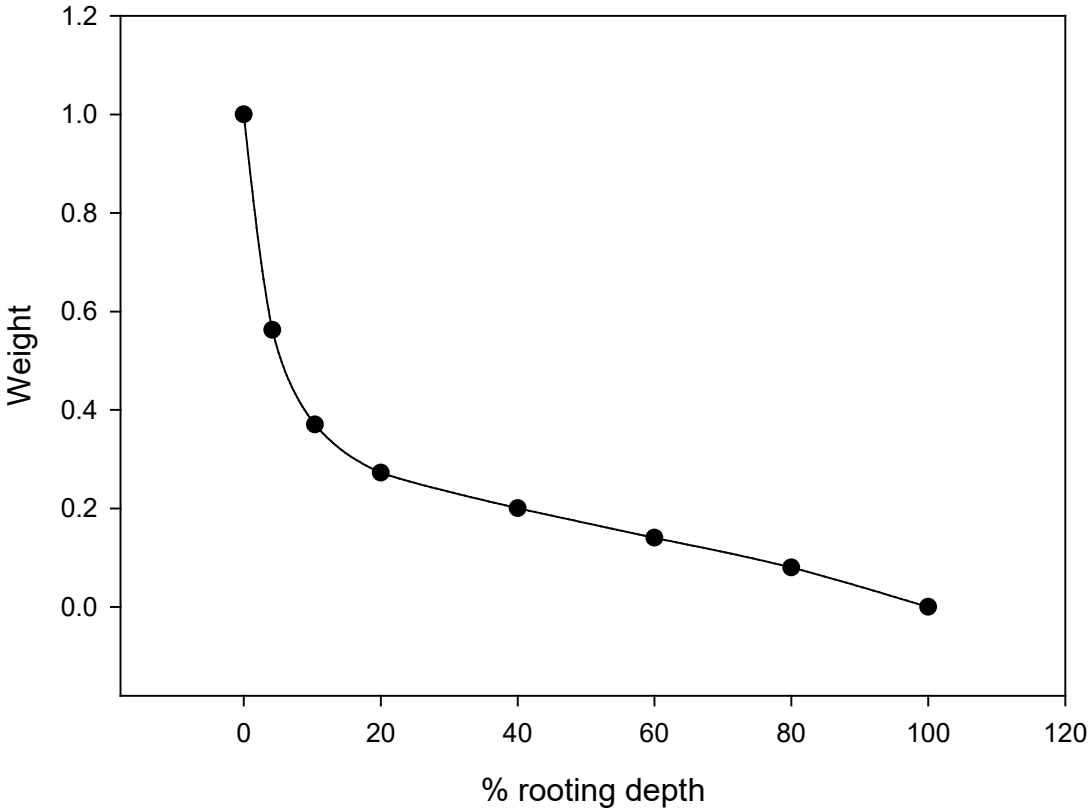

Figure 21. Weighting function for % rooting depth based on McAneney and Judd (1983).

Alternatively, if root length density data is available then this can be used to develop *f*(z) using (Nimah and Hanks, 1973):

$$f(z) = \frac{L_r(z)}{\int_0^{Z_r} L_r(z)\,dz} \tag{29}$$

where $L_r(z)$ is the root length density as a function of depth (m m^{-3}).

However, MEDLI users are unlikely to have root length density data but this could be obtained from literature values or using a function relationship such as Eqn (5) in Cook and Kelliher (2006). Combining Eqns (26) and (28) allows the transpiration (*T*) to be determined by:

$$S_u(z,t) = h_s(z,t)\frac{T_p\int_0^z f(z)\,dz}{\int_0^{Z_r} f(z)\,dz} \tag{30}$$

$$T(t) = \int_0^{Zr} S_u(z,t)\,dz$$

For the MEDLI model, Eqn (28) will need to comply with the discretisation of the model with constant values of h_s and S_p for each depth interval.

Another simple way to determine the transpiration is to use the total soil water deficit as a means to determine the value of T_p and is calculated as (McAneney and Judd, 1983):

$$T(t) = T_p(t), \quad S_t(t) \le S_c$$
$$= T_p(t)\left(\frac{S_m - S_t(t)}{S_m - S_c}\right) \tag{31}$$

where

$S_m = \int_0^{Z_r} \left(\theta_{dul}(z) - \theta_l(z)\right) dz$ is the maximum profile soil water deficit (m)

θ_l is the lower water content or the 15-bar water content

$S_t(t) = \int_0^{Z_r} \left(\theta(t) - \theta_l(z)\right) dz$ is the profile soil water deficit at time t (m)

$S_c = \int_0^{Z_r} \left(\theta_{dul}(z) - \theta_p(z)\right) dz$ is the profile water storage deficit for readily available water (m)

θ_p is the water content at the readily available water limit and S_c is often called the readily available plant water capacity.

The transpiration will still need to be apportioned with depth and soil water status. An equivalent of Eqn (30) can be written for each box in the MEDLI model to give the soil water status and either the weighting function in Figure 21 or Eqn (29) can be used for the depth weighting function. Eqn (31) combined with the weighting function given in Figure 21 would be relatively easily incorporated into MEDLI and would be a first step in modification of the transpiration calculation.

The transpiration losses from each box can be determined and the water content of each box in the MEDLI model reduced. I am suggesting this is done before the drainage flux has been calculated for reasons given above in the drainage section.

2.3.1. Partitioning Potential Evapotranspiration to Evaporation and Transpiration

The potential evapotranspiration (PET) consists of two components: the soil evaporation and the transpiration. In order to determine the potential transpiration (T_p) and the potential evaporation (E_p), various methods are used to determine this partitioning. The model used in MEDLI follows that of Ritchie (1972), which has been adopted in many water balance models. Here an alternative is given, which is used in HYDRUS1D (Sutanto et al. 2012).

2.3.1.1 Soil evaporation

The evaporation from soils involves a two-stage process. The first stage is soil controlled by the energy to evaporate the water while the second stage is controlled by the rate at which water can be transported through the soil to the soil surface. These processes can be described by:

$$E_{os} = E_p, E_p \ge E_{os}$$
$$E_s = \frac{1}{2} D_e \sqrt{t'}, E_s < E_p \tag{32}$$

where

E_p and T_p are given by (Sutanto et al. 2012):

$$E_p = PET\left[\exp(-0.463LAI)\right]$$
$$T_p = PET - E_p = PET\left[1-\exp(-0.463LAI)\right] \quad (33)$$

LAI is the leaf area index

E_p is the potential soil evaporation (m)

T_p is the potential plant transpiration (m)

E_{os} is the evaporation rate during first stage (m)

E_s is the evaporation rate during second stage (m)

t' is the time since the last wetting event occurred (s)

D_e is the desorptivity and can be obtained from the diffusivity with methods of calculation given in Lockington (1994) (m $s^{-1/2}$).

Since D_e is determined from the water content of the first box in MEDLI, small rainfall events may not cause stage 1 evaporation to occur. D_e is equivalent to the CONA parameter used in the present MEDLI model.

For the plant cover factor MEDLI uses Beers law with an extinction coefficient of -0.65. A comparison with the crop factor in Eqn (33) (1-exp(-0.463LAI) and the MEDLI plant crop factor is shown in Figure 22 and indicates that Eqn (33) would give a lower value than that currently calculated with MEDLI. The MEDLI method would give larger estimates of soil evaporation than Eqn (33). This would result in less soil evaporation if Eqn (33) was used and more transpiration. Sutanto et al. (2012) found that estimates using Eqn (33) in HYDRUS1D gave results for soil evaporation that were greater than those obtained with isotope analysis and water balance methods. Changing to Eqn (33) would be unlikely to have a large effect on evapotranspiration calculated with MEDLI but given that evapotranspiration is convolved with drainage it could affect the deep drainage. Further investigation of LAI on evaporation with the present method in MEDLI and Eqn (33) will require comparisons with measured data.

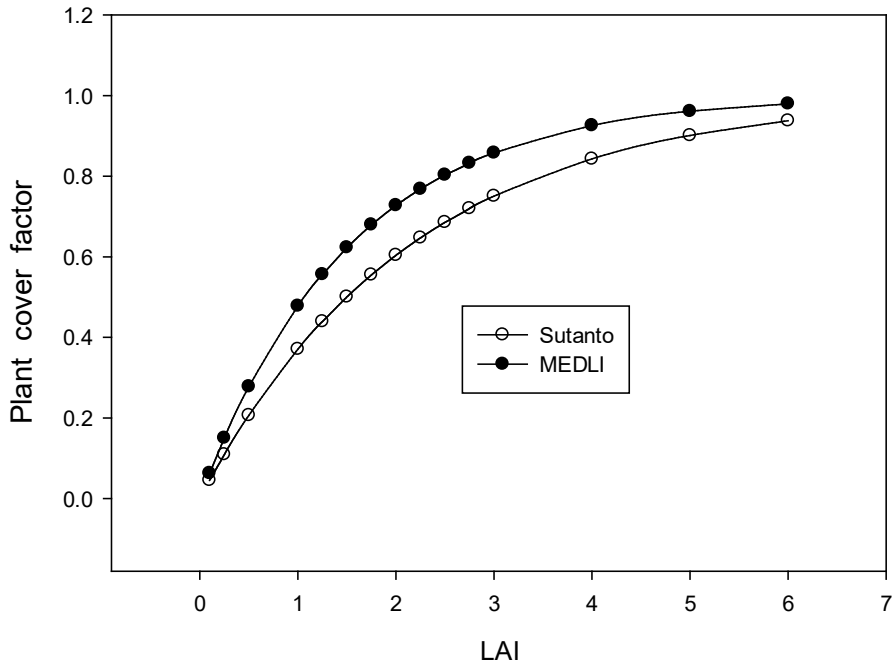

Figure 22. Comparison of plant crop factor from Sutanto et al. (2012) (1-exp (-0.463LAI)) and MEDLI (1-exp(-0.65LAI)).

The above methods for evaporation require that *t'* is reset to zero after each wetting event. The soil evaporation comes only from the first two boxes in the MEDLI model with the less water being taken from the second layer, which can only dry to the lower storage limit. This does now allow for rewetting of the first layer from the second layer. Cook et al. (2008) adopted the Deardoff (1977) force-restore method for calculating the soil evaporation. This method allows for rewetting of the first layer by upward diffusion of water from the second layer due to the water content gradient. Deardoff (1977) used this method to overcome the fact that soil evaporation is often underestimated in box models. However, as full crop cover is likely in MEDLI modelling, any error may be very small, and the extra complication would not be sensible in MEDLI.

The synthesis report on the MEDLI Science Review (Gardner, 2021) covers the MEDLI approach to calculating the soil evaporation and transpiration. The present MEDLI evaporation model considers both plant cover and residual dead plant material but does not take into account the depth or mass of the residual dead plant material. Soil evaporation is considered to be zero under residual dead plant material, regardless of mass. The HowLeaky (McClymont, 2018) model uses an algorithm that does account for this and is given by:

$$E_{pr} = E_p \exp\left(0.22TCR/1000\right) \tag{34}$$

where

E_{pr} is the potential evapotranspiration considering the crop residual (m)

TCR is the total crop residual in (tonnes ha^{-1})

Equation (34) could be added to MEDLI to account for the impact of residual plant material mass left after harvesting on the soil evaporation rate. This may be an important addition especially as soil evaporation will increase, leading to the prediction of higher irrigation demand. The evapotranspiration will affect the drainage rate and leaching of solutes to the ground water. E_{pr} would replace E_p in Eqn (32) when calculating the soil evaporation.

3. Solute Transport

Solute transport in soils occurs due to two main processes: advection where the solute travels along with the water, and dispersion. The dispersion is made up of two aspects, solute movement due to molecular diffusion because of solute concentration gradients and smearing out effects due to different soil water velocities in different sized pores, and different velocities across the diameter of any given pore.

3.1. Piston flow

Advective transport is analogous to the Green and Ampt infiltration model with a sharp front between the invading solution and the resident solution in the soil. This is often called piston flow and is shown schematically in Figure 23.

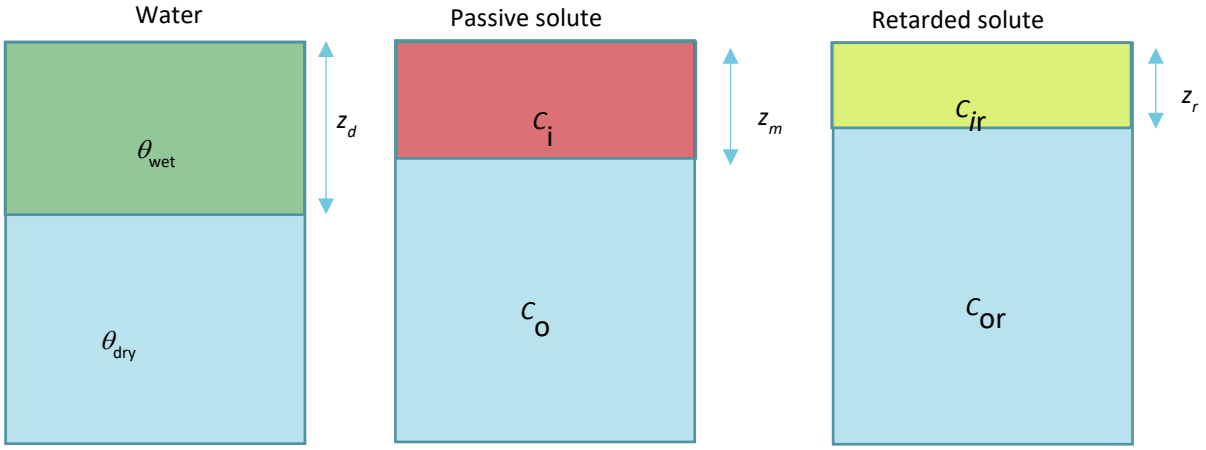

Figure 23. Schematic diagram of piston flow during infiltration into a soil showing idealised the water and solute fronts. The water wetting front is deeper (z_d) into the soil as water in the soil prior to infiltration is pushed out of the pores ahead of the water that has infiltrated. C_i is the concentration in the infiltrating water and C_o is the solute initially present in the soil for a non-absorbed passive solute like chloride or nitrate. z_m is the depth that the infiltrating solute has moved to. A retarded solute like ammonium or phosphate will sorb onto the soil solids, which slows its progress through the soil so that $z_r < z_m$. The concentration of the retarded solute in the infiltrating water is C_{ir} and the initial concentration in the soil is C_{or}.

The sharp fronts of water, solute & retarded solute are such that $z_d > z_m > z_r$, which in turn can be calculated by:

$$z_d(t) = \frac{I(t)}{\left(\theta_{wet} - \theta_{dry}\right)}$$
$$z_m(t) = \frac{I(t)}{\theta_{wet}} \qquad (35)$$
$$z_r(t) = \frac{I(t)}{R_s \theta_{wet}} = \frac{z_m(t)}{R_s}$$

where

R_s is the retardation factor > 1.

Retardation of a solute occurs because the solute interacts with the soil matrix until an equilibrium is reached between the solutes on the soil solids and the solute in solution due to chemical adsorption reactions, which are usually reversible. This means that the solute gets retarded in its transmission through the soil.

The volume of water that was in the soil to the depth z_m is displaced downward (sometimes called the snow plough effect). This water has a concentration of the original soil solute concentration (c_o). The new water with an inert solute (such as chloride or nitrate) with a concentration of c_i will move **by advection** to the depth z_m. However, if the solute interacts with the soil solids as it is transported (e.g., because of anion adsorption) it will be retarded, and the reduced solute front will be given by z_r.

It has been shown this advective front coincides with the centre of mass of the dispersed front. This is illustrated in Figure 24, which is taken from Clothier and Scotter (1985). This assumption works well for infiltration when the Green and Ampt model is used, as the value of $I(t)$ and the depths z_d, z_m and z_r are easily calculated. This means that for infiltration of water with a solute concentration of c_i, the soil water to a depth z_m or z_r will have a solute concentration equal to this input concentration c_i. Below these depths, the concentration will be at the initial soil water concentration of c_o.

Dispersion at the solute front can be estimated using a method developed by Elrick et al. (1987). This spreads the solute out around the centroid of the solute front and is calculated by:

$$c(z,t) = \frac{(c_i - c_o)}{2} \operatorname{erfc}\left(\frac{z(t) - z_m(t)}{2R\sqrt{D_s t}} \right) + c_o \quad (36)$$

where

c_i is the input concentration (kg m^{-3})

c_o is the original concentration in the soil (kg m^{-3})

R is the retardation factor

D_s is the solute dispersion coefficient (m^2 s^{-1}), which can be approximated as 1/10 of the solute travel distance.

For a model such as MEDLI, the development of the actual shape of the solute distribution may not be as important as calculating where the solute front is. This is because the values of z_m and z_r are unlikely to occur at the exact boundaries of the boxes in the MEDLI model. The result will be that for the box where the front ends up, the solute concentration will be mixed throughout the box. If this occurs in the kth box, then for the concentration at the end of the time step this will be given by:

$$c_k = \left[c_i \left(z_m - z_{k-1} \right) + c_o \left(z_k - z_m \right) \right] / \left(z_k - z_{k-1} \right) \quad (37)$$

This means that rather than a sharp transition from c_i to c_o the front will get dispersed due to the structure of the model. This is termed numerical dispersion as it arises due to the discretisation of the space (see Cook 2017). The initial concentration is given here as uniform throughout the soil profile, but this is not a strict requirement. The initial concentration could vary with depth, and the water in the depth increment between z_d and z_m would contain the displaced solute. This would be transferred from one box to the next as it is displaced downward, and the concentrations in the boxes that are wetted are calculated from the water content and mass of displaced solute. This advection only model is relatively easy to implement and is already the basis of the solute transport in MEDLI. The difference would be related to the infiltration model if the GA model was implemented.

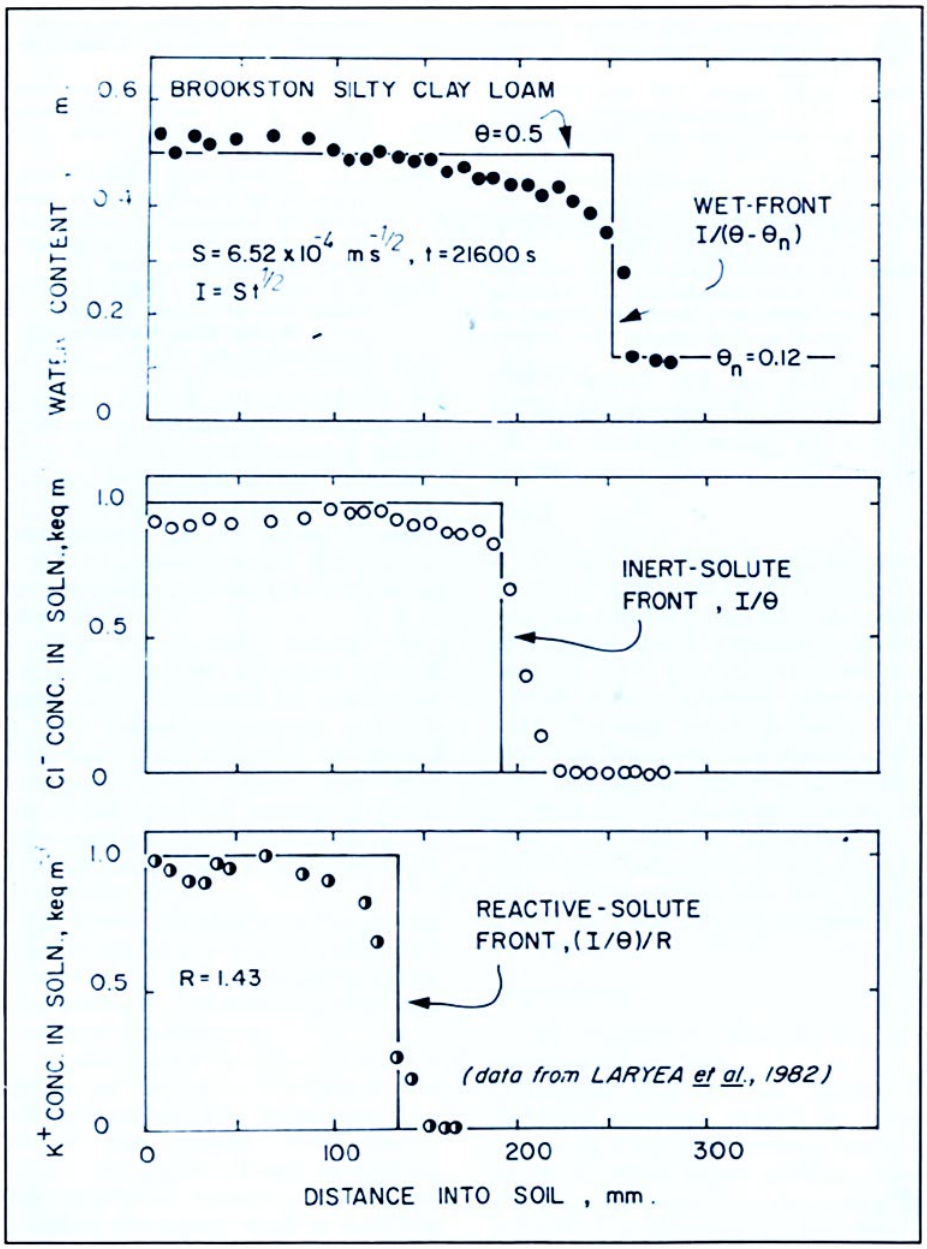

Figure 24. Illustration of horizontal water and solute transport in soil and how the advective solute front (solid lines) compares with the actual dispersed front (data dots). Note that I is cumulative infiltration, θ is water content of the transmission zone, θ_n is the initial soil water content, and R is the retardation factor. The data are profiles of a) water, b) chloride (Cl^-) and c) potassium (K^+) for a Brookston silty clay loam after 21600 sec of adsorption of 1.0M KCl. The Data are from Laryea (1982).

The simplified advection model can also be used to develop a stochastic approach to solute transport if the soil is considered as a collection of stream tubes, with the infiltration in each tube controlled by the local soil physical properties. Biggar and Nielsen (1976) found that the velocity of water flow measured at numerous points across a field plot had a log normal distribution. The mean and standard deviation of the log transformed velocity were calculated from this data set. Hence the mean solute concentration with depth, assuming the same boundary conditions as in Figure 23 can then be written as (Warrick, 2003):

$$c(z,t) = \frac{c_i - c_o}{2} \operatorname{erfc}\left[\frac{\ln\left(\frac{z}{t}\right) - \mu}{\sigma\sqrt{2}}\right] + c_o \qquad (38)$$

where

μ is mean of the log normal velocities with the velocities in units of (m s^{-1})

σ is the standard deviation of the log normal velocities.

Warrick (2003) used the data of Biggar and Nielsen (1976) to compare the difference in solute concentration calculated using a mean velocity and a piston front assumption (calculated with Eqn (35)) vs the assumption of advection and dispersion due to velocity differences in the stream tubes (described by Eqn 38). The comparison is shown in Figure 25 where the much more dispersed nature of the real solute concentration with soil depth is evident. The values for μ and σ were respectively 3.01 and 1.25. This results in a mean value of the velocity of 44.3 cm day^{-1} ($\exp(\mu+0.5\sigma^2)$) on day 5. The mean piston flow solute front will be at a depth of 2.22 m (5x44.3 = 221.6/100) as shown in Figure 25. In comparison the stream tube model shows that some solute would have reached 4 m by day 5. The concentration distribution with depth shown in Figure 25 for the stream tube model is that which would be measured by sampling the whole field with multiple soil cores and calculating the mean concentration at each depth.

The stream tube concentration with depth shape is similar to that for the resident concentration given in Scotter and Ross (1994), which is not surprising as they are both using a velocity distribution to calculate the solute concentrations. More details on the Scotter and Ross (1994) approach are given in Section 3.3.

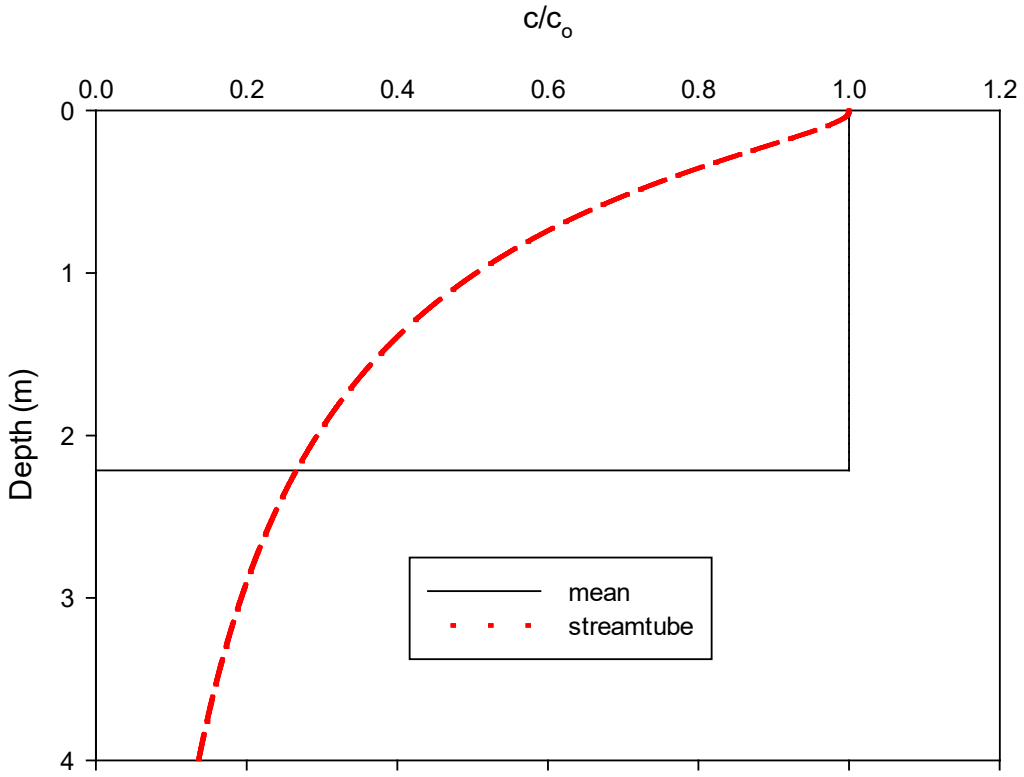

Figure 25. Comparison of relative concentration of a solute with depth at day 5 following a step change of concentration in the infiltrating water at the soil surface. The piston value is calculated from Eqn (35). Using the mean velocity and assuming piston flow. The stream tube model uses Eqn (38) and the log normal distribution of velocities to calculate a mean relative concentration from an infinite number of stream tubes. More detail is given in the text above.

3.2. Advective Dispersive Equation (ADE)

The advection dispersion equation (sometimes called the convection dispersion equation) combines the effects of the *advection* of the solute due to the transport with the soil water, with *dispersion* due to hydrodynamic dispersion and molecular diffusion. The hydrodynamic dispersion occurs due to differences in the velocity between pores of varying diameter and also due to variation in the water velocity across a soil pore due to friction. The ADE equation in one dimension (vertical) is given by (Warrick, 2003):

$$\frac{\partial C}{\partial t} = D_s \frac{\partial^2 C}{\partial z^2} - V \frac{\partial C}{\partial z} \tag{39}$$

where

C is the concentration (kg m^{-3})

$D_s = D_a/\theta$ is the dispersion coefficient (m^2 s^{-1})

D_a is the apparent dispersion coefficient (m^2 s^{-1})

$V = J_w/\theta$ is the velocity of water through the soil pores (m s^{-1})

θ is the water content at time t at depth z.

J_w is the macroscopic water flux density (m^3 water /m^2 soil cross section/unit time) through the soil matrix (m s^{-1}) and can be obtained by solving Eqn (2).

There have been many publications on transport of solutes in soil with different boundary conditions using the advective dispersion equation. Many useful analytical solutions are available for equation (36) and have been summarised by van Genuchten and Alves (1982) and Warrick (2003). Field solute transport experiments showed that the ADE equation does not always give a good representation of the solute distribution in the soil due to preferential flow. This has resulted in development of the *mobile-immobile water* concept which, when incorporated into Eqn (39), gives:

$$\theta_m \frac{\partial C_m}{\partial t} + \theta_{im} \frac{\partial C_{im}}{\partial t} = \theta_m D_m \frac{\partial^2 C_m}{\partial z^2} - J_w \frac{\partial C_m}{\partial z} \tag{40}$$

where

θ_m is the mobile water phase

θ_{im} is the immobile water phase

and $\theta = \theta_m + \theta_{im}$

C_m is the concentration in the mobile water phase (kg m^{-3})

C_{im} is the concentration in immobile water phase (kg m^{-3})

The solute is assumed to only be transferred in the mobile water phase, whilst transfer between the immobile and mobile phases occurs at a rate limiting first order equation given by:

$$\theta_{im} \frac{\partial C_{im}}{\partial t} = \alpha \left(C_m - C_{im} \right) \tag{41}$$

where α is the first order rate constant (kg s^{-1}).

The solute will transfer from the mobile to the mobile phase when $C_m > C_{im}$ and from the immobile to the mobile phase when $C_m < C_{im}$. The amount transfer will depend on the difference in the concentrations and the values of α and θ_{im}. To implement this model in MEDLI would be both computationally intensive and is fraught with difficulties associated with numerical instabilities that can develop when using numerical solutions.

3.3. Transfer Function Model

Jury (1982) developed an alternative method for addressing the log normal distribution of pore water velocities on the solute distributions found in field situations. He used a transfer function that uses a probability density function to predict the solute distribution in the soil profile and is described by:

$$C(z,t) = \int_0^t C(0,t')f(z,t-t')dt' \tag{42}$$

where

t' is the dummy variable in the integral (s)

$f(z, t - t')$ is the probability density function (pdf) (dimensionless).

Examples of normal (gaussian) and log normal pdfs are shown in Figure 26. The normal distribution has a bell-shaped curve centred on the mean whilst the log normal curve has a long tail to the right with higher values of the variable (x). When x is transformed using the natural logarithm (ln) of x, the distribution becomes gaussian.

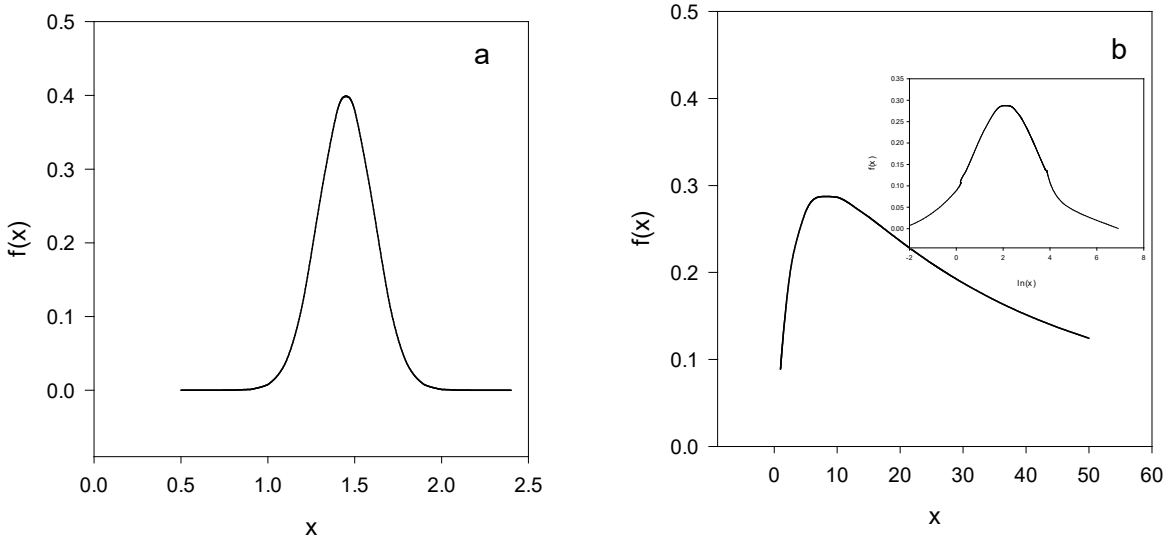

Figure 26. Probability density functions for a) a normal probability distribution f(x) versus variable (x) and b) a lognormal distribution. The probability distribution becomes normal when x is transformed to ln(x). (see insert in panel b).

The mean and variance at a particular depth can be obtained from Eqn (42) for known pdfs, and the concentration as a function of depth can then be obtained. The methods to do this can be found in Jury and Roth (1990). However, the detail required to implement this in a model like MEDLI is fraught with difficulty compared to using the piston flow model.

A simpler version of this was provided by Scotter and Ross (1994). They developed a simple stochastic solute distribution function that is based on soil hydraulic properties. It is an alternative to the approach that treats the soil as a 'black box'. Their model assumes that the velocity in the pores is related to the differential of the hydraulic conductivity with respect to the water content:

$$v(\theta) = \frac{dK(\theta)}{d\theta} \tag{43}$$

This gives a relationship between how fast water is flowing in different pores sizes with the water content. For the Brooks and Corey type of model (see Figure 10) the hydraulic conductivity function is $K(\theta) = K_s\left(\frac{\theta-\theta_r}{\theta_s-\theta_r}\right)^m$ this gives:

$$v(\theta) = \frac{mK_s}{(\theta_s-\theta_r)}\left[\frac{(\theta-\theta_r)}{(\theta_s-\theta_r)}\right]^{m-1} = \frac{mK(\theta)}{(\theta-\theta_r)}$$
$$v_{\max} = \frac{mK_s}{(\theta_s-\theta_r)} = \frac{mK_s}{\theta_s'} \tag{44}$$
$$\theta_s' = (\theta_s-\theta_r)$$

where

K_s is the saturated hydraulic conductivity (m s^{-1})

θ_s is the saturated water content (m^3 m^{-3})

θ_r is the residual water content (m^3 m^{-3}), which is the water content at which capillary water flow is considered to be zero

$m = 2\lambda+3$ is the power coefficient for the Brooks and Corey hydraulic conductivity function

$v(\theta)$ is the pore water velocity of the water at θ

v_{max} is the maximum pore water velocity of the water at θ_s

Scotter and Ross (1994) only considered a v_{max} for saturated soil. However, during non-ponded infiltration when $t < t_p$, the water content in the wetting zone will be < θ_s. This means that the maximum velocity under these circumstances will be less than v_{max} but can still be calculated with Eqn (44).

The relationship between v/v_{max} and the reduced water content $(\theta-\theta_r)/(\theta_s-\theta_r)$, could be used to define the proportion of the solute in the soil that is resident and does not readily move, and the proportion that of solute that is mobile. For example if we considered the boundary between resident and mobile regions of the soil as being defined by v/v_{max} = 0.1, then for m = 10, the reduced water content $(\theta-\theta_r)/(\theta_s-\theta_r)$ at which this occurs is 0.77, which implies that 23% of the reduced water content is in the mobile region and 77% in the resident or immobile region (Figure 27). For m = 4, the reduced water content at which v/v_{max} = 0.1 is 0.46, which implies 54% of the pore space is in the mobile region and 46% in the resident or immobile region. This approach could be used to determine the proportion of the solute mass that is transferred between boxes in the MEDLI model when drainage is occurring. The water content at this divide between resident and mobile regions of the soil may not coincide with the θ_{dul} as was pointed out by Scotter et al. (1993).

For this method to be used to define the resident and mobile regions of the pore space the soil physical parameters listed in Eqn (44) will be required. These are not always available; in Section 5

methods to measure or estimate these parameters are referenced. Also, values of the moisture properties for a range of soil textures are given in Appendix 2.

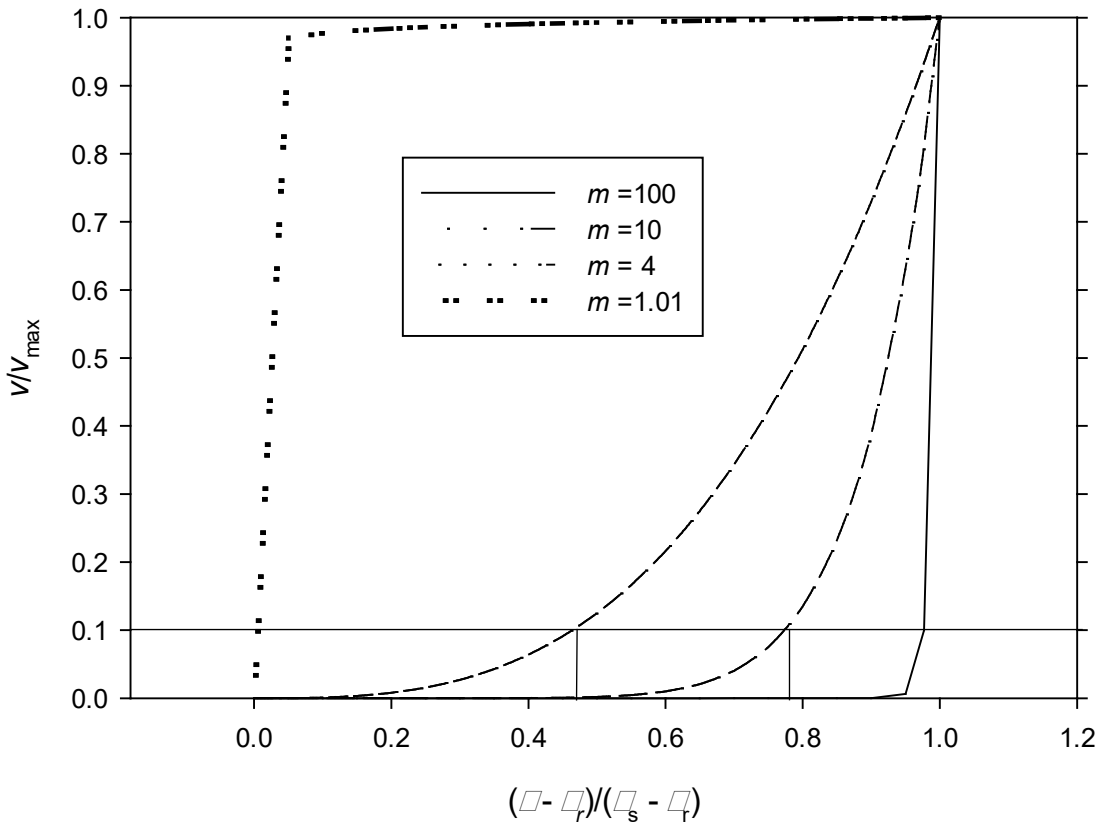

Figure 27. Comparison of the relative pore water velocity (v/v_{max}) with reduced water content ($\theta - \theta_r$)/ ($\theta_s - \theta_r$) for different values of m. A sand is likely to have an m value of 10 whilst a clay will have an m value of 25 or more. At a reduced water content of 0.77, the relative pore water velocity for m = 10 has reduced to about 0.1 of the V_{max}. At m = 4, it has reduced water content of 0.46, at v/v_{max} = 0.1.

The minimum travel time (t_{min}) for a solute to move from the surface to any depth, *z,* is given by:

$$t_{\min} = \frac{z\theta_m^{'}}{mK_m} \tag{45}$$

where

$\theta_m^{'} = \left(\theta_m - \theta_r\right) / \left(\theta_s - \theta_r\right)$ is maximum reduced water content at which t_{min} is calculated

K_m is the hydraulic conductivity at $\theta_m^{'}$ (m s^{-1}).

An analogy is the time taken by a solute travelling in the fastest stream tube to get from the surface to depth *z*. This means that no solute will reach *z* before t_{min}. Eqn (45) could also be used to calculate the time it would take for a solute to get to *z* for stream tubes with any value of θ'. A comparison of t_{min} for a sandy loam and clay to reach a depth of 0.5 m shows that although the proportion of solutes transported are not too different (97% versus 86%) the minimum time for the solutes to travel 0.5 m is

very different (Figure 28) due to the difference in mK_m for the two soils of about 3 orders of magnitude.

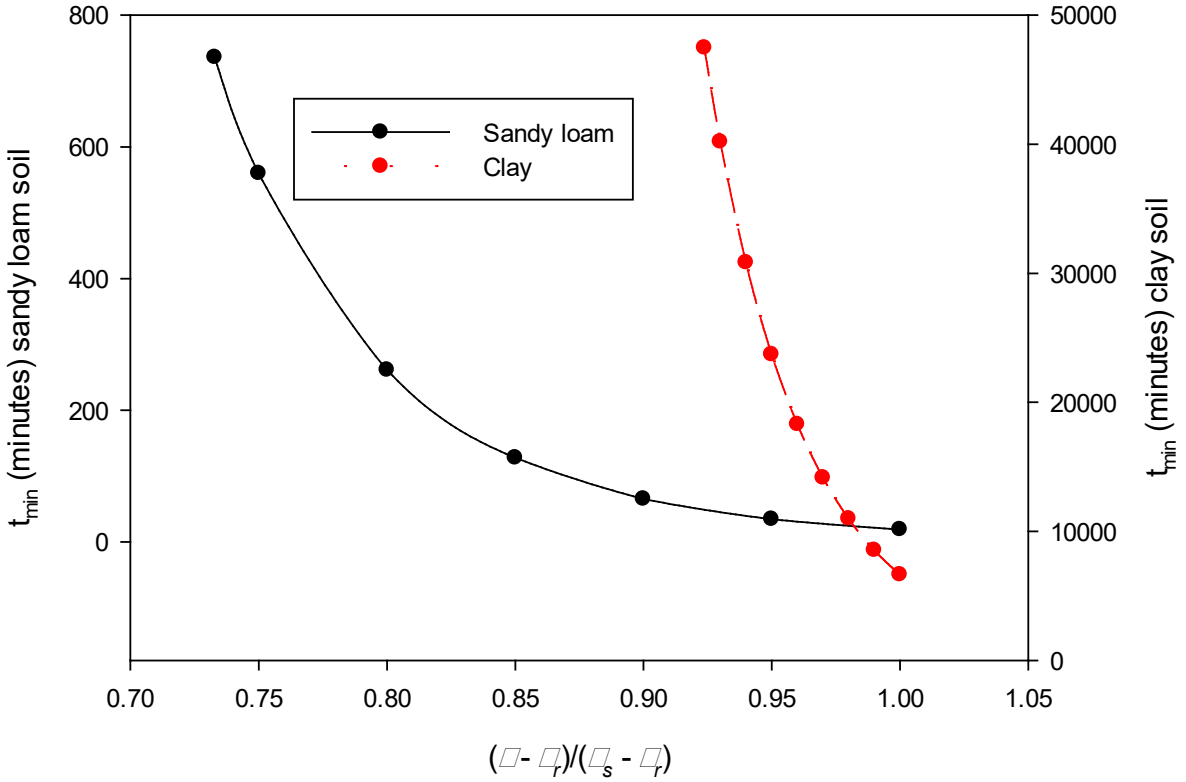

Figure 28. Minimum time (t_{min}) for a solute to reach a depth of 0.5 m calculated with Eqn (45) from saturation reduced water content = 1 to an estimate of the reduced water content at the drained upper limit.

This approach of Scotter and Ross (1994) (Eqn (44)) could be combined with the piston flow model (Eqn (35)) or with the MEDLI model to determine the proportion of solute that was mobile when solute transport was occurring. It can also be used when drainage is occurring with **proportion** of solute being transferred between boxes reducing as the reduced water content decreases towards the θ'_{dul}.

3.4. Corwin Bypass model

A method using a similar solute transport model to MEDLI but using a fixed bypass flow coefficient (γ) of 0.5 was used by Corwin et al. (1991). This means that they considered that only 50% of the solute (chloride) in the soil was mobile and could be leached. This same modelling approach was used by van der Laan et al. (2010) except they used a value for γ of 0.3 for nitrate suggesting that only 30% of the water in the soil was mobile. This difference may reflect a difference in the soil rather than the solute, as the 'field capacity' for the soil used by Corwin et al. (1991) was 0.29 and that of van der Laan et al. (2010) is not stated but from their figures would appear to between 0.15 to 0.3 depending on the depth.

The use of a fixed value for the partition of the mobile and resident solute transport would be a possible way to improve the solute transport model in MEDLI, and in the first instance a value of 0.5 as used by Corwin et al. (1991) along with their computational methodology would seem an appropriate estimate if no other data were available. This method would also provide a relatively simple way to modify MEDLI to accommodate the mobile/immobile concept into MEDLI and if combined with the Scotter and Ross (1994) approach to determining the mobile/immobile regions would result in a more realistic solute transport model.

3.5. Burns Equation

The Burns equation (Burns, 1975) considers the transport of solute in a soil subject to the net infiltration (infiltration less evapotranspiration) of *Du*(*t*) where *Du* is the sum of the net infiltration at elapsed time *t*. Burns (1975) original equation is unsound due to some of the assumptions in it but the concept is very useful (Scotter et al., 1993). Towner (1983) found that if the spatial (depth) discretisation (Δz) is small compared to *Du* then the Burns equation can be simplified to:

$$X(z, Du) = \exp\left[-z\theta_d / Du(t)\right] \tag{46}$$

where

X is the fraction of solute that has leached below depth *z* at time *t* since the fertilizer was applied at the soil surface

$Du(t) = \int_0^t i(t') - Et(t')\,dt'$ is the net infiltration (m) with *i* the infiltration rate (m s^{-1})) and *Et* (m s^{-1}) is the evapotranspiration (E_s + *T*) (see Section 2.3) up to time *t* and *t'* is the dummy variable of integration.

θ_d is the water content of the mobile region. Burns originally had this as the field capacity water content but as Scotter et al. (1993) suggested, this should be treated as an operationally defined function. See Section 3.3 above.

The fraction of solute leached (*X*) below a depth of 0.25 m with *Du* for three values of θ_d shows that as θ_d increases less solute is leached as there is more soil pore volume for the excess water (*Du*) to be stored in (Fig. 29). The fraction of solute leached also increases as the amount of drainage increases.

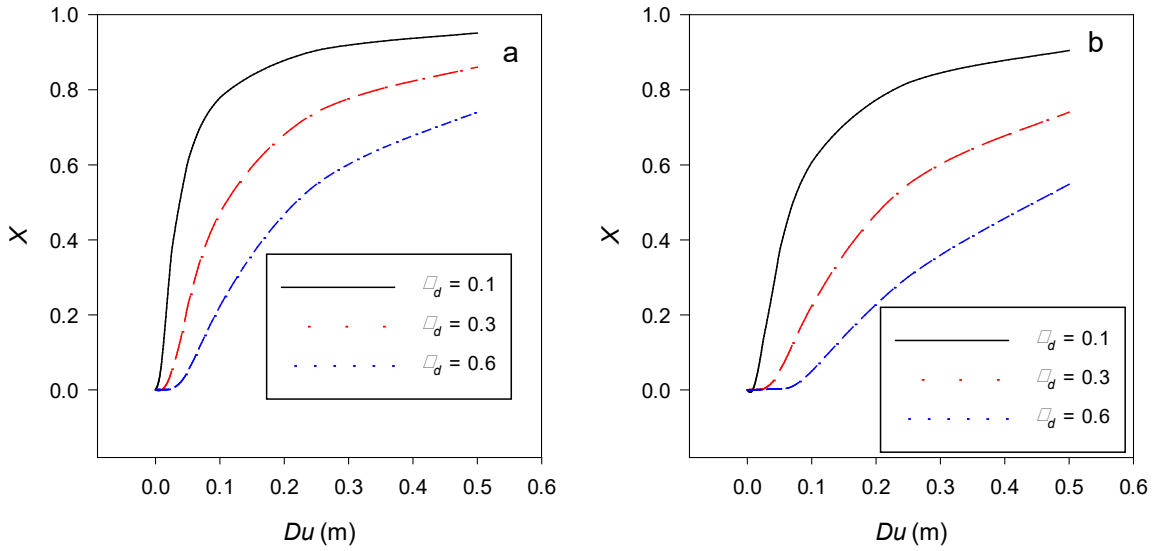

Figure 29. Fraction of surface applied solute leached beyond a) 0.25 m and b) 0.5 m with three values of θ_d as a function of Dw. The curves are calculated with Eqn (46).

Scotter et al. (1993) also provide solutions for the situation where the soil initially had a concentration of C_0 (kg m^{-3}) present and is then leached by the water with zero concentration this results in the leaching fraction for the solute being given by:

$$X(z,Du)=\frac{Du}{z\theta_d}\left[1-\exp\left(-\frac{z\theta_d}{Du}\right)\right] \quad (47)$$

This solution would be applicable to MEDLI for solutes that were initially present in the soil but not in the wastewater.

For MEDLI, a solution of when the solute is applied in the irrigation water and a solute mass of M_i (kg m^{-2}) is applied can be obtained using, (Scotter et al. 1993):

$$X_k(z,Du_k)=1-\left(\frac{z\theta_d}{Du_k}+1\right)\exp\left(-\frac{z\theta_d}{Du_k}\right) \quad (48)$$

where

$Du_k = Du(t) - Du_{k_0}$ is the net infiltration since the start of the *k*th irrigation event (m)

Du_{k_0} is the net infiltration prior to the *l*th irrigation event (m).

Using the principle of super positioning we can then calculate the mass of solute leached beyond any depth by:

$$MT(z,Du(t))=C_0Du(t)\left[1-\exp\left(-\frac{z\theta_d}{Du(t)}\right)\right]+\sum_{k=1}^{n}\left[M_k\left\{1-\left(\frac{z\theta_d}{Du_k}+1\right)\exp\left(-\frac{z\theta_d}{Du_k}\right)\right\}\right] \quad (49)$$

$$M_k = Cs_k Ir_k$$

where

$MT(z,Du(t))$ is the total mass density of solute leached beyond z (kg m^{-2})

$Du(t)$ is the total drainage at time t since t = 0

M_k is the solute mass density applied in the kth irrigation (kg m^{-2})

Cs_k is the concentration of the solute in the irrigation water during the kth irrigation (kg m^{-3})

Ir_k is the depth of irrigation applied during the kth irrigation (m)

k is the irrigation index parameter

n is the total number of irrigations up to time t

The fraction of the mass applied and initially present in the soil that has been leached beyond the depth z is given by:

$$X(z,Du(t))=\frac{MT(z,Du(t))}{C_0.Z_T+\sum_{k=1}^{n}M_k} \quad (50)$$

where Z_T is the depth to bottom of the model domain (m). When $z = Z_T$ in Eqn (50) then this is the fraction of the mass of solute leached out of the soil.

The concentration as a function of Du_k and z can also be calculated using the principal of super positioning by:

$$C(z,t) = \sum_{k=1}^{n}\left[M_k \left\{ \frac{(z\theta_d)^2}{Du_k)^3} \exp\left(\frac{z\theta_d}{Du_k} \right) \right\} \right] + C_0 \left[1 - \exp\left(\frac{-z\theta_d}{Du(t)} \right) \right] \quad (51)$$

where k is the index for the number of irrigation events with a total number of n events by time t. In Eqn (51) when $k = 1$, $Du_0 = 0$ as this will be the first irrigation event and so no drainage prior to $t = 0$ has occurred.

This approach could be incorporated into MEDLI with the leaching fraction solutions (Eqns (47, 48 50 and 51) used with bottom depth of the modelling domain to give the fraction of solute mass leaching out of the soil to deep drainage. This would require summing the fractional loss for each irrigation event. Magesan et al. (1999) used the Burns equation approach described here to successfully model chloride, tritium and nitrate in cores and a tile drained field but was less successful in modelling bromide in the field.

The concentration as a function of depth could be calculated from Eqns (49) and (50) either using the mid-point depth of the boxes in MEDLI or the top and bottom depths and then averaging the concentration.

There are some problems with the use of the Burns approach in MEDLI. The main issue is that the analysis assumes that the solute is conserved within the soil. For nitrate, this implies that no losses occur due to transformations (e.g., denitrification or plant uptake), and no additions occur due to nitrification from ammonia.

The above equations do not consider retarded solutes but multiplication by the retardation factor would allow retarded solutes to be modelled. For layered soil profiles the value of θ_d could be different between the layers, but it is trivial to modify the equations to account for this. For a two layered soil this would modify $z\theta_d$ in the above equations by:

$$\begin{aligned} z\theta_d &= z\theta_{d1}, \qquad 0 < z \le z_1 \\ z\theta &= z_1\theta_{d1} + (z - z_1)\theta_{d2}, z_1 < z \end{aligned} \quad (52)$$

where

z_1 is the depth of layer (m)

θ_{d1} is the value of θ_d for layer 1

θ_{d2} is the value of θ_d for layer 2.

The Burns equation approach only requires knowledge of one soil factor θ_d which makes it attractive. This could be obtained either using the approach given in Section 3.3 or by allowing $\theta_d = \theta_{dul}$.

4. Discretization of Water and Solute Transport and Sequence of Calculation

The transport of water and solutes are coupled by the velocity of the water in the soil pores, which moves the solutes through the soil profile. This has been shown in Section 3. The order in which the various processes are solved will influence the results especially for drainage.

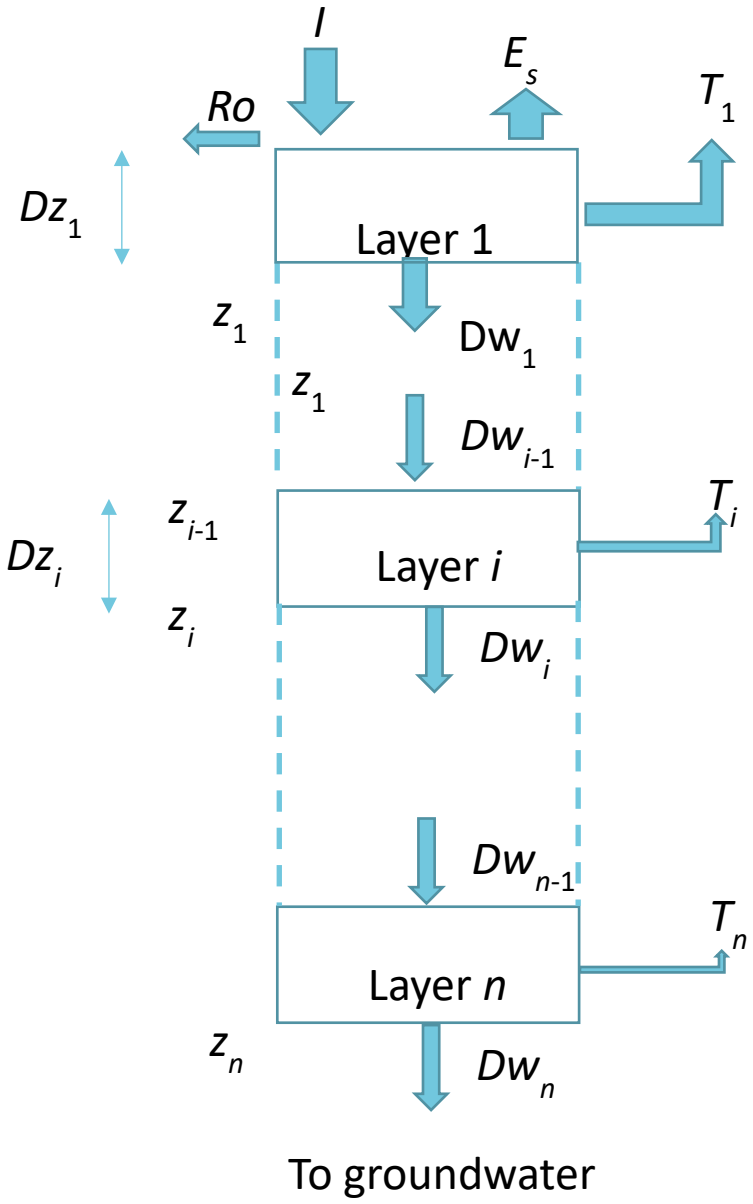

Figure 30. Schematic diagram of water transport in a box model. I is the infiltration, E_s is the soil evaporation, RO is runoff, T is the transpiration and Dw is drainage. Dz is the thickness of the boxes and z is the depth to the bottom of a box.

The processes for water transport are illustrated in Figure 30 with infiltration entering through the first box. For the Green and Ampt model, infiltration could be added to multiple boxes depending on the model time step. E_s is the soil evaporation, which comes only from the first two boxes. Water uptake will occur from all the boxes (that contain roots) until the transpiration demand is met. Drainage (*Dw*) occurs between the boxes, but only when the water content is greater than the drained upper limit.

The sequence of solving is suggested as follows:

- Added infiltration into the soil profile. The Green and Ampt model as given in Section 2.1.3.1 is suggested as the best approach. However, the GA method will require a smaller time step than 1 day if it is to be implemented. The use of the GA method should not be difficult to implement for irrigation events as the surface application rate and the application time is known. However, for rainfall this could be more difficult to implement as often only daily rainfall will be known. The daily rainfall data could be disaggregated to give the necessary duration and intensity data using the method of Connolly et al. (1998). Alternatively, a hybrid approach could be implemented with the GA method used for the irrigation events and the present Curve Number approached used for rainfall.
- Calculate the runoff. The method if the hybrid infiltration model was used would calculate runoff as given in Section 2.1.6 for irrigation events and use the curve number for rainfall events.
- Calculated soil evaporation and transpiration as given in Section 2.3.
- Calculate drainage by the Sisson method as suggested in Section 2.2 and Appendix 3.
- Update the water content in each box.

The water transport should be solved before calculating the solute transport. The processes for solute transport are given in Figure 31.

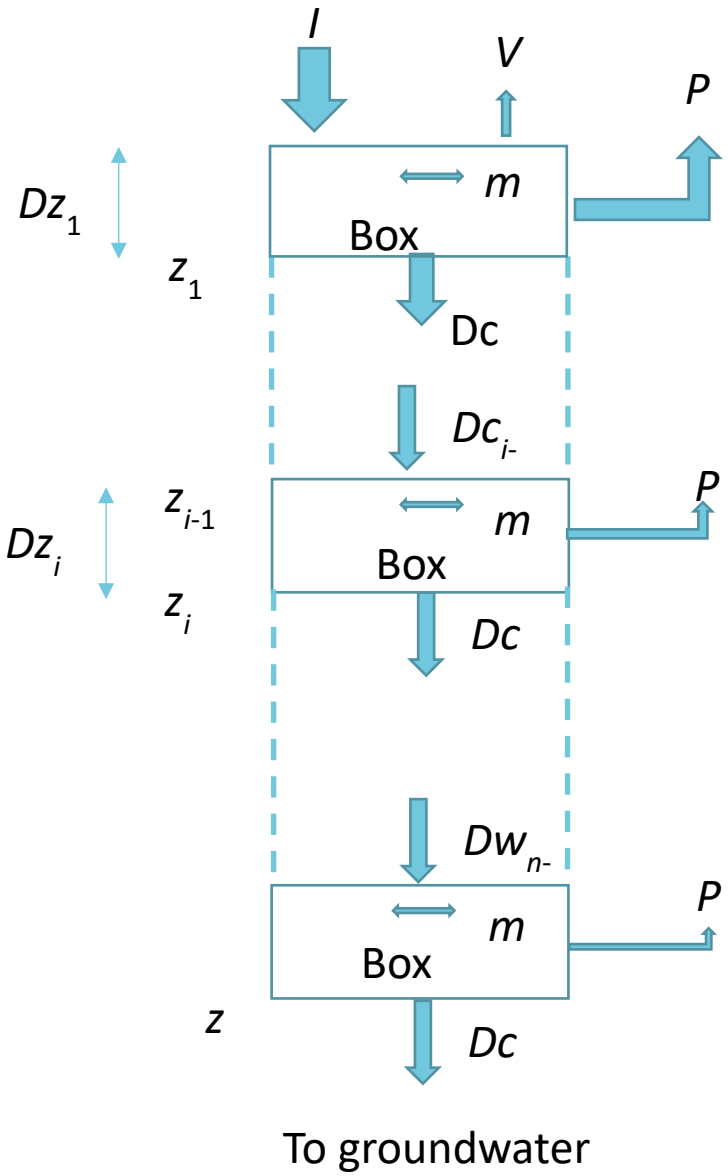

Figure 31. Schematic diagram for solute transport in a box model. Ic is the solute that enters the soil via infiltration, V is volatilisation of solutes such as nitrous oxides and ammonia, P is uptake by plants and m is microbial transformations and mineralisation immobilisation processes (kg s^{-1}).

Infiltration of effluent will introduce new solutes into the model domain. Volatilisation from the soil is likely to be small unless urea is added in the effluent. Oxides of nitrogen will volatilise if denitrification occurs and are assumed to be lost to the atmosphere and has been shown in Figure 31.

Plant uptake of dissolved solutes will occur in the transpiration water. Microbial transformations and mineralisation/immobilisation processes will result in gains or losses to the nitrogen pool.

The easiest way to modify the solute transport in the present MEDLI model would be to only allow the solute in the mobile pore space to be transported during drainage. The simplest way to do this would be to adopt the split suggested by Corwin et al. (1991) and have only 50% of the solute mass in a box available for transport and adopt the methodology of Corwin et al. (1991). This would require only a minimal recoding of the MEDLI model and the computational methodology is well set out by Corwin et al. (1991).

The Burns solute transport model (Section 3.5) would seem the easiest to implement but it does not have the ability to incorporate plant uptake and gains and losses. However, since time is incorporated into the model via the net infiltration parameter *Du* it would be possible to modify the concentration at a depth by the cumulative gains or losses up to this time. The Burns model would be particularly easy to implement for the deep drainage loss at the bottom boundary of the model domain.

The value of mobile water content region for solute transport (θ_d) should be calculated with the Scotter and Ross (1994) approach if the data is available, otherwise the drained upper limit θ_{dul} could be used as an estimate. The present approach in MEDLI which assumes all solute is displaced by the infiltrating solution will overestimate leaching.

With regard to the development of upgrades the recommendations are:

1. Implement the Corwin et al. (1991) methodology with 0.5 as the bypass flow coefficient. If the data is available use the Scotter and Ross (1994) method to alter the proportion of the flow in the mobile region.
2. The Burns equation should be further considered but will require modification to account for gains and losses of solutes. The methodology provided in this report is a first step to implement this but may overestimate the concentrations and leaching losses as these assume that the net losses and gains is zero. The Burns equation may be a particularly good approach for determining the leaching of solutes beyond the bottom boundary of the model domain.

5. Data required and measurement methods or estimation

In order to use the methods described in this report certain soil properties will be needed. These can (best) be derived from measurements or estimated from pedo-transfer functions. The ASRIS (www.asris.csiro.au) soil data base is also available and information can be obtained from this. In Queensland the SALI (https://www.data.qld.gov.au/dataset?organization=environment-and-science&q=soils&sort=score%20desc%2C%20metadata_modified%20desc) has data that could be used along with pedo-transfer functions to obtain some of the data required to use the pedo-transfer models. The minimum required data are:

1. Saturated hydraulic conductivity, Ks. If the GA model is used for infiltration and the soil is bare some account of the surface sealing (reduction in Ks) will be required. Information on this can be found in Connolly et al. (1997; 2001).
2. The air entry potential or bubbling pressure of the soil, ψb
3. Slope of the relationship between water content and matric potential, λ
4. Saturated water content, θs
5. Residual water content, θr. This is the water content at which capillary flow of water is deemed to have ceased.
6. Water content at the drained upper limit (field capacity), θdul

The saturated hydraulic conductivity can be measured by a variety of methods and their pros and cons are given by Mckenzie and Cresswell (2002) along with a description of the other methods in the book by (Mckenzie et al. 2002).

The water content parameters can be derived using laboratory methods on undisturbed soil samples (Cresswell, 2002). The value of θ_s can be derived for the topsoil when K_s measurements are being made. The two-point method proposed by Cresswell and Paydar (1996) with measured matric potential points of -1.0 and -150 m and either bulk density or saturated water content would provide a method that is not too time consuming nor expensive.

The hydraulic conductivity can be measured with a number of methods in the field and laboratory (see various chapters in Mckenzie et al. 2002) and Cook et al. (2007) and Cook and Broeren (1994). Relatively rapid field methods such as those of Vandervaere (2000), the sorptivity method in Cook

and Broeren (1994) or the Beerkan method (Bagarello et al., 2017) would be useful in obtaining hydraulic conductivity measurements.

Methods to predict the hydraulic properties of soils from simpler soil measurements (texture, soil cation exchange capacity, -15 bar moisture content etc.) are called pedo-transfer functions (PTFs), and have been summarised by Cook and Cresswell (2007). These methods are improved if one or more water content - matric potential pairs are available. Recently Zhang and Schaap (2017) have released a newer version of the Rosetta PTF (http://www.u.arizona.edu/~ygzhang/rosettav3/), which they claim is an improvement on earlier versions. PTFs often have a large uncertainty associated with the estimated soil physical properties, especially hydraulic conductivity. There is also a large degree of uncertainty in measured soil physical properties especially at the spatial scales where MEDLI will be applied, so the use of PTFs to obtain soil physical properties for MEDLI modelling may be acceptable.

6. Conclusions

This report considers how developments in soil physics for water entry, storage and drainage could be included to provide incorporation of more physically based models for water transport in the MEDLI model. This analysis suggests that the Green and Ampt infiltration model with the implicit solution of Barry et al. (1995, 2005) along with the time to ponding model of White and Broadbridge (1988) (Eqn (16)) and the time-compression analysis of Salvucci and Entekhabi (1994), could result in a physically based infiltration/runoff model (see Appendix 1). This new infiltration/runoff model will almost certainly require the time step of the MEDLI model to be less than 1 day when infiltration is occurring. The model has been extended to nonuniform soil water content profiles and soil physical properties using the methods of Bouwer (1969). *Testing of this new model against the CN infiltration/runoff model in MEDLI should be a first step in any evaluation.*

For drainage, two models are presented: one from Sisson et al. (1980) that relies on gravitational (free) drainage from an initially saturated or uniformly wet soil profile, and the other from Youngs (1960) that uses the Green and Ampt approach, which assumes that a shallow water table is present. For MEDLI the more likely situation is free drainage so the Sisson et al. (1980) model is suggested. This model works well for uniform initial conditions and soil physical properties and has been adapted in this report to non-uniform initial conditions and soil physical properties. In order to use this model a timer to be set when drainage first starts in the soil profile will be required. The analysis here also shows that all cascading box models are highly dependent on the time step and are unreliable.

The root water uptake models introduced here use the Feddes type modelling approach to determine the uptake potential and combined with a depth weighting function developed from the McAneney and Judd (1983) study should provide a way to provide a physically based transpiration and evaporation model.

The *solute transport* models based on Corwin et al. (1991) would be the simplest to implement in MEDLI and when combined with the partitioning model of Scotter and Ross (1994), should provide an improved methodology that is only slightly more complicated than that currently used in MEDLI. Alternatively, just using the partitioning model of Scotter and Ross (1994) with the present MEDLI model would be a good first step. The Burns equation would provide a good method for estimating leaching loss to deep drainage but will need to be modified to account for gains and losses of solutes due to plant uptake and soil transformational processes.

This report has put forward a number of methods that could be used to have more physically based methods implemented in MEDLI. Unfortunately, time has not allowed for the comparison and evaluation of the different methods, but this should be done before their implementation in MEDLI.

7. Recommendations for future actions and investigation

A number of issues relevant to this report were identified but could not be addressed within the time frame provided. These are listed here as recommendations for future investigations.

1. Runoff

The runoff predictions from CN and Green and Ampt should be compared against data from a range of soil types under irrigation to determine if Green and Ampt approach could provide a significantly better estimate of runoff from irrigated soils than CN. This comparison study should use the White et al. (1989) method for calculating t_p.

Such a study is necessary because King et al. (1999) found that GA was better than CN at the daily time scale, where CN underestimated runoff. The GA model was considered to give better results when the duration and intensity was included in the daily estimates of runoff. More recently Ficklin and Zhang (2013) indicate that the CN was better at predicting runoff in a catchment than GA. The GA overestimated the runoff in small events but gave better results than CN method for large events.

However, these papers use the Mein and Larson (1973) method for calculating time to ponding (t_p). This would create a bias in the results for small storms, which is what the authors found. So the comparison study should use the White et al. (1989) method for calculating t_p.

2. Drainage

*The deep drainage predictions from cascading bucket models should be compared with Sisson et al. (1980) model predictions using data from irrigated soils to determine if the Sisson approach could provide a significantly better estimate of deep drainage. It may also be worth exploring if the **K- θ** function could be to better inform the Drainage Factor parameter used in cascading bucket models and so improve their performance in predicting deep drainage.*

3. Solute Leaching

Comparison and evaluation of the different methods proposed (Corwin et al. (1991), Scotter and Ross (1994) and Burns Equation should be done before their implementation in MEDLI.

Consideration of more complex models such as SWIM (in APSIM) has pros and cons. The pros are this will be more accurate because the drainage flux will be better calculated using the Richards equation, so long as the parameters used in it are correct.

The cons are that this will require both the K-θ and ψ-θ relationships and these are often not available. The K-θ and ψ-θ relationships can be estimated using pedo-transfer functions. As SWIM solves the advection dispersion equation (ADE) to determine solute transport, it is considerably more complicated than what is proposed here. It will be slower to run as it will use much smaller time steps and soil layer depth increments to avoid oscillation and mass balance problems. Adoption of SWIM will require greater knowledge and skill in running numerical models.

The utility of the simple approach of assuming piston flow leaching of solutes between soil layers with partial or complete mixing is that it is simple to calculate.

Performance for modelling solute leaching in irrigated soils should be considered.

The Transfer function model has been used for practical modelling in irrigated soils, but only at experimental sites.

4. Obtaining input parameter values

Simple methods of determining the K-θ and ψ-θ relationships for soils could be compared and validated. There are a number of reviews on this topic in the literature and such a comparison for Australian soils has been done (Minasny and McBrateney, 2000).

Such a study could consider measuring bulk density and particle size analysis of each soil layer and then using pedo-transfer functions to estimate the soil properties. This study would build on what has been done by Minasny and McBrateney (2000) and Cook (2017).

Neil Huth (Huth et al., 2012) method for estimating **Ψ- θ** and K- **θ** involved using spline functions to determine for the moisture content at any matric potential from measurements at four points: saturation, drained upper limit, lower limit and oven dry. They estimated the hydraulic conductivity from these moisture data points and measurements of the saturated hydraulic conductivity and matric hydraulic conductivity. In order to use their methods these measurements would be required.

5. Implications of issues identified

Implications of the issues identified in this report are summarised and provided in Table 1.

Table 1. Strategic overview of the issues and implications raised by this review.

Model Process	Issue(s) identified	Current handling	Proposed alternative(s)	Implications	Degree of difficulty	Importance	Recommendation
Infiltration/ Runoff quantity	Curve number (CN) – Dryland only, not tested under irrigation. Datasets underlying model testing limited to heavy textured soils.	CN used as a pragmatic solution in most daily time-step hydrological models	Green & Ampt (G&A) improved with better approach to calculating time to ponding, be considered to replace CN.	Can't be adopted immediately into MEDLI. Need to compare the improved GA model with the CN model before the infiltration model in MEDLI is changed. Proposed G&A model will require the rainfall input to be at a time step of less than 1 day. and also requires additional parameters for each soil horizon: • Sub-daily rainfall data • Lambda – defines relationship between water content and matric potential. • Sorptivity – a measure of the how rapidly a dry soil is wetted due to capillarity only. • Air-entry matric potential	Currently high, as limited resources to adapt the model; Limited availability of datasets (with the exception of sub-daily rainfall for many areas), Limited in-house soil physics expertise	Infiltration is a key factor in determining deep drainage and solute transport and if incorrectly handled, will have significant implications reef models.	Investigate need and develop a detailed case for dedicated resource(s) to: Adapt G&A model to non-uniform soils and to develop datasets for new parameters using pedo-transfer functions (PTFs) where possible which will need to involve both field studies and "mining" of the soil physics literature.

Model Process	Issue(s) identified	Current handling	Proposed alternative(s)	Implications	Degree of difficulty	Importance	Recommendation
Deep drainage	The prediction of drainage in the soil by MEDLI and other cascading box models is dependent on the thickness of the soil layers chosen and time step used in the model. The draining profile shape is also unrealistic. Hence, daily cascading box models poorly represent actual drainage. Also, the order of calculation of the drainage and evaporation process can affect the drainage if they are implemented sequentially Datasets underlying model testing limited to heavy textured soils – possibly under rain-fed conditions.	Cascading bucket using daily time-step where the drainage factor (proportion of drainable water draining) is calculated using an exponential function based on the saturated hydraulic conductivity and drainable porosity of the soil layer. As such, the drainage factor has no real physical meaning.	Consider using the Sisson model, based on gravitational drainage (must have no shallow water tables). NOTE: *shallow water tables are unlikely to be modelled by MEDLI.* Refer Appendix 3	Sisson model requires additional parameters as it is based on the K-**θ** function, but these may be able to be estimated from known parameters. Sisson method assumes that at the soil surface, the water content reduces to a specified value (less than DUL) as drainage proceeds. A value of 0.83 x DUL may be suitable but this will need to be checked by comparison with numerical models such as HYDRUS1D.	Currently high, proposed Sisson model not currently built or tested. Limited resources to adapt the MEDLI model Limited availability of datasets (with the exception of sub-daily rainfall for many areas) Limited in-house soil physics expertise	High	Investigate need and develop a detailed case for dedicated resource(s) to: • Adapt Sisson model to non-uniform soils • Develop datasets for new parameters using pedo-transfer functions (PTFs) - methods to predict the hydraulic properties of soils from simpler soil measurements - where possible which will need to involve field studies.
Root water uptake	MEDLI transpiration algorithm does progressively reduce root water uptake as plant available soil water approaches zero.	Partitioning of potential transpiration favours wetter layers and excludes layers with no plant available water. The upper two soil layers are also weighted more heavily as these layers will contain more roots. The actual transpiration from each layer is then limited to the amount of plant available water stored in that layer.	Feddes model uses a *bent stick* approach with two zones– • for near saturation/ aeration limitation. • for when soil dried below a specified limit.	Relatively easy to adopt into MEDLI. Will need extra parameter for the soil lower water content threshold. Note: Transpiration and soil evaporation will affect drainage predictions. Order of calculations important	Low.	Improves transpiration modelling in schemes where irrigation is well below irrigation demand.	Include in current planning for model development with current resources

Model Process	Issue(s) identified	Current handling	Proposed alternative(s)	Implications	Degree of difficulty	Importance	Recommendation
Soil evaporation for soils with dead cover (crop residues)	MEDLI poorly models the impact of crop residual cover on soil evaporation.	The fraction of soil surface with any cover (transpiring or non-transpiring) is deemed to show zero soil evaporation.	The residual cover function from HOWLEAKY? should be considered/adopted to account for the mass of residual dead plant material reducing soil evaporation.	Relatively easy to adopt into MEDLI. No new parameters would be required. A "Desorptivity" parameter is equivalent to "CONA" used in MEDLI. Improved soil evaporation modelling in schemes where residual cover occurs following crop removal or as plant canopy regrows following harvest.	Moderate as some further investigation into the HOWLEAKY residual cover function is required. However, adoption into the MEDLI model appears straight forward	Moderate to high Transpiration and soil evaporation will affect irrigation demand and drainage predictions. Order of calculations important	Consider including in current planning for model development subject to availability of resources
Soil evaporation from bare soil	MEDLI does not model re-wetting of soil surface towards the second soil moisture content in the absence of rain or evaporation, potentially underestimating soil evaporation from bare soils.	Ritchie (1972) evaporation algorithms are used to estimate soil evaporation which is then subtracted from the water content of the top two soil layers. Upward flux is ignored.	Force-restore method proposed by Cook et al. (2008).	As bare soil scenario would be rarely modelled within MEDLI, the extra complication may be unwarranted.	Moderate – need for investigation	Low	Consider including in current planning for model development subject to availability of resources
Plant cover factor	Sutanto et al. 2012 calculates a plant cover factor from LAI uses Beers law with an extinction coefficient of -0.463 while MEDLI uses and extinction coefficient of -0.65.	In the pasture model, MEDLI uses a sine curve function of plant transpiring cover over thermal time. The transpiring cover, expressed as the proportion of soil area is then used to calculate potential transpiration. The crop module taken from EPIC uses LAI which is converted to transpiring cover using Beers law with an extinction coefficient of -0.65.	Plant cover function of Sutanto et al. (2012) (used in HYDRUS1D)	This would apply to the crop module.	Moderate as some further investigation into the Sutanto model is required. Adoption into the MEDLI model appears straight forward. Need further investigation of LAI on evaporation with measured data.	Transpiration and soil evaporation will affect irrigation demand and drainage predictions. Order of calculations important	Consider including in current planning for model development subject to availability of resources

Model Process	Issue(s) identified	Current handling	Proposed alternative(s)	Implications	Degree of difficulty	Importance	Recommendation
Solute Transport	Simple piston-flow model assumes all the existing soil water with its dissolved solutes is displaced by the infiltrating solution, hence overestimating leaching. For a model such as MEDLI, the development of the actual shape of the solute distribution may not be as important as calculating where the solute front is.	Simple piston-flow model	Adopt Corwin et al. bypass model (uses mobile/ immobile concept) + Scotter & Ross (1994) to determine mobile/immobile regions for a more realistic solute transport model. The solute would be transported in the mobile pore space during drainage. Adopt the split suggested by Corwin et al. (1991) and have only 50% of the solute mass in a box available for transport. And/or The Burns equation could be incorporated into MEDLI using the leaching fraction algorithms to give the fraction of solute mass leaching out of the bottom boundary of the soil model domain to deep drainage. .	This would require only a minimal recoding of the MEDLI model and the computational methodology is well set out by Corwin et al. (1991). Extra parameters include a fixed bypass flow coefficient for the soil. The Burns equation works on cumulative drainage and either a uniform profile or pulse input. Unlike the Corwin et al. model, It would be more difficult to incorporate into MEDLI's bucket model approach. The Burns equation also assumes that the solute is conserved within the soil (does not allow for plant uptake and gains and losses of solutes from mineralisation/ immobilisation). However, it may be possible to do this with a time-based function, but this would have to be investigated further	Moderate as the Corwin model is well described and the Burns equation is also easily implemented. Equations need explanation for implementation. The Burns equation approach only requires knowledge of one soil factor (the water content of the mobile region).	High	Investigate need and develop a detailed case for dedicated resource(s) to: Develop solute transport model and to develop datasets for new parameters using PTFs where possible which will need to involve field studies.

Model Process	Issue(s) identified	Current handling	Proposed alternative(s)	Implications	Degree of difficulty	Importance	Recommendation
Runoff Quality*	Need to estimate dissolved P concentration and hence P loss in runoff from effluent irrigation areas.	No attempt to model quality of runoff water. MEDLI will indicate any effluent-sourced P lost in runoff if the runoff is likely to contain effluent.	A relationship between soil solution P and soil Colwell-P and Phosphorus buffer index could be used to estimate runoff P concentration	Cannot be adopted immediately into MEDLI. This will need further development and testing against field data	Currently high, due to requirement of investigations and due to limited resources.	High. P loss in runoff is of greater concern than P leaching losses in most soils (with the exception of sandy soils)	Investigate need and develop a detailed case for dedicated resource(s) to: Field trials/data needed; Soil Chemist input needed
Denitrification*	No denitrification model has been validated against datasets. Models assume a potential denitrification rate for the soil (depends on soil pH etc) which can then be scaled back within the model according to soil water content (> DUL) and temperature and soil carbon. This potential value needs validation.	A first order kinetic equation between nitrate-N and denitrification per mass soil per day is assumed which is suitable for high strength effluents. The potential denitrification rate is defined by the user for the soil but uses 10%/day as default. This is scaled back according to soil water content (> DUL) and temperature and presence of labile soil carbon.	Approaches used in APSIM and DairyMod and others need to be reviewed in the light of data.	Cannot be adopted immediately into MEDLI.	Limited availability of datasets. Uncertainty of predictions from such an approach could be high (e.g., see Cook et al 2019; Wallach et al 1990).	High Denitrification is a poorly estimated in the nitrogen mass balance. It represents a possible legitimate sink for nitrogen during effluent irrigation.	Investigate need and develop a detailed case for dedicated resource(s) to: Field trials/data needed (see Beggs et al. 2011 for a good review and method); Soil Chemist input needed
Soil organic carbon specification	The current MEDLI suite of lab analysis only offers to measure OC in topsoil layer.		The need to specify the full thickness of organic carbon layer in the soil rather than just use the default value could be made more explicit?				

* From QWMN MEDLI Science Review Report by Phil Moody.

8. References

Addiscot T, Smith J and Bradbury N (1995). Critical evaluation of models and their parameters. *Journal of Envirtonmental Quality* **24**: 803-807.

Ali S, Islam A, Mishra PK and Sikka AK (2016). Green-Ampt approximations: A comprehensive analysis. Journal of Hydrology **535**: 340-355.

Bagarello V, Di Prima S, and Iovino M (2017). Estimating saturated soil hydraulic conductivity by the near steady-state phase of a Beerkan infiltration test. *Geoderma*, *303*, 70-77.

Barry DA, Parlange J-Y and Sander GC (1995). Comment on "Explicit expressions for Green-Ampt (delta function diffusivity) infiltration rate and cumulative storage" by G.D. Salvucci and D. Entekhabi. *Water Resources Research* **31(5)**: 1445-1446.

Barry DA, Parlange J-Y, Li L, Jeng D-S and Crapper M (2005). Green-Ampt approximations. *Advances in Water Resources* **28**: 1003-1009.

Beggs, RA, Hills, DJ, Tchobanoglous, G, Hopmans, JW (2011). Fate of nitrogen for subsurface drip dispersal of effluent from small wastewater systems. Journal of Contaminant Hydrology, **126 (1-2):** 19-28.

Beven KJ and Freer J (2001). Equfinality, data assimilation, and uncertainty estimation in mechanistic modelling of complex environmental systems using the GLUE methodology. *Journal of Hydrology* **249**: 11-29.

Biggar, JW and Nielsen, DR (1976). Spatial variability of the leaching characteristics of a field soil. *Water Resources Research* **12**: 78-84.

Bridge BJ and Ross PJ (1985). A potable microcomputer-controlled drip infiltrometer. II. Field measurement of sorptivity, hydraulic conductivity and time to ponding. *Aust. J. Soil Research* **23**: 393- 404.

Bower H (1969). Infiltration of water into nonuniform soil. *Journal of the Irrigation and Drainage Division, Proc. ASCE* **95(IR4)**: 451-462.

Bower H (1978). Groundwater Hydrology. First ed., Wiley, New York.

Brooks RH and Corey AT (1964). Hydraulic properties of porous media. Colorado State University, Fort Collins. Hydrology Paper no. 3, 27p.

Brooks RH and Corey AT (1966). Properties of porous media affecting fluid flow. *Journal of the Irrigation and Drainage Division* **92(2)**: 61-88.

Broadbridge P, Knight JH and Rogers C (1988). Constant rate rainfall infiltration in a bounded profile: Solutions of a nonlinear model. *Soil Science Society of America Journal* **52(6)**: 1526-1533.

Broadbridge P and White I (1987). Time to ponding: Comparison of analytic, quasi-analytic, and approximate predictions. *Water Resources Research* **23(12)**: 2302-2310.

Broadbridge P and White I (1988). Constant rate infiltration: A versatile nonlinear model 1. Analytic solution. *Water Resources Research* **24(1)**: 145-154.

Brutsaert W (2005). Hydrology-An Introduction. Cambridge University Press, UK,ISBN 978-0521824798.

Burns IG (1975). An equation to predict the leaching of surface-applied nitrate. *Journal of Agricultural Science* **85**: 443-454.

Carslaw HS and Jaeger JC (1959). Conduction of Heat in Solids. 2nd. Ed., Oxford University Press, New York.

Clapp RB and Hornberger G (1978). Empirical equations for some soil hydraulic properties. *Water Resources Research* **14(1)**: 601-604.

Clothier BE, Scotter DR and Kerr JP (1977). Drainage flux in permeable soil underlain by a coarse-textured layer. *Soil Science Society of America Journal* **41**: 671-676.

Clothier BE and Heiler TD (1983). Infiltration during sprinkler irrigation: Theory and field results. *Advances in Infiltration*, Chicago, Illinois, ASAE.

Clothier BE and Scotter DR (1985). Water and solute movement in the root zone. *New Zealand Journal of Agricultural Research* **19(4)**: 187-192.

Connolly RD, Freebairn DM and Bridge BJ (1997). Change in infiltration characteristics associated with the cultivation history of soils in south-eastern Queensland. *Australian Journal of Soil Research* **35**: 1341-1358.

Connolly RD, Schirmer J and Dunn PK (1998). A daily rainfall disaggregation model.. *Agricultural and Forest Meteorology* **92**: 105-117.

Connolly RD, Freebairn DM, Bell MJ and Thomas G (2001). Effects of rundown in soil hydraulic condition on crop productivity in south-eastern Queensland – a simulation study. *Australian Journal of Soil Research* **39**: 1111-1129.

Cook, FJ. (1983). Water distribution over the soil surface and within the soil during sprinkler irrigation. New Zealand *Journal of Experimental Agriculture* **11**: 69-72.

Cook FJ (1988). Design criteria for droplet irrigation of effluent in Waingawa Freezing Works. *NZ Soil Bureau Contract Report*, 88/13.

Cook FJ (2007). Chapter 80. Near-saturated hydraulic conductivity and sorptivity: Laboratory measurement. *In* Soil Sampling and Methods of Analysis. M.R. Carter and E.G. Gregorich (Eds.), Canadian Society of Soil Science, Taylor and Francis, LLC, Boca Raton, Fl, 1075-1087.

Cook FJ (2017). Estimation of soil physical properties for soils in the Great Barrier Reef catchments. Freeman Cook and Associates, Bureau of Meteorology, 16pp.

Cook FJ and Broeren A (1994). Six methods for determining sorptivity and hydraulic conductivity with disc permeameters. *Soil Science* **157(1)**: 2-11.

Cook FJ, Eyles M, Cowie B, Bosomworth B and Silburn M (2019). Modelling nitrogen transport in sugar cane from soil to runoff from banded surface and buried fertiliser using HYDRUS2D and a post-processing algorithm. *Proceedings from* 23rd International Congress on Modelling and Simulation, Canberra, ACT, Australia, 1 to 6 December 2019. mssanz.org.au/modsim2019

Cook FJ and Kelliher FM (2006). Determining vertical root and microbial biomass distributions from soil samples. *Soil Science Society of America Journal* **70**: 728-735.

Cook FJ and Cresswell HP (2007). Chapter 84 Estimation of Soil Hydraulic Properties. In Soil Sampling and Methods of Analysis. M.R. Carter and E.G. Gregorich (Eds.), Canadian Society of Soil Science, Taylor and Francis, LLC, Boca Raton, Fl, 1139-1161.

Cook FJ, Carlin GD, Hartcher MG, Su X, Asseng S and Campbell P (2008). A water balance model for agent based modeling. *CSIRO Land and Water Science Report*, 47/08, 20p.

Cook FJ (2017). Dispersion in solute transport models: Concepts and limitations in simple models. 22nd World IMACS Congress and MODSIM17 International Congress on Modelling and Simulation, Hobart, Australia 3-8 December 2017, 1857-1863.

Corwin D, Waggoner B, Rhoades J (1991). A Functional Model of Solute Transport that Accounts for Bypass. *Journal of Environmental Quality* **20**: 647-658.

Cresswell HP (2002). The soil water characteristic. Chapter 4 In Mckenzie NJ, Coughlan KJ and Cresswell HP, Soil Physical Measurements and Interpretation for Land Evaluation, Australian Soil and Land Survey Handbook Series: vol. **5**, 59-84.

Cresswell HP and Paydar Z (1996). Water retention in Australian soils. I. Description and prediction using parametric functions. *Australian Journal of Soil Research* **34**: 195-212.

Davidson JM, Stone LR, Nielsen DR and Larue RE (1969). Field measurement and use of soil-water properties. *Water Resources Research* **5**: 1312-1321.

Dawes WR and Short DL (1993). The efficient numerical solution of differential equations for coupled water and solute dynamics: WAVES model. CSIRO Division of Water Resources, Technical Memorandum 93/18.

Deardoff JW (1977). A parameterization of ground-surface moisture content for use in atmospheric prediction models. *Journal of Applied Meteorology* **16(1)**: 1182-1185.

Du X, Yao T, Stone WD and Hendrickx JMH (2001). Stability analysis of the unsaturated water flow equation: 1. Mathematical derivation. *Water Resources Research* **37(7)**: 1869-1874.

Elrick DE, Clothier BE and Smith JE (1987). Solute transport during absorption and infiltration: A comparison of analytical approximations. *Soil Science Society of America Journal* **51**: 282-287.

Feddes RA, Kowalik PJ and Zaradny H (1978). Simulation of field water use and crop yield. Oudoc, Wageningen. Simulation Monographs.

Feddes RA, and Raats PAC (2004). Parameterizing the soil–water–plant root system. *Unsaturated-zone Modeling: Progress, Challenges, Applications* **6**: 95-141.

Ficklin DL and Zhang M (2013). A comparison of the curve number and Green-Ampt models in an agricultural watershed. Transactions *ASABE* **56(1)**: 61-69.

Franz TE, Zreda M, Ferre TPA, Rosolem R, Zweck C, Stillman S, Zeng G and Shuttleworth WJ (2012). Measurement depth of the cosmic ray soil moisture probe affected by hydrogen from various sources. *Water Resources Research* **48**: W08515 1-9.

Franz TE, Zreda M, Rosolem R, Ferre TPA (2013). A universal calibration function for determination of soil moisture with cosmic-ray neutrons. *Hydrology and Earth System Sciences* **17**: 453-460

Gardner T (2021). MEDLI Science Review: Synthesis report. Report to the Queensland Water Modelling Network, Department of Environment and Science.

Germann PF and Beven KJ (1985). Kinematic wave approximation to infiltration into soils with sorbing macropores. *Water Resources Research* **21(7)**: 990-996.

Germann PF and Beven KJ (1986). A distributed function approach to water flow in soil macropores based on kinetic wave theory. *Journal of Hydrology* **83(1-2)**: 173-183.

Green WH and Ampt GA (1911). Studies on soil physics: I. Flow of air and water through soils. *J. Agric. Sci.* **4**: 1-4.

Gowdish L and Munoz-Carpena R (2009). An improved Green-Ampt infiltration redistribution method for uneven multi storm series. *Vadose Zone Journal* **8(2)**: 470-479.

Huth NI, Bristow KL and Verburg K (2012). SWIM3: Model use, calibration and validation. *Transactions of ASABE* **55(4)**: 1303-1313.

Jury WA (1982). Simulation of solute transport using a transfer function. *Water Resources Research* **18**: 262-368.

Jury WA and Roth K (1990). Transfer Functions and Solute Movement through Soil: Theory and Applications. Birlhauser Verlag, Basel Switzerland.

King KW, Arnold JG and Bingner R L (1999). Comparison of Green-Ampt and curve number methods on Goodwin Creek watershed using SWAT. *Transactions of the ASAE*, ***42*(4)**: 919-925.

Knight JH (1973). Solutions of the nonlinear diffusion equation: Existence, uniqueness, and estimation. PhD Thesis, Australian National University, Canberra, Australia.

Knight JH and Philip JR (1973). On solving the unsaturated flow equation: 2. Critique of Parlange's method. *Soil Science* **116(6)**: 407-416.

Laryea KB, Elrick DE and Robin MJL (1982). Hydrodynamic dispersioninvolving cationic adsorption during unsaturated, transient water flow in soil. *Soil Sci. Soc. Am. J.* **46**: 667-671.

Littleboy M, Silburn DM, Freebairn DM, Woodruff DR, and Hammer GL (1989). PERFECT. Productivity erosion, runoff functions to evaluate conservation techniques. *Training series QE93010, Dept. Of Primary Industries, Brisbane*.

Lockington DA (1994). Falling rate evaporation and desorption estimates. *Water Resources Research* **30(4)**:1071-10784.

Ma Y, Feng S, Su D, Gao G and Huo Z (2010). Modeling water infiltration in a large layered soil column with a modified Green-Ampt model and HYDRUS-1D. *Computers and Electronics in Agriculture* **71s**: s40-s47.

Magesan GN, Scotter DR and White RE (1999). The utility of Burn's equation to describe solute movement thrpough soil under various boundary and initial conditions. *European Journal of Soil Science* **50**: 649-656.

McAneney KJ and Judd MJ (1983). Pasture production and water use measurements in the central Waikato. *New Zealand Journal of Agricultural Research* **26**: 7-13.

McClymont D (2018). HowLeaky Model V5 Documentation: Version 1.06. Toowoomba: Department of Environment and Science. Government of Queensland.

McJannet, D, Cook, F, Hartcher, M and Burn, S (2008). Maximising water storage in South-East Queensland reservoirs: Evaluating the impact of runoff interception by farm dams. *Urban Water Security Research Alliance Technical Report*, 12p.

McJannet, D, F. Cook, Hartcher, M and Burn, S (2008). Maximising water storage in South-East Queensland reservoirs: Evaluating the potential of runoff and infiltration enhancement, *Urban Water Security Alliance* **5**: 22.

Mckenzie NJ and Cresswell HP (2002). Selecting a method for hydraulic conductivity. Chapter 6 In Mckenzie NJ, Coughlan KJ and Cresswell HP, Soil Physical Measurements and Interpretation for Land Evaluation, Australian Soil and Land Survey Handbook Series: vol. **5**, 90-107.

Mckenzie NJ, Coughlan KJ and Cresswell HP, Soil Physical Measurements and Interpretation for Land Evaluation, Australian Soil and Land Survey Handbook Series: vol. **5**, 379p.

Mein RG and Larson CL (1973). Modeling infiltration during steady rain. *Water Resources Research* **14**: 384-397.

Minasny B and Cook FJ (2011). Sorptivity of soils. In Encyclopedia of Agrophysics, Eds Glonski J, Horabik J and Lipiec J, Springer, 824-826.

Minasny B and McBrateny SAB (2000). Evaluation and development of hydraulic conductivity pedotransfer functions for Australian soils. *Australian Journal of Soil Research* **38**: 905-926.

Moore ID and Eigel JD (1981). Infiltration into two layered soil profiles. *Transactions of the ASAE* **24(6)**: 1496-1503.

Narsilio GA, Buzzi O, Fityus S, Yun TS and Smith DW (2009). Upscaling of Navier-Stokes equations in porous media: Theoretical, numerical and experimental approach. *Computers and Geotechnics* **36**: 1200-1206.

Neuman SP (1976). Wetting front pressure head in the infiltration model of Green and Ampt. *Water Resources Research* **12(3)**: 564-566.

Nimah MN and Hanks RJ (1973). Model for estimating soil water, plant, and atmospheric interrelations. I. Description and sensitivity. Soil Sci. Soc. Am. Proc. 37(4): 522-527.

Parlange J-Y (1971). Theory of water movement in soils.1. One-dimensional absorption. *Soil Sci.* **111**: 134-137.

Parlange J-Y (1975). On solving the flow equation in unsaturated soils by optimization: horizontal infiltration. *Soil Sci. Soc. Am. Proc.* **39**: 415-418.

Parlange J-Y and Hill DE (1976). Theoretical analysis of wetting front instability in soils. *Soil Sci.* **122**: 236-239.

Philip, JR (1957). The theory of infiltration:4. Sorptivity and algebraic infiltration equations. *Soil Science* **84(3)**: 257-264.

Philip, JR (1966). Linearization technique for the study of infiltration. *Proceedings of UNESCO Netherlands Symposium, Water Unsaturated Zone, Wageningen.*

Philip, JR (1969). Theory of infiltration. *Advances in Hydroscience* **5**: 215-296.

Philip, JR (1987). The infiltration joining problem. *Water Resources Research* **23(12)**: 2239-2245.

Philip JR and Knight JH (1974). On solving the unsaturated flow equation: 3. New quasi-analytical technique. *Soil Science* **117(1)**: 1-13.

Prasad R (1988). A linear root water uptake model. Journal of Hydrology 99(3/4):297-30.

Prendergast JB (1995). Soil water bypass and solute transport under irrigated pasture. *Soil Science Society of America Journal*, **59(6)**: 1531-1539.

Probert ME, Dimes JP, Keating BA, Dalal RC, and Strong WM (1998). APSIM's water and nitrogen modules and simulation of the dynamics of water and nitrogen in fallow systems. *Agricultural systems*, ***56*(1)**: 1-28.

Raats PAC (2001). Developments in soil-water physics since the mid 1960s. *Geoderma* **100**: 355-387.

Raats PAC (1983). Implications of some analytical solutions of drainage of soil water. *Agricultural Water Management* **6**: 161-175.

Ralston A (1965). A First Course in Numerical Analysis. McGraw-Hill, Inc., New York, 578 pp.

Rawls WJ and Brakensiek DL (1986). Comparison between Green-Ampt and curve number runoff predictions. *Transactions of the ASAE* **29(6)**: 1597-1599.

Richardson, LF (1922). Weather Prediction by Numerical Process. Cambridge University Press, 236p.

Richards LA (1931). Capillary conduction of liquid through porous media. *Physics* **I**: 318-333.

Ritchie, JT (1972). A model for predicting evaporation from a row crop with incomplete cover. *Water Resources Research* **8**: 1204-1213.

Salvucci GD and Entekhabi D (1994). Equivalent steady moisture profile and the time compression approximation in water balance modelling. *Water Resources Research* **30(10)**: 2737-2749.

Salvucci GD and Entekhabi D (1995). Ponded iunfiltration into soils bounded by a water table. *Water Resources Research* **31(11)**: 2751-2759.

Scotter DR and Ross PJ (1994). The upper limit of solute dispersion and soil hydraulic properties. *Soil Science Society of America Journal* **58**: 659-663.

Scotter DR, White RE and Dyson JS (1993). The Burns leaching equation. *Journal of Soil Science* **44**: 25-33.

Sharpley AN and Williams JR (Eds.) (1990). EPIC - Erosion/Productivity Impact Calculator: 1. Model documentation. USDA. Agriculture Technical Bulletin. No. 1768. 235 pp.

Short D, Dawes WR and White I (1995). The practicability of using Richards' equation for general purpose soil-water dynamics models. *Environmental International* **21(5)**: 723-730.

Silburn DM and Connolly RD (1995). Distributed parameter hydrology nodel (ANSWERS) applied to a range of catchment scales using rainfall simulatort datal: Infiltration modelling and parameter measurement. *Journal of Hydrology* **172**: 87-104.

Simunek J, Sejna M, Saioto H, Sakai M and van Genuchten MT (2008). The HYDRUS-1D Software Package for Simulating the One-Dimensional Movement of Water, Heat, and Multiple Solutes in Variably-Saturated Media. Riverside, Department of Environmental Sciences, University of California.

Sisson JB, Ferguson AH and van Genuchten M Th (1980). Simple method for predicting drainage from field plots. *Soil Science Society of America Journal* **44**: 1147-1152.

Steiner JL, Williams JR, and Jones OR (1987). Evaluation of the EPIC Simulation Model Using a Dryland Wheat-Sorghum-Fallow Crop Rotation 1. *Agronomy Journal*, **79(4)**, 732-738.

Sutanto SJ, Wenninger J, Coenders-Gerrits AMJ and Uhlenbrook S (2012). Partitioning of evaporation into transpiration, soil evaporationand inmterception: a comparison between isoptopemeasurements and a HYDRUS-12D model. *Hydrology and Earth System Sciences* **16**: 2605-2616.

Towner GD (1983). A theoretical examination of Burn's (1975) equation for predicting the bleaching of nitrate fertilizer applied into a surface soil. *Journal of Agricultural Science* **100**: 293-298.

Van der Laan M, Stirzaker R, Annandale JG, Bristow K L and du Preez CC. (2010). Monitoring and modelling draining and resident soil water nitrate concentrations to estimate leaching losses. *Agricultural Water Management* **97**: 1779-1786.

Vandervaere JP, Vauclin M and Elrick DE (2000). Transient flow from tension infiltrometers: I. The two-parameter equation. *Soil Science Society of America Journal* **64**: 1263-1272.

Van Genuchten, MT and Alves WJ (1982). Analytical solutions of the one-dimensional convective-dispersion solute transport equation. Technical Bulletin, United states Department of Agriculture, Agricultural Research Service. No. 1661.

Verburg K (1996). Methodology in soil-water-solute balance modelling: An evaluation of the APSIM-SoilWat and SWIM v2 models. Division of Soils institutional report. K Verburg Canberra, CSIRO: 88.

Wang Z, Tuli A, Jury WA (2003). Unstable flow during redistribution in homogeneous soil. *Vadose Zone Journal* **2**: 52-60.

Wallach, R, van Genuchten, MTh (1990). A physically based model for predicting solute transfer from soil solution to rainfall-induced runoff water. Water Resources Research 26, 2119-2126.

Warrick WA (2003). Soil Water Dynamics. Oxford University Press, New York, 391p.

Watson, KK (1966). An instantaneous profile method for determining the hydraulic conductivity of unsaturated porous materials. *Water Resources Research* **2(4)**: 709-715.

Watson, KK (1967). The measurement of the hydraulic conductivity of unsaturated porous materials utilizing a zone of entrapped air. *Soil Science Society of America Journa*l **32**: 716-720.

White I and Broadbridge P (1988). Constant rate rainfall infiltration: A versatile nonlinear model 2. Applications of solutions. *Water Resources Research* **24(1)**: 155-162.

White I and Sully MJ (1987). Macroscopic and microscopic capillary length and time scales from field infiltration. *Water Resources Research* **23(8)**: 1514-1522.

White I, Sully MJ and Melvill MD(1989). Use and hydrological robustness of time-to-incipient-ponding. Soil Science Society of America Journal 53: 1343-1346.

Yao T and Hendrickx JMH (2001). Stability analysis of the unsaturated water flow equation 2. Experimental verification. *Water Resources Research* **37(7)**: 1875-1881.

Zhang Y and Schaap MG (2017). Weighted recalibration of the Rosetta pedotransfer model with improved estimates of hydraulic parameter distributions and summary statistics (Rosetta 3). *Journal of Hydrology* **547**:39-53.

Youngs EG (1960). The drainage of liquids from porous media. *Journal of Geophysical Research* **65(12)**: 4025-4030.

Youngs EG and Aggelides (1976). Drainage to a water table analysed by the Green-Ampt approach. *Journal of Hydrology* **31**: 67-79.

Appendix 1. Solutions for infiltration into non-uniform initial conditions and layered soils

A1.1 Prior to ponding

Prior to ponding the cumulative infiltration into the soil is given by:

$$I(t) = \int_0^t R(t)\,dt \tag{A1}$$

$I(t)$ is the cumulative infiltration (m)

t is time (s)

$R(t)$ is the rainfall rate (m s^{-1})

Consider a soil consisting of n layers with thicknesses of Dz_1, Dz_2, … Dz_n and corresponding water content storage volumes of $\Delta\theta_1$, $\Delta\theta_2$, … $\Delta\theta_n$ (Figure 32). When the piston wetting front is at the bottom of the first layer the cumulative infiltration will be $I_1 = Dz_1\Delta\theta_1$. This cumulative infiltration must equate to the value of $I(t_1)$ given by Eqn (A1) at the time t_1 when the piston is at the bottom of layer 1 so that:

$$I(t_1) = \int_0^{t_1} R(t)\,dt = Dz_1\Delta\theta_1 \tag{A2}$$

To obtain the time that the wetting front reaches the bottom of the second and subsequent layers we follow the procedure used by Bouwer (1969). Firstly, we calculate the fictitious time, $t_1^{'}$, for the wetting front to reach the bottom of the first layer but now with the water content storage of layer 2 ($\Delta\theta_2$) by substituting $\Delta\theta_2$ for $\Delta\theta_1$ in Eqn (A2). Then we calculate the fictitious time, $t_2^{'}$, for the wetting front to reach the bottom of layer 2 as:

$$I(t_2^{'}) = \int_0^{t_2^{'}} R(t)\,dt = \left(Dz_1 + Dz_2\right)\Delta\theta_2 \tag{A3}$$

The difference between $t_2^{'}$ and $t_1^{'}$ is the time it will take for the wetting front to move through layer 2. Thus, we can calculate the actual time, t_2, the wetting front reaches the bottom of layer 2 as:

$$t_2 = t_1 + \left(t_2^{'} - t_1^{'}\right) \tag{A4}$$

The infiltration at t_2 is the $I(t_2)$ or $I2 = Dz_1\Delta\theta_1 + Dz_2\Delta\theta_2$. This procedure can be repeated for all layers until ponding occurs or the rainfall ceases.

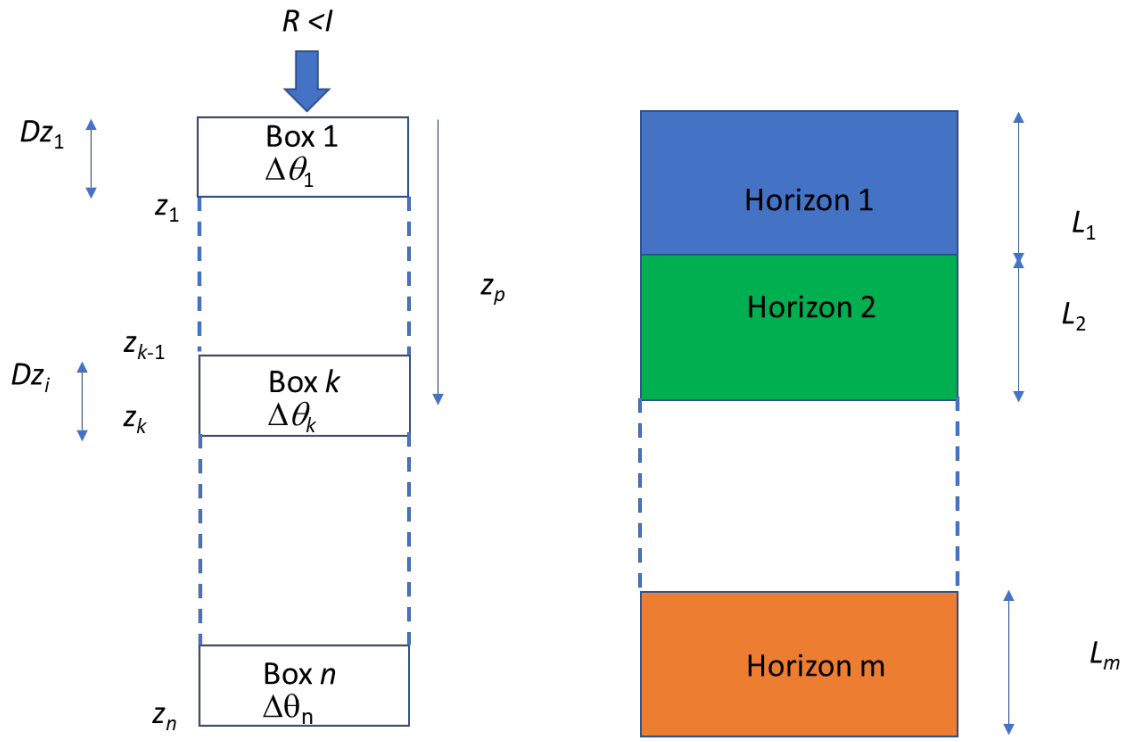

Figure 32. The left-hand diagram is a schematic of the spatial discretisation and showing the wetting front depth z_p as being in box k. The right-hand diagram is a schematic of the soil profile with soil horizon of thickness L_x.

A1.2 Time to ponding

The non-uniformity of the water content will also affect the calculation of the time to ponding (t_p). At t_p H = 0 and substituting Eqn (9) into Eqn (16) and using M = 0.55 gives:

$$\bar{R}_p t_p = 1.1\Delta\theta\psi_f \ln\left[\frac{R(t_p)}{R(t_p)-K_s}\right] = I_p(t_p) \qquad \text{(A5)}$$

Infiltration into each box needs to be tested to determine in which layer the wetting front is when ponding occurs. The box in which this occurs, k, will be the one where:

$$\bar{R}(t_k)t_k > 1.1\Delta\theta_k\psi_f(k)\ln\left[\frac{R(t_k)}{R(t_k)-K_s}\right] \qquad \text{(A6)}$$

The time when ponding occurs can be calculated using Eqn (A5) with $\Delta\theta = \Delta\theta_k$. This will have to be achieved by using an iterative procedure like Newton-Raphson with a good starting value being $t_p = (t_k + t_{k-1})/2$. The cumulative infiltration at the time of ponding is $I_p = \bar{R}_p t_p$ and the depth of the wetting front at t_p (z_p) is given by:

$$z_p = \left[I_p - \sum_{i=1}^{k-1} Dz_i \Delta\theta_i \right] / \Delta\theta_k + \sum_{i=1}^{k-1} Dz_i \quad \text{(A7)}$$

where

i is the index counter for the box.

If the soil hydraulic properties change at some depths L_1, L_2, … L_m then this also needs to be accounted for. If $z_p \le L_1$ then Eqn (A6) is correct with K_s the value of the soil for horizon 1. When z_p is in horizon 2 then then the harmonic mean ($\overline{K}$) must be used for Ks in Eqn (A6) given by:

$$\overline{K} = \frac{z_p}{\left(\frac{L_1}{K_1} + \frac{z_p - L_1}{K_2} \right)} \quad \text{(A8)}$$

When z_p is at some depth where the wetting front has passed through *u* soil horizons then the value of ($\overline{K}$) is given by:

$$\overline{K} = \frac{\sum_{i=1}^{k} Dz_i}{\left(\frac{L_1}{K_1} + \frac{L_2 - L_1}{K_2} \right)} \quad \text{(A9)}$$

where K_1 and K_2 are the K_s of the soil properties above and below *L*. This can be used for more than two soil horizons by calculation of $\overline{K}$ for the number of soil horizons that are wetted.

The above analysis will only be required if ponding occurs at the soil surface. If ponding does not occur, then the infiltration rate (*i*) is the rainfall rate (*R*) and the cumulative infiltration is:

$$I(t) = \int_0^t R(t)\, dt \quad \text{(A10)}$$

where t is the time it has been raining for. The depth of wetting (z_w) will be in box *k* given by:

$$z_w(t) = \sum_{i=1}^{k-1} Dz_i + \left[I(t) - \sum_{i=1}^{k-1} Dz_i \Delta\theta_i \right] / \Delta\theta_k \quad \text{(A11)}$$

A1.3 Green and Ampt Model

Once ponding has started the GA model can be used to determine the further movement of the wetting front through the soil. The time to the bottom of the *k*th box where the wetting front is when ponding occurs can be calculated using the method proposed by Bouwer (1969). The implicit form of

the GA model (Eqn (7)) is the easier to use for solving for nonuniform soils. The fictitious time for the time to ponding is calculated by:

$$t_p^{'} = \frac{1}{K_k^a}\left\{ I_p + \Delta\theta_k \left(H + \psi_f\right) \ln\left[1 + \frac{I_p}{\Delta\theta_k \left(H + \psi_f\right)}\right]\right\}$$
$$K_k^a = \left(\bar{K}_{k-1} + \bar{K}_k\right)/2 \qquad \text{(A12)}$$

and the fictitious time to the bottom of the *k*th box is:

$$t_k^{'} = \frac{1}{K_k^a}\left\{ I_k + \Delta\theta_k \left(H + \psi_f\right) \ln\left[1 + \frac{I_k}{\Delta\theta_k \left(H + \psi_f\right)}\right]\right\}$$
$$I_k = \sum_{i=1}^{k} Dz_i \Delta\theta_i \qquad \text{(A12)}$$

The real time to the bottom of the *k*th box is then $t_k = t_{k-1} + \left(t_k^{'} - t_p^{'}\right)$. For the next box we can calculate the fictitious time to the top of the box as:

$$t_k^{'} = \frac{1}{\bar{K}_k}\left\{ I_k + \Delta\theta_{k+1} \left(H + \psi_f\right) \ln\left[1 + \frac{I_k}{\Delta\theta_{k+1} \left(H + \psi_f\right)}\right]\right\}$$
$$I_k = \sum_{i=1}^{k} Dz_i \Delta\theta_i \qquad \text{(A13)}$$

And to the bottom of the *k*+1 box as:

$$t_{k+1}^{'} = \frac{1}{K_a^{k+1}}\left\{ I_{k+1} + \Delta\theta_{k+1} \left(H + \psi_f\right) \ln\left[1 + \frac{I_{k+1}}{\Delta\theta_{k+1} \left(H + \psi_f\right)}\right]\right\}$$
$$I_{k+1} = \sum_{i=1}^{k+1} Dz_i \Delta\theta_i \qquad \text{(A14)}$$
$$K_a^{k+1} = \left(\bar{K}_k + \bar{K}_{k+1}\right)/2$$

The real time to the bottom of the *k*th box is then $t_{k+1} = t_k + \left(t_{k+1}^{'} - t_k^{'}\right)$. For subsequent boxes the same procedure is used until the infiltration event is completed. For the last box if infiltration reaches the bottom of the box, then any further infiltration goes out the bottom of the box to deep drainage.

A spreadsheet with examples has been provided to assist with implementation of the methods described in this report.

Appendix 2. Soil Properties used in Examples.

The soil properties used in the examples in the text.

Table A2. Soil physical properties for a clay soil from Salvucci and Entekhabi (1994), sandy loam soil from Clapp and Hornberger (1978) and clay loam soil from Sisson et al. (1980)). λ is the slope term and ψ_b is the air entry matric potential in the Books and Corey moisture retention function.

Parameter	Salvucci & Entekhabi	Clapp & Hornberger	Sisson
Soil	Clay	Sandy Loam	Clay loam
Saturated Hydraulic Conductivity (K_s) (mm day^{-1})	29	2995	1000
Saturated water content (θ_s)	0.45	0.435	0.52
Pore size distribution term (λ)	0.44	4.9	0.625
Air entry water potential (ψ_b) (mm)	-900	-218	-
Initial water content (θ_i)	0.1	0.15	0.52
Sorptivity calculated with Eqn (9) (S)	1.4 (mm day$^{-1/2}$)	391 (mm day$^{-1/2}$)	-

Table A3. Representative values of hydraulic parameters (standard deviations in parentheses) (From Table 2 of Clapp and Hornberger (1978). Note the soil texture is based on the USDA particle size ranges. The values of $m = 2\lambda + 3$ are calculated here.

Soil Texture	Clay (%)	λ	m	ψ_b (m)	θ_s ($m^3\ m^{-3}$)	K_s ($m\ s^{-1}$)	S ($m\ s^{-1/2}$)
Sand	3	4.05 (1.78)	11.10 (6.56)	0.121 (0.143)	0.395 (0.056)	$7.33x10^{-6}$	$4.01x10^{-4}$
Loamy sand	6	4.38 (1.47)	11.76 (5.94)	0.09 (0.124)	0.410 (0.068)	$6.51x10^{-6}$	$2.74x10^{-4}$
Sandy loam	9	4.90 (1.75)	12.80 (6.50)	0.218 (0.31)	0.435 (0.086)	$1.44x10^{-6}$	$2.71x10^{-4}$
Silt loam	14	5.30 (1.96)	13.60 (6.92)	0.786 (0.512)	0.485 (0.059)	$3.00x10^{-7}$	$3.32x10^{-4}$
Loam	19	5.39 (1.87)	13.78 (6.74)	0.478 (0.512)	0.451 (0.078)	$2.90x10^{-7}$	$1.83x10^{-4}$
Sandy clay loam	28	7.12 (2.43)	17.24 (7.86)	0.299 (0.378)	0.420 (0.059)	$7.08x10^{-8}$	$1.29x10^{-4}$
Silty clay loam	34	7.75 (2.77)	18.50 (8.54)	0.356 (0.378)	0.477 (0.057)	$1.02x10^{-7}$	$8.17x10^{-5}$
Clay loam	34	8.52 (3.44)	20.04 (9.88)	0.63 (0.51)	0.476 (0.053)	$3.00x10^{-7}$	$1.42x10^{-4}$
Sandy clay	43	10.4 (1.64)	23.80 (6.28)	0.153 (0.173)	0.426 (0.057)	$9.03x10^{-8}$	$5.88x10^{-5}$
Silty clay	49	10.4 (4.45)	23.80 (11.9)	0.49 (0.621)	0.492 (0.064)	$4.31x10^{-8}$	$6.38x10^{-5}$
Clay	63	11.4 (3.70)	25.80 (10.4)	0.405 (0.397)	0.482 (0.050)	$4.86x10^{-8}$	$7.06x10^{-5}$

Appendix 3. Drainage for Non-uniform Soil Profiles.

For drainage following infiltration where the whole profile has been wetted to saturation is given in Section 2.2. When the wetting front does not wet the whole profile then there will be a step change in the water content at some depth zf. This means that the water draining from the saturated part of the soil profile will result in wetting of the soil below depth zf. Other non-uniformity arises if there is a change in soil properties with depth. The models presented in Section 2.2 need to be modified to account for this.

A3.1 Sisson Model

At the end of infiltration, the depth of the wetting front z_f will be in some soil box (x). The amount of water in the soil above z_f at the start of drainage, W_0, is then:

$$W(z_f, t_0) = \int_0^{z_f} \theta \, dz \tag{A15}$$

where

$t_0 = z_f/A$ is the time when drainage commences at z_f. Prior to t_0 the water draining from above maintains the water content at the saturated or initial value.

A is given in Eqn (20)

The water stored in the profile to z_f at t_0 can be calculated by:

$$W_0(z_f, t_0) = \theta_c z_f + \frac{(m-1) z_f}{m} (\theta_s - \theta_c) \left[\frac{z_f}{At'} \right]^{1/(m-1)} \tag{A16}$$

The amount of water having drained from the soil profile at t_0 is then given by:

$$\Delta W_0 = \int_0^{z_f} \theta_s \, dz - W(z_f, t_0) \tag{A17}$$

This drained water will be transported down the soil profile to a depth given by:

$$z_{f1} = z_f + \Delta W_0 / (\theta_s - \theta_1) \tag{A18}$$

where

θ_1 is the water content in the soil below z_f

z_{f1} is the new depth of the wetting front at t_0 (m)

This process is repeated until a value of $z_{fn} - z_{fn-1} < 1$ mm.

The value of the water storage at t_0 is now adjusted to give:

$$
\begin{aligned}
W(z,t_1) &= \theta_c z + \frac{(m-1)z}{m}(\theta_s - \theta_c)\left[\frac{z}{At'}\right]^{1/(m-1)}, && 0 < z < z_f \\
W(z,t_1) &= W(z_f,t_0) + (z_{f1} - z)\theta_s, && z_f < z \le z_{f1}. \\
W(z,t_1) &= W(z_{f1},t_0) + (z - z_{f1})\theta_1, && z > z_{f1}
\end{aligned}
\tag{A19}
$$

The integral of the flux at time t_0 and $t_1 = z_{f1}/A$ with depth is then calculated and the difference in the integrals is the water drained from the soil above that depth with:

$$
\begin{aligned}
\Delta J(z,t_1) &= \frac{B(z)}{1-\bar{M}}\left[(t_0)^{1-\bar{M}} - (t_1)^{1-\bar{M}}\right] \\
B(z) &= \bar{K}\left(\frac{z}{A}\right)^{\bar{M}}
\end{aligned}
\tag{A20}
$$

where

$\bar{K}$ is the harmonic mean of K_s if the soil properties are nonuniform and is calculated in Appendix 1

$\bar{M}$ is the harmonic mean of M if the soil properties are nonuniform and is calculated in Appendix 1.

The value of $\theta(t_1)$ using:

$$
\theta(z_i,t_1) = \frac{W(z_i,t_1) - W(z_{i-1},t_1)}{z_i - z_{i-1}} \tag{A21}
$$

A new value of t, t_2, is chosen and the procedure is repeated from Eqn (A19) onward. A spreadsheet with the procedure has also been provided.

A3.2 Youngs Model

The Youngs model is not suitable for nonuniform water content as Q_∞ needs to be calculated for a whole profile. Although an attempt was made to develop a method, it was not satisfactory due to it violating assumptions made in the development of the method. No further development will be presented here.